2013

Bit error rate estimation in WiMAX communications at vehicular speeds using Nakagami-m fading model

Biswojit Bose
Edith Cowan University

Edith Cowan University

Copyright Warning

Bit Error Rate Estimation in WiMAX Communications at Vehicular Speeds using Nakagami-m Fading Model

by

Biswojit Bose

This thesis is presented in fulfillment of the requirements for the degree of

Master of Engineering Science

SCHOOL OF ENGINEERING

FACULTY OF COMPUTING, HEALTH AND SCIENCE

EDITH COWAN UNIVERSITY

January 25, 2013

To my father the late Asit Kumar Bose and my mother Shila Bose

USE OF THESIS

The Use of Thesis statement is not included in this version of the thesis.

Abstract

The wireless communication industry has experienced a rapid technological evolution from its basic first generation (1G) wireless systems to the latest fourth generation (4G) wireless broadband systems. Wireless broadband systems are becoming increasingly popular with consumers and the technological strength of 4G has played a major role behind the success of wireless broadband systems. The IEEE 802.16m standard of the Worldwide Interoperability for Microwave Access (WiMAX) has been accepted as a 4G standard by the Institute of Electrical and Electronics Engineers in 2011. The IEEE 802.16m is fully optimised for wireless communications in fixed environments and can deliver very high throughput and excellent quality of service. In mobile communication environments however, WiMAX consumers experience a graceful degradation of service as a direct function of vehicular speeds. At high vehicular speeds, the throughput drops in WiMAX systems and unless proactive measures such as forward error control and packet size optimisation are adopted and properly adjusted, many applications cannot be facilitated at high vehicular speeds in WiMAX communications. For any proactive measure, bit error rate estimation as a function of vehicular speed, serves as a useful tool. In this thesis, we present an analytical model for bit error rate estimation in WiMAX communications using the Nakagami-m fading model. We also show, through an analysis of the data collected from a practical WiMAX system, that the Nakagami-m model can be made adaptive as a function of speed, to represent fading in fixed environments as well as mobile environments.

DECLARATION

I certify that this thesis does not, to the best of my knowledge and belief:

(i) incorporate without acknowledgement any material previously submitted for a degree or diploma in any institution of higher education;

(ii) contain any material previously published or written by another person except where due reference is made in the text; or

(iii) contain any defamatory material.

I also grant permission for the Library at Edith Cowan University to make duplicate copies of my thesis as required.

ACKOWNLEDGEMENT

I would like to express my sincere gratitude and profound indebtedness to my supervisors Prof. Daryoush Habibi and Dr Iftekhar Ahmed for their constant guidance, insightful advice, critical reviews, valuable suggestions, and commendable support, enabling me to complete the thesis. I am fortunate to have worked with wonderful mentors. Their experience was most helpful to ensure the quality of this work.

I would like to thank Dr Steven Richardson for his valuable help to develop the analytical model of this research. I would like to thank Dr Narottam Das, Dr Prabir Kumar Sarker and Dr Eric Dines for their good wishes, encouragement and valuable suggestions. Thanks also to Mr Steve Lawn for proof reading of this thesis.

I am thankful to all the staff and research students at the School of Engineering, Edith Cowan University. Special thanks to Uttam kumar Debnath and Rajesh Ramraj for their valuable help during data collection. Thanks to the research students and the staff members of the Centre for Communications Engineering Research (CCER) for their support during this research. I enjoyed every moment of their friendship. Special thanks to my loving wife for her endless support, patience and encouragement to complete this thesis. Finally I would like to thank my cute son who missed my company while I was busy with this research.

Contents

List of Tables

List of Figures

List of Algorithms

Research Publications

Accepted Paper

1. B. Bose, I. Ahmad and D. Habibi, "Bit Error Rate Analysis Using Nakagami-m Distribution in WiMAX Communication at Vehicular Speeds" is accepted for the IEEE 76th Vehicular Technology Conference: VTC2012-Fall 3-6 September 2012, Québec, Canada.

2. B. Bose, I. Ahmad and D. Habibi, "Estimation of the Nakagami m parameter in WiMAX Communication at Vehicular Speeds " in preparation for The 10th IEEE Annual Consumer Communications and Networking Conference (CCNC), January 11-14, 2013, Las Vegas, Nevada, USA.

Chapter 1

Introduction

Wireless communication is the fastest growing segment of the communications industry and has enjoyed exponential growth in the last decade. Wireless communication has become a critical business tool and an integral part of modern civilization. Wireless technologies have come a long way since their introduction and the current 4G standards are deemed to revolutionise the way everyday communication is done. In this thesis, we explore the suitability of Worldwide Interoperability for Microwave Access (WiMAX), a 4G standard, for vehicular communications. We propose techniques to overcome the limitations of low throughput at high vehicular speeds. In this chapter, we describe the background of the research problems in brief. We then present the research motivation and contributions.

1.1 Wireless Communications

The research and development of wireless communication started in the seventeenth century [1]. The era of modern wireless communication began in the 1980s and is divided into generations. First Generation (1G) wireless communication systems were only able to transmit voice calls and a limited amount of data, but had no roaming capacity. The Second Generation (2G) started during the late 1980s when the roaming capacity was integrated in wireless communication. There were a number of 2G standards published during that decade and 2G was able to transmit high volumes of data when compared to 1G. The 2G systems used individual infrastructure for voice and data transmission. At the end of the 1990s, the data network assimilated with cellular systems and led to the Third Generation (3G) systems. The

International Telecommunication Union (ITU) published the 3G standard, known as International Mobile Telecommunication-2000 (IMT-2000) during the 2000s. The minimum data speeds of the IMT-2000 specification were 2 Mbps, 384 Kbps and 144 Kbps for stationary, pedestrian and moving vehicle speeds, respectively. The 3G provides superior voice quality, global roaming and data service. The Fourth Generation (4G) initiative started at the beginning of the 2000s; developing the next generation Internet Protocol (IP) based wireless mobile network for providing broadband data communication, that can transmit multimedia (voice, video or music) and data, and interface with wired backbone networks[2, 3].

1.2 Fourth Generation Wireless Systems

The International Telecommunication Union published the International Mobile Telecommunication-Advanced (IMT-Advanced) technical requirements in 2008, which is known as the 4G standard[4]. According to the 4G specifications; it should support at least 100 Mbps peak data rate at full mobility in wide area coverage, and 1 Gbps at low mobility in local area coverage. The 4G standard is based on broadband IP and brings improved real world wireless communications. The IMT-advanced supports scalable bandwidth up to 40 MHz and mobility up to 350 km/h. The Institute of Electrical and Electronics Engineers (IEEE) standard IEEE802.16m is a 4G technology standard[5].

1.3 Worldwide Interoperability for Microwave Access

The Worldwide Interoperability for Microwave Access has revolutionised our day to day communication. The first version of WiMAX 802.16 was published by IEEE in 2001 for Line of Site (LOS) communication, and the revised version 802.16a was published in 2003, which supports Non-LOS (NLOS) communications. The mobility enhancement was added to WiMAX 802.16e in 2005 and approved as a IMT-2000 (3G) standard in 2007. The advanced version of IEEE 802.16m, or mobile WiMAX, has been approved as a 4G technology in 2011.

The WiMAX system provides higher throughput than any other conventional

3G technology and gives total freedom to people who are mobile; allowing them to stay connected with voice, data and video services. It has many practical applications for both public and private networks such as: cellular backhaul, banking networks, education networks, offshore communication, campus connectivity, temporary construction communications, theme park, access networks, rural connectivity and public safety. More than 600 vendors deployed WiMAX systems over 149 countries around the world; which is greater than any other conventional 3G technology, and 50% higher than High Speed Packet Access (HSPA) network. Roughly 70% of WiMAX communication deployments are in emerging markets [6]. The WiMAX forum projected more than 93 million mobile WiMAX users globally by 2012 [7].

The IEEE 802.16m version of the WiMAX system is able to meet the individual Quality of Service (QoS) parameters for the individual multimedia classes of; low, medium, high and super high multimedia, defined by the ITU. It offers the throughput up to 1 Gbps and mobility up to 350km/h. The Orthogonal Frequency Division Multiple Access (OFDMA) and Multi user Multiple Input Multiple Output (MIMO) are key features of mobile WiMAX for higher throughput and high mobility. This capacity to deliver higher throughput and high mobility opens a number of new avenues for new applications.

1.4 WiMAX Communications at Vehicular Speeds

Nowadays people want to access internet services anytime and anywhere; consequently the demand for higher data rate broadband access service is increasing rapidly. Public safety is a big issue worldwide and the capacity of WiMAX system opens a new avenue for public safety applications such as real-time video surveillance. Public transport authorities are now moving towards WiMAX communication systems for transmitting video data from video surveillance cameras. Such applications, however, require high throughput.

High data rates in WiMAX systems for fixed environments is beyond any doubt, but the standard is not fully optimized for mobile communication at vehicular speeds. The data rate decreases sharply for mobile communication at vehicular speeds, often providing data rates that are barely sufficient to maintain the connection at high vehicular speeds. The IEEE 802.16m standard also acknowledges this

problem and its system requirements document indicates that the IEEE 802.16m is fully optimized only when stationary or at pedestrian speeds (0-10km/h). At speeds between 10 - 120km/h, WiMAX users are expected to experience gradual degradation of services, as a function of increasing speed. At speeds above 120km/h, a connection can be maintained, but no assurance of any data capability is provided[8]. In the high mobility scenario, relative motion between transmitters and receivers results in rapid time variation, so a significant fluctuation of Received Signal Strength (RSS) is observed in the channel.

1.5 Motivation and Research Questions

At vehicular speeds, spectral efficiency of the WiMAX system reduces, mainly due to the following problems, which are the main challenges for delivering high throughput at vehicular speeds.

1. **Multipath propagation:** Multipath is major drawback in wireless telecommunications. When there is no LOS communication between the transmitter (Tx) and the receiver (Rx), the signal cannot reach the Rx directly. The signal bounces by reflection, refraction and diffraction from the obstructions between the Tx and Rx and reach the receiving antenna by two or more paths. This phenomenon is known as multipath. Multipath propagation causes Inter symbol Interference (ISI) and ISI causes amplitude fluctuation and phase difference of the signal, which is an irreducible error in the detected signal. During the mobile environment at vehicular speeds, the multipath changes dynamically and results in a more severe multipath fading channel.

2. **Doppler spread:** The doppler spread is the spectrum of fluctuations of the received signal. When the electromagnetic wave source moves around a receiver, the signal experiences doppler spread. When the source moves towards the receiver, compared to emitted frequency the received frequency of the receiver increases. The receiver frequency decreases during the recession and remains constant when passing by. This effect is known as the doppler effect, after Christian Doppler. The doppler effect creates Inter Carrier Interference (ICI) and distorts the signal.

Unless any proactive measure is taken to combat the above mentioned problems, the throughput at the Rx becomes insufficient to support many applications, particularly those with multimedia contents. For any proactive measure, Bit Error Rate (BER) estimation plays a vital role and further research is needed for designing resource management schemes at vehicular speeds, so that applications requiring high throughput can be supported at high vehicular speeds. A key requirement for such resource management schemes is to have an analytical model that can estimate BER at high vehicular speeds, so that proactive actions can be taken and proper planning can be done. Fading models are used for bit error rate estimation.

The fading channel caused by multipath and doppler shift and often modeled with the popular Rayleigh distribution. The Rayleigh fading model has not been challenged until very recently when researchers started to focus on high throughput at vehicular speeds. The Rayleigh model works on the assumption that the resultant fading arises from a large number of uncorrelated partial waves, with identically distributed amplitudes, and uniformly $[0, 2\pi]$ distributed random phases. This assumption is highly optimistic in a mobile communication environment at high vehicular speeds. The more realistic assumption is to have many partial waves with amplitudes that follow distributions that are not identical, yet are partially correlated [9, 10]. In an environment like this, signal fluctuation is better modeled by the Nakagami-m distribution [10, 9] and as a result, bit error rate estimation using the Nakagami-m distribution should provide more accurate BER estimates.

The Nakagami-m distribution is used for different types of channel estimation. The shape parameter m of the model defines the fading severity of the channel. If $m > 1$, the channel is considered as Rician fading, where there is a minimum of one LOS communication between the Tx and the Rx. When $m = 1$, the channel is considered as Rayleigh fading where there is no LOS communication between Tx and Rx. If $m < 1$, the channel is considered as Nakagami fading, where the fading is more severe than the Rayleigh fading.

The first aim of this research is to develop a mathematical model for BER estimation in WiMAX communication at vehicular speeds, that can be used for improving throughput at the receiver end.

The second aim of this research is to estimate the fading severity of the channel at different vehicular speeds by estimating the Nakagami parameter m; which can

be used for resource management schemes, to facilitate applications that require high throughput.

1.6 Research Contribution

To improve the throughput of any wireless communication system, a proactive measure is necessary, and for any proactive measure, BER estimation plays the major role. To estimate the BER accurately, a proper analytical model is also necessary. In this research, we developed a BER estimation model for WiMAX system using the Nakagami-m distribution model. We estimated the BER in WiMAX communication at different vehicular speeds in Adaptive Modulation and Coding (AMC) and Partial Use of Sub-Carrier (PUSC) mode; for both 512 and 1024 First Fourier Transformation (FFT). To estimate the BER, we considered the different values of Nakagami parameter m and different SNR. We also compared the BER between Nakagami-m and the Rayleigh fading model.

In this research, we also estimated the value of m for different vehicular speeds ranging from 10 km/h to 100 km/h for NLOS communication. To estimate the value of m, we collected the instantaneous receive signal strength, from a commercial WiMAX communication system providing service to the Australian people.

1.7 Research Outline

The structure of this thesis is as follows

- **In chapter 2,** we first describe the 4G Standards. We include the background of WiMAX communication technology and its key features that make WiMAX system a prime technology for the 4G standard. We will also familiarise the readers with the Nakagami-m distribution model and then discuss the literature and works which are relevant to this research.

- **In chapter 3,** we present the different types of fading characteristics, and the fading model used in wireless communication technology to estimate the channel. We will present the proposed BER analytical model for estimating the BER of WiMAX system at vehicular speeds using the Nakagami-m fading

model. We alsoanalyse the BER in WiMAX communication using the proposed analytical model at different vehicular speeds, considering the different values of Nakagami parameter m. In this chapter we will also compare the estimated BER in the Nakagami-m fading model against the Rayleigh fading model.

- **In chapter 4,** we discuss the Nakagami parameter m and estimate the values of m for a commercial WiMAX communication system at different vehicular speeds. We will also describe the WiMAX system, the environment of the data collection area and collection procedure; and finally estimate the fading characteristics of the channel at vehicular speeds.

- **In chapter 5,** we conclude the thesis with the findings in this research. We also outline future works that are necessary for further improving data rates in WiMAX communication at vehicular speeds.

Chapter 2

Background and Literature Review

The WiMAX system is a state of the art broadband wireless communication technology, which is currently serving more than 160 million people in around 149 countries. It provides a number of new opportunities for researchers and opens a number of new avenues for applications at vehicular speeds. Numerous research studies have been conducted on the WiMAX system by researchers worldwide, for vehicular applications. This chapter outlines the development of wireless communication systems, the WiMAX system and its key features, research and implementation of the WiMAX system at vehicular speeds and the challenges for wireless communication systems in vehicular applications.

2.1 Wireless Communication and 4G Technologies

The development of modern wireless communication started with the observation of electromagnetic phenomena of radio waves in the seventeenth century [1]. Wireless networking is based on either the connection-based voice oriented service or the connection-less data oriented service. The voice oriented service evolved around the wireless connection to the Public Switched Telephone Network (PSTN), and the data oriented network evolved around the Internet, computer and communication networks. Over the last century, the voice oriented service was the biggest revenue provider, but nowadays the data oriented service has taken over, and is the biggest revenue provider world wide.

Table 2.1: 1G to 4G at a Glance

Generation	Basic Requirement	Access Technology	Comments
1G	No standard, Analogue	FDMA	NMT, AMPS
2G	No standard, Digital	TDMA, CDMA	GSM, PCS, WLAN
3G	IMT-2000	W-CDMA, OFDM	UMTS, CDMA-2000, WiMAX
4G	IMT-Advanced	OFDM, OFDMA	LTE-A, WiMAX-2

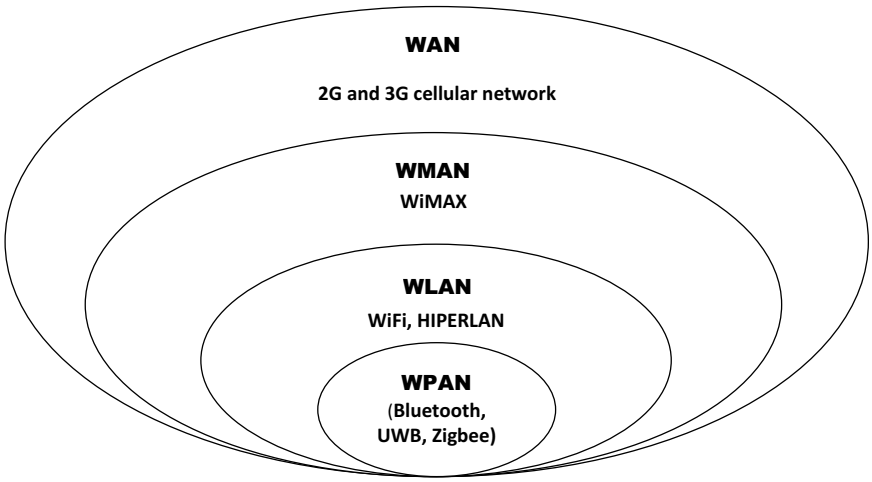

Figure 2.1: Classification of wireless network

The modern wireless network is classified by the network scale (Figure 2.1) as Wireless Personal area Network (WPAN), Wireless Local Area Network (WLAN), Wireless Metropolitan Area Network (WMAN) or Wireless Wide Area Network (WWAN), and is divided into generations by the underlying technology and the capacity of the network (Table 2.1) [5]. The evolution of wireless communication technology is briefly described in the following sections.

2.1.1 Beyond Third Generation (3G) Wireless Systems

The 1G mobile telephone used the narrow band analogue transmission with circuit switching systems based on Frequency Division Multiple Access (FDMA). The FDMA system was developed by AT&T Bell Lab early 1970s. FDMA was first deployed in Nordic Countries by Nordic Mobile Telephony (NMT) in 1981 and then Advanced Mobile Phone System (AMPS) in the US in 1983 [11]. It was only able to communicate voice calls and a small amount of data.

The 2G systems used a narrow-band digital transmission and packet switching system. 2G provides the most advanced roaming services with the highest spectrum

efficiency. The major four standards of 2G are digital cellular, Personal Communication Systems (PCS), WLAN and mobile data [3].

Global System for Mobile Communications (GSM) is the most successful 2G digital cellular system worldwide. The other three 2G digital cellular systems are North American Interim standard (IS-54 or IS-136), IS-95, and Japanese Digital cellular (JDC). The cordless telephone is the only surviving PCS standard still active using the unlicensed Industrial, Scientific and Medical (ISM) band[3] [2]. The 2G WLAN is widely used to access wired LANs and the internet. It is an IEEE 802.11 technology known as Wireless Fidelity (WiFi). Using the unlicensed frequency band, WiFi can provide throughput up to 54 Mbps. HIPERLAN is the European version of WLAN. The IEEE 802.11p version of WLAN is developed for Wireless Access in Vehicular Environment (WAVE). WAVE uses the licensed band of 5.9 GHz which is known as the ITS band.

Some important 2G mobile data services were Advanced Radio Data Information Services (ARDIS), Mobitex, Cellular Digital Packet Data (CDPD), Terrestrial European Trunked Radio (TETRA) and General Packet Radio Service (GPRS). ARDIS and Mobitex use their own independent infrastructure. In the 1990s, CDPD was deployed in the US and shared the spectrum and infrastructure of AMPS, and GPRS was integrated with GSM systems. This assimilation of the data network to into the cellular telephone network led to the next generation cellular systems [3].

2.1.2 IMT-2000 : The Third Generation (3G) Wireless Systems

The ITU published IMT-2000 for wireless communication systems, which is a global standard for 3G. This standard opened a number of new opportunities for innovative applications and services. Until the advent of IMT-2000, the cellular system was being developed following different technology standards, which created a fragmented market. The aim of the 3G standard was to develop an international standard which is a combination of 2G cellular, PCS and mobile data services. It was anticipated that 3G would provide higher transmission rates of up to 2 Mbps for stationary, 384 Kbps for pedestrian speeds and 144 kbps for vehicular speeds [11]. Besides high transmission rates, the 3G systems also envisioned better QoS for voice telephony,

interactive game, web browsing, e-mail, and multimedia streaming with seamless global roaming. In 2001, the first 3G system was deployed in Japan. The key characteristics of 3G are flexibility, affordability, compatibility with existing systems, and modular design. 3G supports six radio interface technologies such as IMT-DS (Direct Spread), IMT-MC (Multi-Carrier), IMT-TC (Time-Code), IMT-SC (Single Carrier), IMT-FT (Frequency Time), and IP-OFDMA. Three widely used commercial 3G standards are CDMA-2000, UMTS, and WiMAX. The CDMA-2000 and UMTS standards are briefly described in the following section.

2.1.2.1 CDMA-2000

The 3G evolution of the IS-95 standard is called CDMA-2000. CDMA-2000 uses the Code Division Multiple Access (CDMA) technology; which is an access method as well as air interface technology [3]. The CDMA2000-1X was the first evolution of IS-95 for the 3G standard and CDMA2000-1XEVDO (EVolution Data Only) had evolved by 2002. It was committed to supporting 2 Mbps minimum data rates. The enhanced version EVDO Rev-A offers peak user data rate up to 3.07 Mbps for downlink (DL), and 1.8 Mbps for uplink (UL) [11].

2.1.2.2 Universal Mobile Telephone System

The Universal Mobile Telephone System (UMTS) is based on a GSM evolution. Following IMT-2000, the Third Generation Partnership Project (3GPP) was founded to develop the UMTS standard on GSM heritage in 1998 and published the first 3G UMTS in 1999. The HSPA technologies such as High Speed Downlink Packet Access (HSDPA) and High Speed Uplink Packet Access (HSUPA), were introduced in UMTS-WCDMA release 5 and release 6 respectively. Theoretically the peak throughputs of UMTS are 14.4 Mbps for UL and 5.8 Mbps for DL [11].

2.1.3 IMT-Advanced :The Fourth Generation (4G) Wireless Systems

The research community continued their efforts to improve the 3G wireless mobile networks to provide broadband data communication in high vehicular speeds. The ITU-R proposed IMT-Advanced technical requirements, which is known as the 4G

standard. The aims of 4G are to provide a high degree of commonality of functionality worldwide, while retaining flexibility to support a wide range of services and applications in a cost efficient manner. The fundamental differences between 3G and 4G are; in 4G the functionality of the Radio Network Controller (RNC) and Base Station Controller (BSC) are distributed to Base Transceiver Stations (BTS), servers, and gateways [5]. By integrating all access technologies, services, and applications; the 4G system will run without restriction through the wired backbone by using IP addresses. The 4G standard provides a global platform on which to build the next generation of mobile services, fast data access, unified messaging, and broadband multimedia; which is a perfect real world wireless or World Wide Wireless Web (WWWW). 4G is compatible with GSM-GPRS, 3G cellular, WiFi, Blutooth and fixed network or digital broad-casting. 4G will provide the freedom and flexibility for the user to select any desired service that requires high QoS with an affordable price any time, anywhere in the world.

The IMT-Advanced systems requirement, specified the peak data rates for any 4G standard to be up to 1 Gbps at low mobility and 100 Mbps for high mobility [11][4]. The envisioned spectral efficiencies of 4G are up to 15 bps/Hz in an antenna configuration of 4x4 for DL or less, and up to 6.75 bps/Hz in an antenna configuration of 2x4 or less for UL. The average user spectral efficiency for DL with inter-site distance of 500 metres, and for pedestrian speeds must be 2.2bps/Hz/cell with MIMO 4x2. The average cell UL spectral efficiency will be 1.4 bps/Hz/cell with MIMO 2x4. In the same scenario with 10 users, cell edge user spectral efficiency will be 0.075 bps in DL and 0.03 bps in UL with MIMO 2x4. 4G supports scalable bandwidth and spectrum agreements with bandwidths, which is more than 40 Mhz in DL and UL, and mobility support up to 350 km/h [4].

The WiMAX release 2 has been approved as a 4G technology by ITU-R and the LTE-Advanced specification has been submitted to the ITU for 4G approval. The evolution and technology of LTE-A and WiMAX system are described in the following sections.

2.1.4 Long Term Evolution-Advanced (LTE-A)

The Long Term Evolution-Advanced (LTE-A) is a 3GPP standard wireless communication of ETSI and an advanced version of Long Term Evolution (LTE). The name

LTE came from the LTE project of the Radio Access Network (RAN) group, and the 3GPP standard release 8 specified as LTE. It was basically an upgrade version of UMTS and is a fully Transmission Control Protocol/Internet Protocol (TCP/IP) based technology. The RAN group initiated the LTE project and the System Aspects group initiated the System Architecture Evolution (SAE) project. The LTE group developed Evolved UMTS Terrestrial Radio Access Network (E-UTRAN) as an evolution of UMTS RAN and the SAE group developed all IP based Evolved Packet Core (EPC) architectures. The core network of LTE is the combination of the E-UTRAN and EPC architectures; which is formally called the SAE. It is designed to increase the capacity of throughput in high speed mobile telephone networks. Instead of W-CDMA, LTE introduce OFDMA for air interface and supports multi antenna configurations. It also included the flexible transmission bandwidth system and advance antenna technology. The theoretical peak spectral efficiency of LTE is 5b/Hz/s for DL and 2.5b/Hz/S for UL. The envisioned DL peak rate is at least 100 Mbps for UL in a moving environment, when operating at 20 MHz channel, and the target one way latency in LTE is 5ms. It was expected that LTE will provide maximum performance at the lower terminal speeds of 0 to 15 km/hr, with a minor degradation at speeds up to 120 km/hr, and will sustain the connection up to 350 km/hr [12]. The anticipated cell size was 5 km for optimum performance and 30 km for reasonable performance. The world's first publicly available LTE-service was implemented by Telia Sonera in Stockholm and Oslo on December 2009.

LTE-Advanced is release 10 of the 3GPP standard and is capable of inter-working with LTE and 3GPP legacy systems. LTE-A uses the OFDMA for DL and single carrier OFDMA (SC-OFDMA) for UL [11]. The main aims of LTE-A are increasing data rate up to 1 Gbps at DL and 500 Mbps for UL. The targeted peak spectrum efficiency is 30 bps/Hz for DL in an antenna configuration of 8x8, and is 15 bps/Hz for UL in an antenna configuration of 4x4. The targeted average user throughput is three times and cell edge throughput is twice that of LTE. It is anticipated that the LTE-A will support mobility up to 500km/h depending on the frequency band. It is able to support scalable bandwidth up to 100 MHz and spectrum aggregation where the non-contiguous spectrum needs to be used.

The main competitor of LTE is WiAMX and the success of LTE-A depends on mobile WiMAX [6]. Some vendors say that LTE-A and mobile WiMAX have

two market segments. LTE-A is suitable for those operators who are already in the market and mobile WiMAX is an economic choice for green field operators. It is also suggested that both technologies can co-exist in a system that will allow cooperation, and allow each system to be enhancement together [13]. This research which focused on mobile WiMAX, is described in the following section.

2.2 Worldwide Interoperability for Microwave Access

Following IMT-2000, the IEEE 802.16 working group was dedicated for the Broadband Wireless Access (BWA) to develop an WMAN standard for high data transmission [14]. WiMAX is the product certification forum of the IEEE 802.16 standard, and the product of the IEEE 802.16 standard is known as WiMAX. The 802 family of standards are maintained by the IEEE 802 LAN/MAN Standards Committee (LMSC). The name 802 come from the first meeting of LMSC held in February, 1980 (80/2). Since 1980, a total of 23 standards have been developed under the LMSC. The first standard was IEEE 802.1 which was published in 1980. IEEE 802.16 is one of the revolutionary standards of this family.

The objective of the WiMAX standard was to fill the gaps between the WLAN and 3G cellular systems. To fill the gaps, some important features were considered such as: flexible architecture, high security, quick deployment, mobility, high throughput, wider coverage, and cost effectiveness. Some others important features were: multilevel service, portability, interoperability, and QoS.

This is a complementary wireless technology to the existing 3G, WLAN and wired broadband. The WLAN standard provides higher throughput for the broadband wireless access to the internet, within a cell radius of 100 meter. On the other hand, the other 3G cellular network provides a low data rate over a large cell. The WiMAX not only provides higher throughput, but also provides a wide coverage area. It is a disruptive technology which is threatening existing technologies, and it has been described as a technology that offers considerable benefits in the broadband markets for business, consumers, and backhaul for WiFi hot spots. It is a quadruple play (voice, data, video, mobility); cost effective and quicker way of providing broadband service for developing countries. The advantage of WiMAX communication is that

there is no need for any external plant construction to deploy the system. In most cases, the deployment of WiMAX communication takes some hours, and when the antenna and equipment are installed and powered, it is ready to use. It saves a lot of the time and money which is required to build up copper or fibre optic infrastructure [7]. It provides high throughput over a long distance in a Point to Multi-point (PMP) LOS or NLOS network [Koon].

The WiMAX system brings total freedom to the user who is highly mobile, and allows them to stay connected with voice, data, and video services for both public and private networks. For private networks, the WiMAX system is used in cellular backhaul, banking networks, education networks, offshore communication, campus connectivity, and temporary construction communications or theme parks. For public networks it is used in wireless service provider access networks and rural connectivity [15]. The other potential areas of WiMAX communication are: telemetering for electricity, gas or water; public safety; emergency and video surveillance [13]. The WiMAX system operates at 2.3 GHz in the Asia Pacific region, 2.5 GHz in the Americas and 5.5 GHz in European Union countries. The WiMAX forum is also considering a 700 MHz version of mobile WiMAX. Some companies are also manufacturing WiMAX accessories for 1.8 GHz frequency.

The first version of the WiMAX system profile was based on DL and UL [12] and published in 2001 by IEEE for LOS communication. The recommended frequency bands were from 10 to 66 GHz. The first version supported Quadrature Amplitude Modulation (QAM) modulation and Time Division Duplex (TDD). The target was providing fixed broadband wireless access via Customer Premises Equipment (CPE). The revised version 802.16a was published in 2003 to support NLOS, and the recommended frequency bands were from 2 to 11GHz. Three physical interfaces were defined for this version, Wireless MAN-OFDM which is commonly known as OFDM, Wireless MAN-OFDMA which is commonly known as OFDMA, and Wireless MAN-Single Carrier which is known as SCa. The 802.16d is the revised version of above two versions and was published in 2004. This version added 256 and 2048 points FFT OFDM physical (PHY) modes. The goal of this version was to use OFDM for both UL and DL. These PHY capabilities envisioned several feature such as frequency diverse and frequency specific sub-channelization, Adaptive Modulation and Coding (AMC), Hybrid Automatic Repeat Request (HARQ), and fast

scheduling based flexible Channel Quality (CQI) [16]. This version added Forward Error Correction (FEC) schemes including Convolution Turbo code (CTC) and Low Density Parity-Check (LDPC) code; multi antenna operation including Advanced Antenna Subsystems (AAS); open loop Space Time Coding (STC) to support two to four transmitting antennas; closed loop MIMO; and UL coordinated Space Time Division Multiple Access (STDMA). The others advanced features of this version are spatial multiplexing and smart antenna beam forming. These are the most powerful techniques in this version, which significantly improved the spectral efficiency and system capacity. This version also supports multicast-broadcast transmission using Signal Frequency Network (SFN), and variable frame size of 2 ms, 2.5 ms and 5 ms. This development enabled the high performance receiving capacity of WiMAX communication in a frequency selective fading channel [17].

Mobility enhancement was added in version 802.16e during 2005; supportting nomadic, portable, and mobile wireless access, with seamless network coverage. The standard was published in the beginning of 2006. The FFT size of 128, 512 and 1024 were added in this version to support scalable bandwidths of 1.25 MHz, 2.5 MHz, 10 MHz and 20 MHz. Other important additions of this version are inter-cell hand off, direct-adjacent cell management, and sleep mode. This version also supports frequency diverse and frequency selective scheduling. The IEEE802.16e standard offers mobility up to 120 km/h and throughput up to 75 Mbps for UL and DL. Theoretically the reasonable cell size of the WiMAX system is 10 km, and the acceptable cell is of 50 km and 112.6 km cell size in ideal conditions. But the practical transmission is 16 km in a rural area and 1.6 km in an urban area. It can support throughput up 10 Mbps at around 10 km for LOS communication [18]. In 2007, IEEE 802.16e was approved as a 3G standard. In comparison, WiMAX 802.16e serves four time better than any others 3G standards [14].

In early 2007, the WiMAX Forum and the IEEE 802.16 working group started the IEEE 802.16m project to enhance coverage, spectral efficiency, throughput, VoIP, latency, and power conservation of WiMAX systems. The focus of this version was to add Frequency Division Duplex (FDD) in WiMAX communication and to enable MIMO and Beam Forming (BF) under FDD. IEEE 802.16m is backward compatible with 802.16e and provides more than twice the spectral efficiency for both UL and DL. It was envisioned that this version would provide full mobility support up to

350 km/h or even 500 km/h, and up to 1 Gbps data at fixed speed at low mobility. IEEE 802.16m is designed to support all licensed IMT bands below 6 GHz frequency using TDD and FDD as well as Half-Duplex FDD (H-FDD). This version provides an improved link budget (at least 3 dB) over Release 1 within same antenna configuration. The other enhancements of this version are Multiuser MIMO (MU-MIMO), improved open-loop and closed-loop power control, and advanced interference mitigation techniques including fractional frequency reuse. The aims were the use of pilot tones more efficiently with new sub-channelization schemes, and to use 1/8 cyclic prefix, in order to reduce layer 1 overhead for both DL and UL.

The key goals of 802.16m are minimizing all aspects of system latency including: link layer up to $<$ 10 ms for DL or UL; hand-off interruption $<$ 30 ms; control plane idle to active time $<$ 100 ms; to guarantee the QoS for all services as per the IMT Advanced standard. These are the significant improvement over 802.16e-2005 latency. This minimization enhanced the QoS for latency-sensitive real-time applications such as: Voice Over Internet Protocol (VoIP); on-line business and financial transactions; real-time gaming; and navigation. IEEE 802.16m also supports channel aggregation of contiguous or non-contiguous channels to provide an effective bandwidth of up to 100 MHz. It is able to support 1600 bidirectional VoIP sessions per sector, or 4800 sessions per 3-sector cell with FDD in a 2x20 MHz channel pair.

IEEE 802.16m is able to provide flexibility to meet individual QoS parameters established in the individual multimedia classes of IMT-Advanced. These classes are defined as low multimedia (Data speed up to 144 kbps), medium multimedia (data speed up 2 Mbps), high multimedia (Data speed up to 30 mbps) and super high multimedia (data speed up to 100 Mbps or possibly 1 Gbps). The ITU approved IEEE 802.16m the WiMAX release 2, as IMT-Advanced technology on 20 October 2010; which is the first technology that came in this track [19]. The combination of OFDMA, advanced antenna techniques, link adaption, and fine granularity QoS classified WiMAX communication as a 4G system [12].

IEEE 802.16m ensures backwards compatibility on the 802.16e-2009 standard, and concurrent operation of IEEE 802.16m and non-802.16m technologies on the same mobile station. Specifically, to ensure seamless connectivity to alternative wireless networks, 802.16m provides a shorter hand off interruption time with other radio access technologies including WiFi, UMTS, LTE, and LTE Advanced, and

CDMA-1X-EVDO.

Jupiter research identified the top applications of WiMAX communication as being Voice/VOIP, gaming, music, TV, and video including social networking. It has been suggested that the WiMAX system is the first technology to have the potential to address broadband connectivity in the developing world for its low installation cost. Motorola conducted a survey in 2007 on WiMAX systems in the US and results showed that the consumers were using WiMAX systems for email on the go, web surfing, mobile TV, and music. The deployed WiMAX communication is greater than any kind of conventional 3G technology and 50% more than the HSPA network. Roughly 70% of WiMAX system deployments are in emerging markets [6]. The WiMAX forum projected more than 93 million mobile WiMAX users globally by 2012 [7]. As described in the following section, OFDM and OFDMA are the key features of the WiMAX system for providing higher throughput and to support high mobility.

2.2.1 MAC layer of WiMAX Systems

The protocol and services of IEEE 802 the Media Access Control (MAC) layer is specified in the data link and physical layer of the Open Systems Interconnection (OSI) model. In the OSI model the data begins to pass from the application layer, the top layer of the model and proceeds to the bottom layer, the physical layer at transmitting station.

The physical layer creates a physical connection between the communicating devices' Tx and Rx. At the receiving station the data is received through the physical layer and passes through the opposite direction towards the application layer. IEEE 802 splits the data link layer, the sixth of OSI model into the Logical Link Control (LLC) and Media Access Control (MAC) layers (Figure 2.4). The MAC layer is responsible for the maintenance of the connection between the Tx and Rx

WiMAX is structured to support many physical layers and different types of system architecture including Point to Point (P2P), Point to Multipoint (P2M), and ubiquitous coverage by scheduling a time slot for each Subscriber Station (SS). If there is only one SS in the network the, Base Station (BS) communicates on a P2P basis. A BS in a P2P configuration use a narrow beam antenna to cover

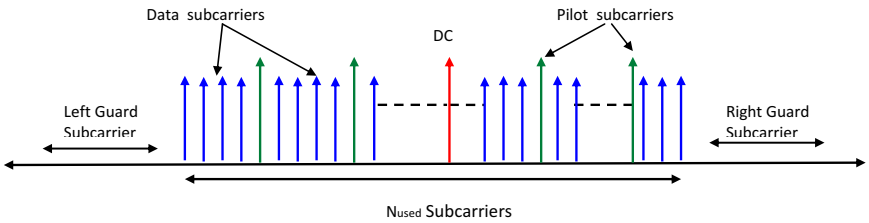

Figure 2.2: The WiMAX OFDM Subcarriers

longer distances. The MAC layer consists of three sublayers, namely theConvergence Sublayer (CS), the Common Part Sublayer (CPS), and Security sublayer [20]

2.2.2 Orthogonal Frequency Division Multiplexing

Orthogonal Frequency Division Multiplexing is a widely used technique for overcoming multipath fading. OFDM is based on Frequency Division Multiplexing (FDM). In FDM all users transmit signals simultaneously and separate themselves by using a guard band. Different frequency bands are used for UL and DL transmission, and a pair of fixed sub-channels are used for communication sessions. Considering the limitation of the frequency bands, the disadvantage of FDM is that it uses extra frequencies for the guard band. In OFDM, all the sub-carriers are orthogonal to each other, and the guard band is no longer required; all sub-carriers being modulated by using QAM or Phase-Shift Keying (PSK).

In December 1966, Robert W. Chang outlined the theory of OFDM for transmitting simultaneous data streams through linear band limited channels, without ISI and ICI. The basic idea of OFDM is that it divides the frequency selective channel into a number of frequency flat sub-channels, and combines the three transmission principles: 1) multi-symbol modulation, 2) multi-carrier modulation, and 3) multi-rate transmission. In OFDM a large number of orthogonal sub-carriers are used for data transmission. OFDM has the ability to cope with a severe fading channel and provides a high data rate when compared to the signal carrier. It is an effective technique for combating delay spread in the frequency selective fading channel.

The basic technique of OFDM is the Inverse First Fourier Transformation (IFFT). The OFDM symbols are generated using IFFT at the Tx and are decoded at the Rx by using the First Fourier Transformation (FFT). The minimum FFT point for OFDM is 64, other FFT points are determined by the multiplication of 64 by an odd number. The dedicated FFT points for WiMAX systems are 128, 256, 512,

1024 and 2048. In OFDM sub-carriers, N is spaced by Fs/N Hz, and modulates at a rate of Rs/N symbols/sec; where N is the number of sub-carriers, and Fs is the sampling frequency. The multi-path effect reduces relative to the symbol interval by the ratio of 1/N. The error control coding can be implemented in OFDM across the symbols and is known as Coded OFDM (COFDM). In the time domain after the IFFT operation, a Cyclic Prefix (CP) is added to the beginning of the OFDM symbols, and the occupied time of CP is called the guard time. In the frequency domain, sub-carriers are divided into four types: 1) the data sub-carrier, 2) the pilot sub-carrier, 3) the null sub-carrier, and 4) the Direct Current (DC) sub-carrier. Data sub-carriers are dedicated for data transmission, pilot sub-carriers are dedicated for channel estimation and synchronization, and the DC sub-carrier is the center frequency of the band used as a guard band to protect the channel from ICI.

The OFDM transmission mode was originally designed for single signal transmission. In order to conduct multiple transmissions, multiple access schemes such as TDMA and FDMA are associated with OFDM, and the developed scheme is known as OFDMA.

2.2.3 Orthogonal Frequency Division Multiple Access

Orthogonal Frequency Division Multiple Access provides multiuser access to OFDM single channel transmission. In OFDMA, sub-carriers are divided into subsets of sub-carriers, and each subset represents a sub-channel. The sub-carriers of one sub-channel may be adjacent to each other or not as the case may be (Figure 2.3). In the DL, a sub-channel is intended for different receivers or groups of receivers. In the UL a transmitter is assigned to one or more sub-channels. For UL and DL, users have a specific time slot, and a sub-channel allocation for each communication.

Mobile WiMAX supports Scalable OFDAM (S-OFDMA). Scalability refers to the ability to change the FFT size and the number of sub-carriers. The S-OFDMA supports FFT sizes of 128, 512, 1024, 2048 and the bandwidths from 1.25 to 20MHz. The 256 FFT is not included in the OFDMA layer, but 512 and 1024 FFT are mandatory for mobile WiMAX communication. Mobile WiMAX achieves this scalability by changing the FFT size, while keeping the sub-carrier spacing fixed. OFDMA provides the tolerance of multipath, frequency selectivity, scalable channel bandwidth, and high compatibility with advanced antenna technology.

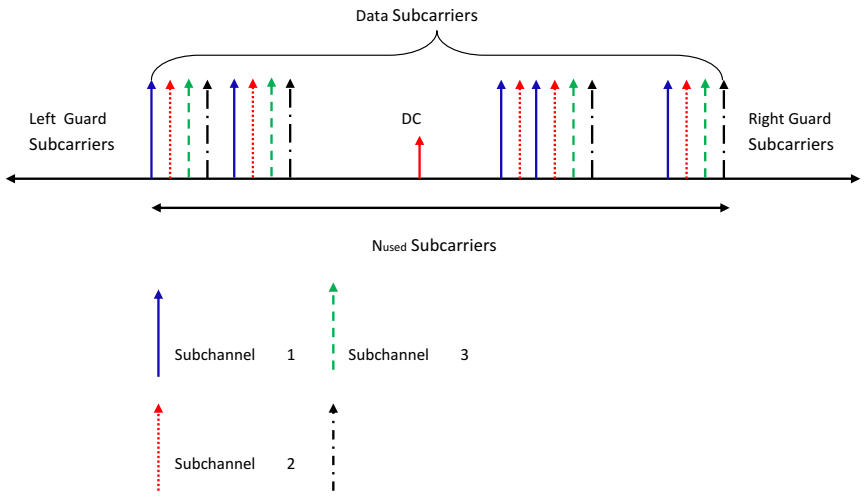

Figure 2.3: OFDMA Principle

Table 2.2: Antenna configuration supported by mobile WiMAX

Parameter	Antenna Configuration	Performance
Peak DL spectral efficiency	(2x2) MIMO	8.5 bps/Hz
	(4x4) MIMO	17.0 bps/Hz
Average DL spectralficiency	(4x2) MIMO	3.2bps/Hz
		0.32bps/Hz/user
DL Cell edge user throughput	(4x2)MIMO	.09bps/Hz
Peak UL spectral efficiency	(1X2) SIMO	4.6 bps/Hz
	(2X4) MIMO	9.3 bps/Hz
Average UL spectral efficiency	(2X4) MIMO	2.6 bps/Hz
		0.26 bps/Hz/user
UL Cell-Edge user throughput	(2X4) MIMO	0.11 bps/Hz/user

Mobile WiMAX OFDMA PHY support diversity and contiguous permutation. In diversity permutation, subcarriers are distributed pseudo-randomly. The main advantages of diversity permutation are the frequency diversity and inter-cell interference averaging. IEEE 802.16m supports the diversity permutation modes of: 1) Full Use of Sub-carrier (FUSC), 2) PUSC, 3) Optional PUSC, 4) Optional FUSC, and 5) Tile Uses of Subchannels (TUSC).

The contiguous permutation is a group of adjacent subcarriers. This family includes the AMC. This permutation leaves the door open to choose the best condition of channel for the highest capacity of bandwidth. The mandatory permutation of mobile WiMAX systems are PUSC, FUSC, AMC for DL and PUSC, and AMC for UL [21]. In this research we considered the AMC and PUSC permutation mode.

OFDM, OFDMA, and modulation are the major building blocks of WiMAX

PHY. There are some other important elements used in WiMAX PHY such as; randomization, FEC, repetition, and interleaving. Figure 2.4 shows the OFDMA PHY transmission chain. OFDMA PHY supports Concatenated Reed-Solomon Convolutional Code (RS-CC), Convolutional Turbo Codes (CTC), and Block Turbo Codes (BTC) for FEC.

The EFC schemes for OFDMA PHY are tail-biting Convolutional Code, Convolutional Turbo Codes (CTC), BTC, and Low Density Parity Code (LDPC). The CTC is the mandatory FEC code for mobile WiMAX communcation[21].

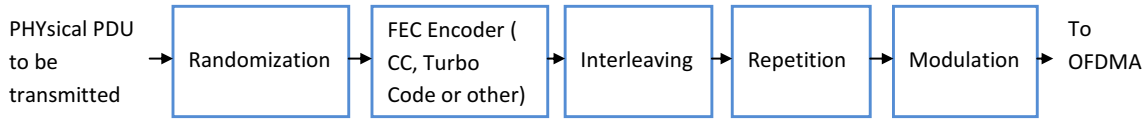

Figure 2.4: OFDMA PHY transmission chain

2.3 Deployment of Wireless Systems in Vehicular Communications

Transportation systems play an important role in modern life. In 1986, the Texas Transportation Institute did a study in the US, and found that the peoples are losing $24 billion dollars every year due to traffic congestion [22]. To alleviate this condition, the concept of the Intelligent Vehicle Highway System (IVHS) was introduced in the US and Europe. Presently the IVHS is known as Intelligent Transportation Systems (ITS), and collectively approaches the problem of enhancing mobility and traffic handling capacity, improving the condition of travel, and reducing the adverse environmental effects in surface transportation systems. The modern research on ITS emphasized cooperative ITS systems connected through wireless communication [23]. Wireless communication is also used in modern railway operations called Communication Based Train Control (CTBC) [24]. In ITS applications, data communication takes place between the Vehicle to Vehicle (V2V), and Vehicle to Infrastructure (V2I), using wireless communication systems. The IEEE Intelligent Transportation Systems Society (ITSS) is actively working to develop and deploy modern technologies for ITS. The deployment and research on ITS using wireless communication is described in the following section.

2.3.1 ITS Deployment

Rapid progress in the development of communications, control technologies, and computers, is helping to produce possible solutions for ITS problems. The current generation of vehicles are already equipped with different kinds of sensors, Central Processing Units (CPUs), software, GPS, and ad hoc and sensor networks. It is anticipated that within the next few years, active in and out vehicle environment sensing will become standard, and will enable intelligence for all drivers and passengers [25]. Different types of ITS applications are being using worldwide under one of five major components [26] that are described briefly in the following section.

2.3.1.1 Advanced Traffic Management Systems

The Advanced Traffic Management Systems (ATMS) is known as the backbone of ITS and is playing an important role in roadway management. The system collects and uses real time traffic data from transit networks, expressways, or from major roads, and sends feedback signals to the transportation system to control the flow of traffic [27]. The major three part of ATMS are: i) Surveillance systems, ii) Real time traffic adaptive control systems, and iii) Operator support systems. The first part monitors the operation status of roadway networks and the second part receives data from the surveillance systems and adapts the network control, and finally the third part facilitates the real time control and network management. The Santa Monica Freeway Smart corridor demonstration project [28], California, USA, COMPASS [29] in Ontario, Canada, and Auckland ATMS in New Zealand [30] are examples of ATMS.

2.3.1.2 Advanced Traveler Information Systems

The Advanced Traveler Information Systems (ATIS) is an intelligent transportation system application which is a combination of computer, communication, and information technology. The system provides a wide variety of information such as: electronic maps; route selection and guidance; information service such as gas station, restaurants, hospital; and real time traffic information through communication between drivers and ATMS [22]. This information helps travelers to reach their destination safely and competently. One of the best examples of GIS based ATIS is implemented in Hyderabad city, India [31]. Some Other examples of ATIS include:

the Road-Management System for Europe (ROMANSE) at Southampton; and the Paris London Corridor Evaluation of Integrated ATT and Drive Experimental Systems (PLEIADES) project at the London-Paris corridor [32]; and the Partners for Advanced Transit and Highway (PATH) program in Southern California in USA [33].

2.3.1.3 Commercial Vehicle Operation

The Commercial Vehicle Operation (CVO) system add features to ATIS which are critical to commercial and emergency vehicles [22]. The CVO is used for dynamic fleet management in government and commercial vehicles. Data communication takes place between moving vehicles and the central control office via two way communications and the tracking system. The Urban Mass Transportation Administration (UTMA), USA, deployed an advanced vehicle monitoring system and CVO system in 1974 [34]. QUALCOMM's OmniTRACs information management system is an another good example of CVO [35]. OmniTRACs provides messaging and positioning services for the user using satellite communications.

2.3.1.4 Advanced Vehicle Control System

Advanced Vehicle Control Systems (AVCS) technologies such as adaptive cruise control, night vision sensor, Radio Detection And Ranging (RADAR), and automating braking to assist the driver in safer travel are already applied to ITS. AVCS interact with ATMS for providing automatic vehicle operation [22]. The ultimate goal of AVCS is to develop an automated highway technology where the driver is no longer required and a car can travel from one place to another without human interaction.

Google's driverless cars is an example of AVCS. The system collects information information from Google's street view map. The artificial intelligence software combines that information with the imputed data through the video cameras inside the car, from the Light Detection And Ranging (LIDAR) sensor on top of the vehicle, RADAR sensors on the front of the vehicle, and from a position sensor attached to one of the rear wheels that helps locate the car's position on the map. In 2010, Google has tested several vehicles equipped with the system, driving 1,609 km without any human intervention. The system provides an override that allows a human driver to take control of the car by stepping on the brake or turning the wheel,

similar to cruise control systems already in cars. The Nevada legislature passed a law in June 2011 to authorize the use of driverless vehicles.

2.3.1.5 Advanced Public Transportation Systems

The Advanced Public Transportation Systems (APTS) provides for advanced navigation and communication technologies to all aspect of public transportation systems. Video surveillance is added to APTS systems for the safety of passengers and is now becoming an important system in security service. In APTS, Closed Circuit Television (CCTV) cameras are used for video surveillance to detect red light crossing, illegal lane change, speeding detection, cordon zone monitoring, or any kind of misleading incident purpose. Enhanced CCTV systems can automatically detect misleading behavior and raise the alarm. After the Madrid rail net bombing in 2003, intelligent vision systems based on enhanced CCTV surveillance started in the London underground, and their plan was to deploy 12,000 CCTV cameras by 2011 [36]. The Public Transport Authority (PTA) of Western Australia have already installed CCTV cameras at train stations and bus ports, as well as inside trains and buses.

2.4 Application and Research of Wireless Systems in Vehicular Communications

Due to mobility requirements, a wireless communication link is needed for ITS, and V2I communication is a key interconnection link for ITS. Different types of wireless communication systems are used in ITS applications. Some widely used wireless communication systems used in ITS are briefly described in the following section.

2.4.1 Infra Red

From early 1990s in Europe, US and Japan, Infra Red (IR) has been used in ITS for carrier information. The effective range of IR is about 60 to 80 metres, and it supports up to 500 Kbps data speeds in urban areas, and it is able to support speeds up to 100 km/h [37] [38]. Since early 1980, Siemens has opted for an IR base communication known as EURO-SCOUT, for dynamic route guidance, and driver information systems in Berlin, Germany . IR is used in the Universal Traffic

Management Systems (UMTS), and the Vehicle Information and Communication System (VICS) in Japan [39] [40].

2.4.2 Mobile Satellite Service

The Mobile Satellite Service (MSS) provides a wide area coverage for short interactive vehicle trips to the dispatcher and traffic management center. It operates on ku bands (12-14GHz), on a secondary basis. The ku band is primarily allocated for fixed satellite service. The system provides two way messaging and GPS service between the user and the control station. QUALCOMM OmniTRACKs is a successful project which implemented the MSS [26]. LOw COst satellite based train location system for signaling and train PROtection for Low-density traffic railway lines (LOCOPROL), and LOw COst LOCalization (LOCOLOC) projects, are employing satellite technologies based on the Global Navigation Satellite System (GNSS), to develop for railways a fail-safe and low-cost positioning system on low-density traffic lines.

2.4.3 Global System for Mobile Communications

The GSM is a widely used mobile communication system used in CTBC. The CTBC system relays; safety control, speed, and other functions, by using two-way, continuous, GSM communication [41]. The control and telemetry data inter-exchange between the train and way side equipment use inductive loop or frequency transmission. The European Rail Network management system (ERTMS) has chosen GSM-rail for voice and data communication for the moving train [42].

2.4.4 WLAN and DSRC

A study on mobile applications using WLAN has been done by G. OHTA *et al.*, in a working group of the Yokosuka Research Park (YRP) Research & Development promotion councils [Ohta]. The researcher developed a wireless infrastructure over a 4 years period (2001-2004), setting up an internet mobile newspaper service for a running train, and patient monitoring system in an ambulance. Researchers built up a wired network from a newspaper office to the research park. A bus was used as a substitute for the train and tried to connect as far as possible. The newspa-

per contents were transported to the research park with a gigabyte Ethernet from Tokyo, then transmitted to the bus by 25 GHz WLAN, and researchers received the transmission by a 5 GHz WLAN terminal in the bus. Later on researchers tested the whole system with the Japan railway express train "Shikoku Ishizuchi", at a speed of 152km/h. The train accelerated up 120 km/h in two seconds, and the carrier restoring period was 2ms. Research found the doppler shift to be 0.0185Hz/2ms. The OFDM subcarrier frequency was 312.5 KHz, and the 0.0013 degree phase shift was caused by doppler's effect. Researchers used 10 dBi horn antennas to reduce the fading effect. Two base stations were installed and connected with optical fibre, which were used to communicate with the WALN unit in the train. Cellular, 2.4, 5.03, 25, and 60 GHz WLAN wireless technologies were provided in the train, and managed by mobile IP technology. The distance between the two base stations was 1 km, and the handover was being controlled by mobile stations on the train. The study achieved a data rate of >2 Mbps, at a distance of 800 metres from base station, at a speed of 152Km/h. Research found a better Packet Error Rate (PER) was achievable in a fully seated train, over that which had no passengers.

For the UL transmission, the researcher transmitted the National Television Systems Committee (NTSC) video output of an ultrasonic diagnostic system from an ambulance. Two built-in two video cameras of 2.5 Mbps, and an electrocardiograph from the ambulance, transmitted a several hundred Kbps data stream. The research was done on adaptive modulation function with BPSK, QPSK, 16 QAM, and 64 QAM modulation. Results showed that the information was transported to the hospital with a 0.03 second delay, and that a doctor can observe the condition of the patient and instruct the rescue team.

The Dedicated Short Range Communication (DSRC) channel is specifically designed for one or two-way, short to medium range wireless communication for automotive use. It is suitable for public safety and private operations in V2V and V2I systems, where the distance between the two nodes is less than 50 meters. In the USA and Europe, the 5.9 GHz band is used for DSRC. Japan and Korea use the 5.8 GHz band [43]. The DSRC uses the IEEE 802.11p protocol and provides very high throughput. This technology is mainly used in Europe and Japan for electronic toll collection. In the USA, a nationwide roadway based communications network is using DSRC, where all the vehicles will be equipped with DSRC equipment with

Figure 2.5: DSRC used for toll collection

5.9 GHz frequency. This vehicular network is providing a wide range of safety and mobility applications, such as: intersection collision avoidance, traffic management, traveler information, and weather sensing [42].

2.4.5 WiMAX System for ITS Applications

The Utah Transit Authority (UTA) in the USA provides internet access by WiFi facilities installed in their double-decker commuter trains, which run from Ogden city to Salt Lake City. They set up WiMAX system base stations to provide wayside connections between the train and the internet world, which can support speeds up to 128 km/h. The base stations were set up on poles at every 0.83 to 4.15 km, and two units were installed in each car. Every base station operates in Point to Multipoint (PMP) mode. A variety of antennae were used, and were mostly 102 ft flat panels and omnis track side, with special antennas on board the trains. Each of the track side BSs connected to the Utah transit office using a fibre optic connection. Broadband internet access facilities were given to the passenger using WiFi. The train travelled a 66 km corridor, providing seamless connectivity to the passenger [44].

Dubai Metro launched a mobile WiMAX network in 2009, at the Dubai Metro railway, to provide internet access for their passengers. The network offers its customers wireless internet access, while traveling on the metro at speeds up to 90km/hr, using: Personal Digital Assistant (PDA), smart phone, or laptop, via Wi-Fi services. The system can achieve average broadband speeds of up to 4Mbps at stations, while backhauling to the network through WiMAX communication. Data speeds reach up to 2Mbps on board the train. Mobiserve began the project in June 2009, and implemented the system over 20 stations within three months. Each train has four access points and can easily connect a large number of passengers

simultaneously.

Taiwan High Speed Rail began a study for implementing WiMAX technologyon the high speed railway system, under the M-Taiwan program in 2007. The aim was to provide broadband facilities to the passengers of Taiwan High Speed Rail (THSR) from early 2012. In that system, passengers will be able to connect to internet and Web via Wi-Fi, or directly if they have a compatible WiMAX device, enabling uninterrupted on board connectivity at speeds of 285 km/h.

For the Public Safety Communication (PSC) system, the narrow band Professional Mobile Radio (PMR) standards such as Terrestrial Trunked Radio (TETRA), TETRAPOL, or P25 were used as a communication media until recently. It is observed that nowadays, the PSC is moving to newer 4G mobile technology. The mobility support at vehicular speeds, and inherent wide coverage capabilities of WiMAX communication, made itself an appropriate technology for PSC and vehicular applications. The PTA Western Australia, is aiming to implement a WiMAX system for video surveillance inside the running train, for the safety of the passengers and properties.

2.4.6 Research on WiMAX Systems for Vehicular Communications

A feasibility study on V2I communication using the WiMAX system has been done by Chien *et al.*, using commercial WiMAX equipment of 3.5 MHz frequency with 7 MHz Bandwidth (BW), where the link speeds was BPSK-1/2 and QPSK-1/2 [45]. The BS was equipped with a 90 degree external antenna and placed beside the road. The transmission power of the BS was 28 dBm. The study found that data transmission is possible up to 1 km, with 1 Mbps throughput using 64-QAM modulation. Research shows that the frame size has a big impact on the performance of WiMAX communication.

Andre *et al.* evaluated the WiMAX communication system for vehicular communication, for both V2I and V2V infrastructure in [46], for a road safety project. The experimental setup was comprised of three WiMAX base stations. To verify the link speeds, a dynamic test was taken when the SS moves at low speeds around the coverage area. The dynamic test shows that it is possible to maintain the link,

but the network entry process did not work properly.

Aguado *et al.* did a simulation study to deploy the mobile WiMAX system for safety applications. The researcher considered two scenarios; the first of which included two mobile nodes that supported real time application and crossed each other. The second one has a high congestion traffic scenario with 40 vehicles. A simulation was run using two Access Service Network (ASN) getways. The backbone was Single Carrier (SC) link of 10 GHz frequency with 25 MHz BW. The access network was of 3.5 Ghz frequency, with 20 MHz BW, with OFDMA PHY. In the first scenario the two vehicle moved at a speed of 160 km/h, crossing each other during the inter ASN handover process. The second scenario is a traffic jam with 40 vehicles, and all the vehicle were connected with the BS. The researcher concluded that their proposed architecture met the requirements to deploy the WiMAX release 1.0 [47].

A techno-economical inspection for high speed internet connection of trains was done by V. Riihimaki *et al.* in Finland [48]; using a WiMAX system, Flash OFDM, and GPRS for the railway track from Helsinki to Tampere. In this study, the researcher considered users (regular traveler, freight companies and train operator in-house customer), service groups (entertainment, infotainment, advertisements, telemetries, billing and security), networking solutions (ground to vehicle communication, on board vehicle communication), and customer terminal (mobile hand set, PDA, laptop and the terminal link of WiFi). The study showed that the Flash OFDM is a pre-stage solution for the train connection, and that WiMAX communication based high speed internet access for passengers is profitable in the most heavily operated railways.

Nikolaos *et al.* proposed a system to provide wireless connection roaming at high speeds over multiple interfaces, that works on WiMAX and WiFi system. The system supports multiple interfaces for rapidly moving devices. It can sustain fast WiFi access point connection switch, and transparently switches between the access points. Connections utilize multiple mediums such as WiFi and WiMAX. The proposed system improved the efficiency of WiMAX communication up to 30%, and the combination of WiMAX and WiFi bandwidth significantly [49].

Kaveh *et al.* proposed a WLAN and WiMAX Double-Technology Routing (WWDTR); for routing the packet in the heterogeneous vehicular network. In WWDTR, the gen-

eral protocol is formed by a combination of WLAN and WiMAX hops [50]. The WWDTR approaches the point based routing over the parts of the route in which the packets are forwarded via WLAN radio. The researcher claims the better results compare to the traditional routing protocol.

Mai *et al.* studied the PER and throughput performance for IEEE 802.16e in [51]as a function of Single to Noise Ratio (SNR) in an urban micro cell; and determined the SNR switching point between each link speeds. This theoretical performance is compared with practical measurement results from mobile tests in an urban cell. Experiments show that 3/4 code rate offers poorer performance than code rate 1/2.

Movement of the subscriber station causes BW variation, handoff error, and transmission error. Channel bandwidth variation causes network congestion when the video transmission rate exceeds the channel BW, and results in packet loss and handoff latency. To solve this problem, Hay-Soo *et al.* proposed a video streaming method on a mobile WiMAX system, which dynamically adjusted the video transmission rate based on the BW. The proposed model firstly analyzed the channel parameters, such as Carrier Interference to Noise Ratio (CINR), and handoff occurrence message. The streaming server adjusts the next transmission according to the estimated channel BW. To avoid the network congestion, the model performs the intra refresh method, that inserts an intra frame right after the handoff [52].

Onsy *et al.* did a performance analysis applying Additive White Gaussian Noise (AWGN) and doppler shift [53]. The Tx was developed according to the IEEE standard and the simulation runs on M-QAM modulation with RS and CC code. The Least Square (LS) and Least Mean Squares (LMS) method was used for channel estimation. Results show that the LS estimator performance degrades at high relative speeds, and LMS provided better performance. The researcher concluded that the interpolation method has a big impact on the mobile channel estimation.

Masrul *et al.* estimated the cluster based DL channel in mobile WiMAX systems, based on LS methods using the DL-PUSC permutation. The simulation was conducted using the Rayleigh fading model. The estimation was taken in terms of the Mean Square Error (MSE) and the BER. The results showed that two OFDM symbols exhibits better performance compared to that of a single OFDM symbol [54].

The performance of mobile WiMAX OFDMA PHY using the Stanford University Interim (SUI) channel model using mobile IP was evaluated by Omar *et al*. The simulation was taken using SUI-1, SUI-2, and SUI-3 channel models using 1024 FFT. Simulation was done for both low and high doppler shift with different coding rate. Results showed that the code rate of 1/2 offers low performance, and that 16-QAM and 64-QAM with 3/4 code rate provided better performance then QPSK 3/4 rate [55].

The mobile WiMAX standard offers mobility up to 350 km/h. But the mobility develops doppler spread and results in an irreducible error. George *et al*. examined the possibility of using directional antennas with the WiMAX standard to reduce the doppler spread and improve the performance [56]. The researcher developed a simulator in accordance with the IEEE 802.16-2004 standard. The simulation runs with CC with 1/2 punctured rate. Comparing this sectorised antenna array, the result showed that uneven beam widths result in better performance at high speeds, which reduce the doppler spread and increases the channel coherence time.

It is expected that the IEEE 802.16 based on BWA technologies, will play the central role in the next generation wireless network. It can form the foundation upon which operators can delivers ubiquitous internet access in the near future. The central concern regarding next generation wireless systems, is the need to provide seamless support in mobility, while taking advantage of different access networks. IEEE has been working on the 802.21 draft standard, which will enable media independent handover. It is anticipated that when IEEE 802.21 will be employed, the mobility management will be harmonized. Pedro *et al*. proposed an architecture which integrates WiMAX, QoS and mobility management framework over a heterogeneous network, integrating QoS and mobility; which is compliant with WiMAX Network Reference Model (NRM) [57].

Hyunkee *et al*. proposed two new pilot pattern and channel estimation models to mitigate the ICI for IEEE802.16m standard [58]. In the proposed channel estimation model, a group of pilot pattern and linear properties of the channel variation was used. In the first proposed model, two Physical Resource Units (PRUs) are inserted into the left and right part adjacent to the null sub-carrier. In addition four pilots are inserted into fixed position of each PRU. In the second proposed model, the PRU was changed to 18x7 to reduce the density compared to 18x6. Here the pilots are

inserted in the first , third, and seventh symbols. BER performance was measured between the speeds of 3 km/h to 350 km/h. The proposed models showed the better performance during 30 dB SNR.

Research on high vehicular speeds, investigating high speed dynamics of power control, UL timing correction, and doppler mechanisms was done by Alan *et al.* [59]. For this research an experimental WiMAX network was deployed at the BMW test facility, South Carolina using commercial products. The researcher concluded that WiMAX standards are ready to connect to the car, and that with a good system design, it can provide excellent performance at high mobility up to 250 km/h. From the study, the researcher provided a WiMAX equipment production guideline for automobile use at up to 240 km/h speed.

Rebeca *et al.* studied DL performance of mobile WiMAX vehicular multipath fading channel using the ITU-R set of channel model [60]. In the simulation, the data transmission takes place at vehicular speeds of 60 km/h and 120 km/h. The study determined that the SNR threshold is needed for the system to jump from one modulation scheme to another. The observation of this study is that 16 dB is the minimum SNR for vehicular multipath channel to imposed QoS parameter, and the complex modulation scheme can be used when the SNR is >30dB. Research shows that 29 dB SNR is required for jumping to QPSK-3/4 link speed from QPSK-1/2 link speed; and >24dB SNR is required for jumping to 16-QAM-1/2 link speed.

The performance of IEEE 802.16e for vehicular networks is investigated under different existing empirical propagation models, hand-off scenarios and different speeds of MS by Nargis *et al.*; in order to select a suitable propagation model. The simulation is done using NCTUns simulation tools, with design paradigms specified for the WiMAX system [61]. The simulation was conducted on 2.3 GHz with SOFDMA. The research shows that the ECC 33d model is suitable for analysis for WiMAX networks, which provide the low path loss, and better throughput compared to the Okumara hata open area and large urban model.

Beibei *et al.* studied the performance of mobile WiMAX on the OFDMA air interface in two mobile V2V channels. One is the open area high traffic density channel and other is urban channel. For modeling the channel, both antennas were placed inside and outside of the car. The study considered the 512 FFT with UL PUSC subcarrier permutation. Data passes through QAM modulation with CC

and block interleaver. The MSE is used to quantify the accuracy of the channel estimation method. The simulation was taken at 100 km/h speeds in different SNR conditions. The result showed that the IEEE 802.16e system performance in the non stationary channel is more unstable than stationary channels [62].

For real time video surveillance systems on a moving vehicle, wireless is the most suitable communication system. But the throughput is still insufficient for streaming video data from all cameras mounted in the public transport at one time. Ahmad *el al.* proposed a new scheme "live_feeding_status_check" algorithm, to estimate the utility for different cameras for real time video surveillance in the public transport. The algorithm assists WiMAX MAC to make a decision. In the proposed scheme, the system first estimates the utility of the cameras, then puts some low utility camera offline and makes high utility cameras active [63].

In the US, the 50MHz wide frequency band is allocated for public safety communication on 4.9 GHz center frequency. Considering this frequency, Bultitude *et al.* proposed a model to characterize the emergency vehicle-to-indoor radio channel, using WiMAX communication for public safety applications [64].

Hand over technique is one of the most urgent issues for successful mobile deployment. In order to support IP mobility, the Mobile IP (MIP) is added to the WiMAX standard. Due to long handover latency of MIP, real time services such as video streaming and VOIP are still challenging. Jun *et al.* proposed a fast cross layer handover scheme based on movement prediction in mobile WiMAX systems. The proposed scheme is based on the signal strength prediction, and the signal strength samples have been taken from the mobile users. The simulation was run using the WiMAX forum recommended propagation mode. The researcher claims the proposed scheme can support fast and efficient handover [65].

2.4.6.1 Research on Rayleigh Fading Model

For any NLOS wireless communication, where muitipath propagation reduces the signal strength, the Rayleigh distribution model is widely used for channel estimation. Ahmad *et al.* investigated the BER of WiMAX communication system at high speed vehicular environments in [18], and proposed a mathematical scheme to compute the packet size based on the estimated Bit Error Probability (BEP) at different speeds of the mobile station. For estimating the BEP, the researcher considered the

channel to be Rayleigh fading, and the Rayleigh distribution model was used for the simulation. The simulation was conducted using NS2, assessing a centralized video surveillance system in public trains. The train was equipped with four video cameras. Each camera sent video data at a rate of 512 Kbps to the WiMAX BS, and then the central control room through an optical fibre network. The carrier frequency was 2.6 GHz with 12 MHz BW. The simulation used 2048 FFT point, and the maximum data rate of the channel was10 Mbps. The train started from the station, and gradually increased speed to 40 km/h within 20 sec, and 70 km/h within 60 sec, and continued to run with in the speed of 110 km/h before stopping at the next station at 180 sec.

Research showed that the BEP is higher when the terminal moves at high speeds, and during the higher BEP the packet error probability is increased. A comparative study has been done at 256 and 512 packet size, with standard 64 byte and 128 bytes packet sizes. The result showed that the smaller packet size offers a higher chance of uncorrupted packets; but when the terminal speed is low, the data rate fails badly due to extra cost caused by higher numbers of packet headers. But when the terminal moves at high speed, smaller packets offer a comparatively high data rate. But when the speed is low, the larger packet size reduces the extra header bits, and comparatively achieves higher throughput. From the study result, researchers offer a packet size adjusting scheme in response to the BEP, according to the speeds of the mobile terminal.

Ahmad *et al.* proposed a new an adaptive FEC scheme in [66], using RS-CC for WiMAX communication in vehicular communication. The proposed scheme monitors the channel condition at an sampling interval, and sends the BER information to the sender by the receiver, which notifies the changes of channel condition at various vehicular speeds. So the sender can promptly adjust the FEC size for the next interval, and can promptly correct the error without the need of retransmission. The simulation was conducted using the same properties used in the research [18]. From this research, the researchers achieved a good throughput which was sometimes 800 Kbps. In [67] Ahmad *et al.* proposed new CAC for the WiMAX system at vehicular speeds, considering parameters in [18]which is described with the Rayleigh fading model. The proposed model improved the capacity at 4.5% during the study time over 120 sec.

Boudali *et al.* evaluated the high mobility effects on the CC and RS coded OFDM system for the return link, considering doppler effects; and examined the BER performance in [68]. The sub optimal estimation technique based on the Minimum Mean Squared Error (MMSE) was used in this research, and focused on the development of LS and Maximum Likelihood (ML) performance using MMSE. The Rayleigh distribution with Jake's spectrum was used as a channel model. The velocity of the MS was 130 km/h and 345 km/h. Results show that LS channel estimations degrade as the increasing of time dispersion, and the ML channel estimations perform robustly in the variable environment. The noise gap between LS and ML was 8 dB, and this gap increased when the channel time variation increased.

The Rayleigh distribution model is a standard channel model for heavily built-up urban areas where the signal reflects and refracts from different objects. But when the fading condition is more severe, the Rayleigh fading channel treated as sub-Rayleigh fading, or Nakagami fading, and the Nakagami-m distribution model is suitable for that sub-Rayleigh fading. Literature reviews on the Nakagami-m fading model are described in the following section.

2.4.6.2 Researh on Nakagami-m Fading Model

K. Zhengjiu *et al.* did research [69] on a frequency selective Nakagami fading channel. The research found that the magnitude of the channel responses are Nakagami distributed random variables. Its fading parameter 'm' and mean power Ω are the explicit functions of the Channel Impulse Response (CIR). The researcher concluded that the number of multipaths have different impacts on the BER performance depending on values of m. When $m < 0.5 < 1$ or $m > 1$, the number of multipaths has significant impact and when $m = 1$ the number of multipaths has no impact.

A precise BER calculation for the asynchronous direct spectrum CDMA system has been done by Julian *et al.* using the Nakagami-m distribution model. The result shows when $m = 1$, the integrand function is strictly non-negative and decays exponentially. For $m > 1$, the integrand function is both positive and negative. Another finding of this research is that the largest BER improvement is obtained between $m = 1$ and $m = 2$ for small numbers of users in the system [70].

Mohammad *et al.* developed an analytical model, to evaluate the cell, and user throughput, under the correlated and uncorrelated Nakagami fading channel for

HSDPA using the rake receiver. The study investigated the composite uncorrelated and correlated multipath channel, where the path amplitude follows the Nakagami-m distribution. The average throughput indicated that the system performance decreases by 5% when the correlation increases from 0 to 0.07. When the Nakagami parameter m increases from 1 to 4, the result shows that the system performance increases approximately 10 to 12% [71].

Error rate performance analysis of OFDM for frequency selective Nakagami–m fading channels, has been done by D. Zhang *et al.* in [72] for slow fading environments. Analysis is done in multi-channel reception with Maximal Ratio Combing (MRC). The gain of each channel is made proportional to the Root Mean Square (rms) signal level and inversely proportional to the mean square noise level in that channel. The observation of this research is that at the same SNR, the BER decreases with increasing the value of m, when the number of CIR taps are three.

In [73], Subotic *et al.* analyzed the BER performance of an equalized OFDM system in the Nakagami $m < 1$ fading channel. Researchers used semi-analytical methods to evaluate the BER of a QPSK-OFDM system, and used the pilot assisted linear channel estimation and channel equalization. The observations of this research are "due to the ICI caused by high doppler the error floor is not observed for slower fading and the BER increases with decreasing m."

X. Chen *et al.* did a BER performance analysis of MIMO-OFDM systems with Space Time Block Coding (STBC) over the Nakagami-m fading model in [74]. To analyse the performance, researchers used the MATLAB at a different simulated condition. The results show that when the antenna number is 4, the capacity is nearly 20 Mbps more than SISO at $m = 1$. The other observation is that BER declines as the SNR grows. For different values of m, it is shown that the BER declines as the value of m increases.

Research has been conducted by R. Guo *et al.* in [75] to improve the BER of MIMO-OFDM systems over the Nakagami-m fading channels. Performance of a Rate-Compatible Punctured Convolution (RCPC) and STBC encoded MIMO-OFDM system, with transmitter and receiver diversity used in the research. The MRC is used at the receiver and the results showed that the RCPC encoded systems provide better results than with a non RCPC encoded system.

Srigowri *et al.* did a study in [76], on a D-QPSK-OFDM system over a frequency

selective slow fading channel using the Nakagami-m distribution model. The researcher calculated the phase shift, degradation of energy per bit (E_b) and interference in channels caused by doppler frequency shift.

A Symbol Error Rate (SER) performance analysis of an OFDM system over a correlated Nakagami-m fading channel was done by Vivek *et al.* using MRC diversity. The conculsion of this research was that the SER performance of the system decreases with the correlation increasing [77]. Vivek *et al.* did another study on ICI characteristics over the above scenario and estimated the BER [78]. Research found that the value of SNR has a different impact on the BER depend on m.

The impact of MS velocity on the performance of frequency selective scheduling in WiMAX IEEE 802.16e has been done by Ashley *et al.* in [79] both in AMC and PUSE mode. The researcher came to the conclusion that the frequency selective scheduling is viable, and nearly doubled the throughput at low velocity under ideal conditions. The researcher recommended a frequency selective scheduling scheme for WiMAX at band AMC mode in urban cells. In rural environments where the system is deployed on rail or road for vehicular application, the researcher recommended the frequency interleaving approach, such as the PUSC mode operation.

H. Balta *et al.* analyzed the performance of turbo codes on Nakagami flat fading radio transmission channels in [80]. To compare coded and uncoded transmission, researchers calculated the BER as a function of mean SNR at different values of m (2,3,4 and 5). The study shows that the uncoded transmission decreases performance as time selectivity increases.

A. Ramesh *et al.* conducted research on BER performance in [81], using union bounding techniques for TC on the Nakagami fading channel with diversity combining. The researcher evaluated the BER probability at punctured rate-1/3. The study found that with TC, the EGC performs close to the diversity scheme. The researcher undertook other research in [82] for the analysis of turbo coded, coherent communication systems on independent and identically distributed (i.i.d) Nakagami-m fading channels with SC.

Research on BER performance of OFDM-BPSK and OFDM–QPSK over the Nakagami-m fading channel was done by N. Sood *et al.* in [83] for a flat fading channel. The approach was the decomposition of Nakagami random variables into orthogonal random variables with Gaussian distribution envelopes. The study shows

that with increasing m, BER decreases. The researchers concluded that the threshold value of Nakagami parameter m for flat fading channel is 1.4.

2.4.6.3 Estimation of Nakagami Parameter m

The Nakagami shape parameter m indicates the fading severity of a channel. A significant amount of research has been done to estimate the Nakagami m parameter. Simon *et al.* did a study on bodyworn wireless PAN operating at 868 Mhz frequency. The data was taken in three environments: 1) echoic chamber, 2) open office area and 3) a hallway; both in LOS and NLOS communication. Research uses ML and the Akakie Information Criterion (AIC) method to calculate the Nakagami m value. The study shows that the multipath has a role to reduce the signal strength, and the mean m value is sharply reduced to 1.3 from 7.8 due to multipath [84].

Simon *et al.* did another study in [85]to characterize channel condition on Wireless Body area Network (WBN) using the Nakagami fading parameter m. To estimate the Nakagami parameter m, the researcher took data from anechoic chamber, open office space and a hallway using the 2.45GHz channel. Experiment results show that, in stationary conditions, fading is very little and the Nakagami parameter m is always > 1.

A channel fading statistical analysis using empirical data for DSRC standard was done by Jijun *et al.* in [86] using the Nakagami-m distribution. The researcher characterized the fading as a function of distance from mobile to mobile channel in a vehicular environment. To get an unbiased and accurate m for the Nakagami distribution, the researcher collected data from a stationary random process. The relative speed between two vehicles was 1.6 km/h. The doppler spread was around 100 Hz and the channel coherence time was around 10 ms. The result found that when the distance is less then 70 -100 metres, the m value is 1.0 for MLE, and 1.8 for the CDF method. Beyond 100 metres, the m value is 0.7 for MLE and 1 for CDF respectively.

In literature various studies are presented, which report findings on vehicular communications using different wireless technologies such as GSM, CDMA, Infra Red, DSRC and WiMAX. Almost all of these studies used Rayleigh distribution for modelling the channel fading and bit error rate estimation. Nakagami-m distribution is a relatively new model which is known for better accuracy at vehicular speeds,

but there is no research reported in the literature that investigates bit error rate estimation in WiMAX communication system using Nakagami-m distribution."

2.5 Technical Challenges for Wireless Communications at Vehicular Speeds

Different studies have been done to analyse the medium of wireless communication during the last century. There are a number of alternatives in wired medium such as twisted pair cable, coaxial cables, and optical fibre. But the Electromagnetic Wave (EMW) is the only medium for wireless communications.

Compared to the wired medium, the wireless medium is unreliable, and has low bandwidth. Received signal strengths of EMW rapidly fluctuate due to mobility of the receiver or transmitter or surrounding objects, which develop the doppler spectrum and change the multipth dynamically. In the following, we discusses the multipath effects and doppler shift problems in Wireless communications at vehicular speeds.

In the WiMAX system, the delay spread is typically over several micro seconds, which is longer than the guard interval. Therefore it is very challenging to maintain the BER performance of the system for NLOS channel at a high rate data transmission. In mobile WiMAX access architecture in a high speed environment, there are several problems, such as handoff, doppler spread and non uniform RF power etc. Due to OFDM, deep frequency selective fading is a big problem at high speeds, and the performance of the transmission channel is affected by two important factors; the multipath effect and the doppler shift [87].

2.5.1 Multipath Effects

Multipath is the propagation phenomenon in wireless telecommunications. When there is no LOS communication between the Tx and the Rx, the signals reach the receiving antenna by two or more paths. The signals bounce by reflection and refraction from mountains, buildings or any other obstruction between the Tx and Rx. As a result, some of the signals travel longer paths and encounter more delays at the receiver. Due to the path delay, the signal may reach the receiver either in phase

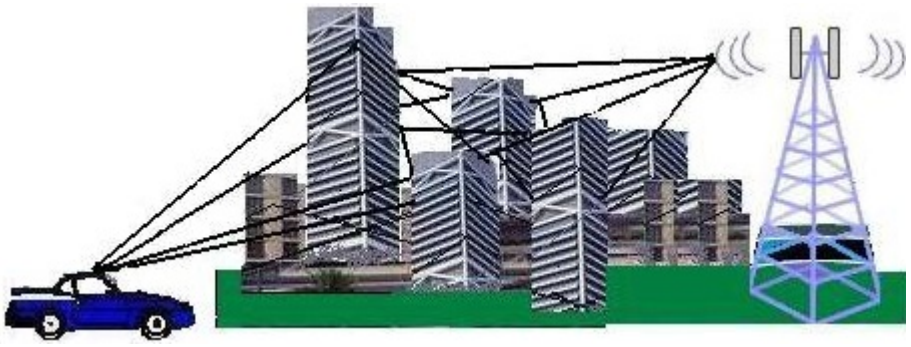

Figure 2.6: Multipath effects

or out of phase. If the signal arrives out of phase, it cancels certain frequencies at the receiver, which is called ISI. This phenomenon occurs when the multipath delay spread is larger then the symbol duration and the wave spread to the neighbour symbol. The ISI is a significant problem that causes fluctuation in signal amplitude, and results in phase difference and irreducible errors in the detected signal[3][88]. The mathematical model of the multipath can be presented using the method of the impulse response.

$$h(t) = \sum_{n=0}^{N-1} \rho_n e^{j\phi_n} \delta(t - \tau_n) \qquad 2.1$$

where $h(t)$is the impulse response function, N is the number of received impulses, τ_n is the time delay of the generic n^{th} impulse and $\rho_n ej\phi_n$ is the complex amplitude of the generic received pulse.

2.5.2 Doppler Spectrum

The doppler spectrum is the spectrum of fluctuations of the received signal. When the electromagnetic wave source moves around a receiver, receiver frequency is observed to be high when the source move towards it, constant when passing by, and lower during the recession compared to the emitted frequency. These effects are known as doppler effects after Christian Doppler who proposed this theory in 1842. The change of frequency is given by

$$f_d = \frac{f_c v}{c} \qquad 2.2$$

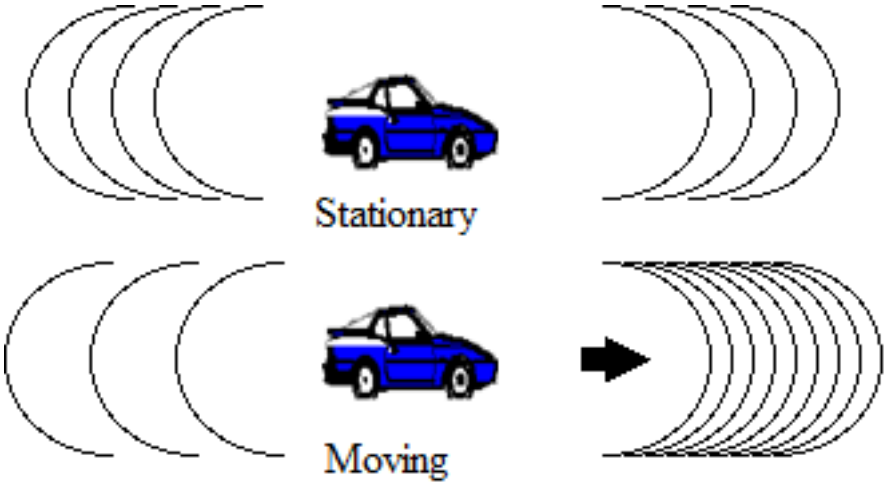

Figure 2.7: Doppler spectrum

where f_d is the doppler shift, f_c is the carrier frequency, v is the speed of the mobile Tx or Rx, c is the speed of light ($3*10^8$ metre/s). The normalized doppler frequency (δ) can also be calculated using

$$\delta = f_d/f_{sd} \qquad 2.3$$

The ICI is caused by doppler shift. When the δ is larger then 5%, the doppler shift is severe and when the δ is smaller then 2.5 %, the doppler shift is slight. Doppler compensation is required for WiMAX operation because this operates in 2 to 11 GHz [87].

In a mobile scenario the signal strength fluctuates rapidly due to multipath effects and doppler spectrum, and the coherence times become small relatively with the delay constraint of the channel and results in small scale fading or fast fading. Amplitude and phase of the signal varies considerably over the period of time. In a fast-fading channel, the transmitter takes advantage of the variations in the channel conditions and may cause deep fade; which temporarily erases some of the transmitted information, and this fast fading is the cause behind the high bit error of the channel at vehicular speeds.

As we discussed in earlier chapter, the high data rate in WiMAX communication at fixed environment and pedestrian speeds is beyond any doubt, but it is not fully optimized for mobile communication at vehicular speeds. At vehicular speeds, the data rate decreases sharply to the point that it is only sufficient to maintain

connection, but no assurance of data, especially the data with multimedia contents is given. The IEEE 802.16m acknowledged this problem. Its system requirement document indicates that at speeds between 10 -120 km/h, there is a gradual degradation of services as a function of speed. At speed above 120 km/h, a connection can be maintained only.

2.6 Summary

WiMAX system is a popular 4G wireless communication technology which provides services to millions of people world wide. The 4G version of WiMAX communication offered throughput up to 1 Gbps at specific conditions which open a new avenue of new applications. OFDMA and MIMO are the key features of the WiMAX system for higher throughput. Different types of wireless communication technology has been used for data communication in ITS, but recently the focus has shifted towards WiMAX. WiMAX has already been deployed in ITS for data communication in different countries. During high mobility, the throughput in the WiMAX system is not sufficient to transmit multimedia content. Dynamically changed multipth and doppler effects are the main causes behind the degradation of the channel capacity. In this chapter we have discussed the background of wireless communication systems, their generations and types, as well as the vehicular application of wireless systems. We have discussed the WiMAX communication system and its application and research in vehicular application. We have discussed the research on the WiMAX system in vehicular communication, using different types of stochastic models such as the Rayleigh distribution, and the Nakagami-m distribution model. Lastly we have discussed the challenges of wireless communication systems to get the optimum throughput specially in vehicular applications.

Chapter 3

Bit Error Estimation in WiMAX Communications at Vehicular Speeds using Nakagami-m Fading model

As we discussed in chapter 2, the doppler effects and dynamically changed multi-path cause severe fading of the channel, and reduce the throughput so low, that without any proactive measure the throughput at high vehicular speeds drops to zero. The BER is a measure of end to end performance of the channel, and the estimation of BER is an integral part of any proactive measure that aims to maintain high throughput at vehicular speeds. In this chapter, we propose an analytical model to estimate the BER in WiMAX communication at vehicular speeds using the Nakagami-m distribution model. The proposed model is adaptive and can be used with resource management schemes designed for fixed, nomadic, and mobile WiMAX communications.

3.1 Introduction

The WiMAX system is popular for its capacity to deliver high throughput in a fixed communication environment. In a mobile communication environment at high vehicular speeds, this throughput decreases sharply, often providing a connection with service only, with no guaranteed data rate. The 802.16m version of the WiMAX standard acknowledges this problem and indicates that the 802.16m is fully optimized for stationary and pedestrian speeds (0-10km/h) [8]. Unless any proactive measure

is taken to combat this problem, throughput becomes insufficient to support many applications, particularly those with multimedia content. Table-3.1 summarizes the primitives used for mobile WiMAX PHY. At high speeds, doppler shift causes ICI and due to small sub-carrier spacing in WiMAX system, the ICI possibilities on larger FFT is higher than the smaller FFT. The WiMAX forum therefore recommends smaller FFT and simpler modulation at high vehicular speeds. The WiMAX forum specified OFDMA PHY for mobile WiMAX with 512 and 1024 FFT, and PUSC, FUSC and AMC subcarrier permutation. According to the specification, PUSC mode is mandatory for DL and optional for UL. The AMC is optional for both DL and UL and FUSC is potentially optional only for DL [21]. The mandatory modulation schemes specified in the specification are QPSK and 16-QAM for both UL and DL. The 64-QAM is an optional modulation scheme.

The WiMAX communication standard incorporates OFDM and Orthogonal OFDMA [89] for achieving better spectral efficiency and data rates. The OFDM is a robust technique that overcomes the frequency selectivity problem of the channel and provides higher throughput. In OFDM systems, total bandwidth is divided into multiple sub-carriers using FFT operation where the sub-carriers are orthogonal to each other. Sub-carriers are divided into data, pilot, DC, and guard sub-carrier. The data, pilot, and guard sub-carriers are used for transmitting data, pilot symbols, and guard information for limiting interference, respectively. The OFDMA technique is based on OFDM, which provides multiuser access to a channel by dividing the sub-carriers into subsets of sub-carriers. For supporting mobility, the mobile WiMAX system extends its physical layers and incorporates the Scalable OFDMA (SOFDMA) technique. By adopting scalable PHY architecture, the WiMAX system supports a wide range of BW. The scalability is implemented by varying the FFT from 128 and multiples of 128, up to 2048 to support bandwidth from 1.5 MHz to 20 MHz.

In a high mobility scenario, relative motion between transmitters and receivers results in rapid time variation and high doppler shift. Accumulating dynamically changed multipath effects and noise, a significant fluctuation in received signal strength is observed in the channel. Fading like this is often modeled in the literature with the Rayleigh fading model. The Rayleigh fading model has not been challenged until very recently when researchers started to focus on the throughput

Table 3.1: WiMAX forum specification primitives for mobile WiMAX PHY.

Parameters	Value			Value		
Bandwidth (BW)	3.5, 5			7, 8.75, 10		
Sampling Factor (n)	BW is multiple of 1.75 is 8/7, multiple of 1.25, 1.50, 2, and 2.75 is 28/25 not otherwise specified then n=8/7					
Cyclic Prefix time ratio (G)	1/8					
Number of Sub-carriers	512			1024		
Permutation mode	AMC	PUSC		AMC	PUSC	
		DL	UL		DL	UL
Used sub-carriers	433	421	409	865	841	841
Guard sub-carriers, Left	40	46	52	80	92	92
Guard sub-carriers, Right	39	45	51	79	91	91

problem at vehicular speeds. The Rayleigh model works on the assumption that the resultant fading arises from a large number of uncorrelated partial waves with identically distributed amplitudes and uniformly $[0, 2\pi]$ distributed random phases. This assumption is highly optimistic in a mobile communication environment at high vehicular speeds, and the more realistic assumption is to have many partial waves with amplitudes that follow distributions that are not identical, yet are partially correlated [9, 10]. In an environment like this, signal fluctuations are better modeled by the Nakagami-m distribution [10, 9], and as a result, estimated BER is more accurate in the Nakagami-m model than in the Rayleigh model. Moreover, the Nakagami-m model can be made adaptive to suit fixed, pedestrian, and high speed mobility environments by changing the fading parameter m, which is used to reflect the fading severity. The parameter value $m < 1$ is considered as Nakagami/sub-Rayleigh fading, and the fading process is considered as a product of complex Gaussian process and a square root beta process. Rayleigh distribution ($m = 1$) and Rician distribution ($m > 1$) are considered as a special case of the Nakagami distribution [10, ?]. In the following sections, we develop and present an analytical model for BER estimation in WiMAX communication systems using the Nakagami-m fading model.

3.2 Channel Condition at Vehicular Speeds

The development of wireless technology has opened a number of new paths for implementation, but some unavoidable circumstances attenuate the signal energy and make barriers to achieving optimum results from the system. By its nature, the radio signal strength attenuates with the distance between the BS and SS, and the distance power relationship provides a mean value of the signal. In a real type implementation the mean value is not always constant with the distance. This variation of the received signal strength depends on the environment, location, surrounding infrastructure, and the speeds of Tx or Rx. The surrounding infrastructure such as hills, large buildings, walls on side of the buildings, and any another objects in the main signal path between that Tx and the Rx, block the signal. So the signal reflects, refracts, or diffracts from the obstruction, and reaches at receiver via a number of different paths, and takes a longer times to reach the Rx. The different between longest and shortest path is commonly known as multipath delay spread counting only the path significant energy.

If the multipath delay spread is larger than the symbol duration, the channel experiences ISI[3]. If Tx and Rx are stationary, the multipath delay spread is constant, but during mobility this delay spreads rapidly changes with the movement of Tx or Rx. As a result, the amplitude and phase of the signal varies considerably over the period of time. Multipath delay spread also creates frequency selectivity of the channel. When the coherence bandwidth (W_c) of the channel is smaller than the bandwidth of the signal, different frequency components of the signal therefore experience de-correlated fading. This is known as frequency selective fading. The coherence bandwidth approximately is given by the equation

$$W_c = \frac{1}{2\pi(max|\tau_i(t) - \tau_j(t))} \tag{3.1}$$

where $(max|\tau_i(t) - \tau_j(t)$ is the multipath delay spread, which is defined as a function t and τ is the delay spread of the signal [90] . During the mobility of MS, the coherence bandwidth varies over the channel due to multipath delay spread and varies from point to point.

Doppler spread is another effect of mobility which change the signal frequency

over time. When the coherence time (T_c) becomes small relative to the delay constraint of the channel, it results is a fast fading channel. Coherence time is the minimum time that is required for the magnitude change of the channel which is used to measure the fading. It is inversely related to doppler spread. For OFDM transmission system, the coherence time has a special significance because the symbol duration should be chosen to be much smaller then T_c to avoid ICI. It is inversely proportional to the maximum doppler shift [91]and typically expressed as:

$$T_c = \frac{k}{D_s} \tag{3.2}$$

where T_c is the coherence time, D_s is the doppler spread, and k is a constant taking on values in the range of 0.25 to 0.5.

Fading causes of bit errors at the Rx and the BER depends on the fading severity of the channel. The dynamic multipath effects and doppler shift result in severe variations of the channel, and this variation may cause deep fade which temporarily erases some of the transmitted information.

According to the fading severity, the channel is divided into three categories, and different distribution models are used to estimate that channel according to the type of fading, which is described in the following section.

3.2.1 Rician Fading Channel

Rician fading occurs when one of the paths, typically a line of sight signal, is much stronger than other signals. The amplitude gain of the signal is characterized by the Rician distribution. The *pdf* of the received signal amplitude in the Rician distribution model is given by

$$f(r) = \frac{2(K+1)\gamma}{\Omega} exp\left(-K - \frac{(K+1)\gamma^2}{\Omega}\right) I_o\left(2\sqrt{\frac{K(K+1)}{\Omega}}\gamma\right) \tag{3.3}$$

where K is the ratio between the power of the direct path and the power of the other scattered path, Ω is the total power of the both paths, and $I_0(.)$ is the 0th order of the modified Bessel function for the first kind.

3.2.2 Rayleigh Fading Channel

In a heavily built-up urban area or alpine area where there is non- LOS communication between Tx and Rx, the objects of the environment attenuate, reflect, refract, and diffract the signal before it arrives at the receiver. This propagation environment is known as Rayleigh fading, and the Rayleigh distribution model is a specialized stochastic fading model for this type of fading channel. Rayleigh fading has a small-scale effect, and is appropriate for this environment if the fading statistic is short term. How rapidly the channel will fade depends on how fast the receiver and/or transmitter will move. The amplitude gain of this fading channel is characterized by the Rayleigh distribution [18]. The *pdf* of the received signal amplitude gain in Rayleigh distribution is given by

$$p_R(\gamma) = \frac{2\gamma}{\Omega} exp^{-\gamma 2/\Omega,} \qquad \gamma \geq 0 \tag{3.4}$$

where $\Omega = E(\gamma^2)$

3.2.3 Sub-Rayleigh Fading Channel

The term sub-Rayleigh fading refers to fading which is more severe than Rayleigh fading. This severity is caused by the high variability of the channel. The cause behind high variability is the high speed movement of the transmitter or receiver, especially in heavily built-up areas where the direct propagation path of the signals are severely obstructed by the objects, and few indirect multi-path components reach the receiver [92]. This more severe fading channel is observed by Nakagami [73] for long distance high frequency communication links. The amplitude gain of the sub-Rayleigh fading channel can be characterized by the Nakagami-m distribution [93]. Sub- Rayleigh fading is also known as Nakagami fading.

3.3 Channel Model for Nakagami Fading Channel

When mobile nodes move at high vehicular speeds, doppler shift and dynamic multipath effects cause complex fading and reduce throughput. Following [10, 73], this complex fading process $x(t)$ can be modelled as a product of two independent processes $y(t)$ and $z(t)$; where $y(t)$ is the zero mean complex gaussian random process

and $z(t)$ is the exponentially correlated random process. The correlation function $\Re_x(\tau)$, of the process $x(t)$ is a product of correlation process of $y(t)$ and $z(t)$, which can be given as

$$R_x(\tau) = |y(t)y(t+\tau)z(t)z(t+\tau)| = R_y(\tau)R_z(\tau) \tag{3.5}$$

The marginal distribution $p_x(x)$ of $x(t)$ does not depend on the correlation of these components. Therefore, the marginal distribution $p_z(x)$ of the modulation component $z(t)$ affects the desired distribution. If γ is the symbol energy to noise ratio at the receiver, then the pdf of the Nakagami process is given by

$$pdf(\gamma) = \frac{2m^m\gamma^{2m-1}}{\Gamma(m)\Omega^m} exp\left(-\frac{m}{\Omega}\gamma^2\right), \quad \gamma \geq 0, 0.5 \leq m < 1 \tag{3.6}$$

where $\Gamma(.)$ is the gamma function and

$$\Omega = E[\gamma^2] \tag{3.7}$$

$E(.)$ is the mathematical expectation and the fading parameter m is defined as

$$m = \frac{\Omega^2}{E[(\gamma^2 - \Omega^2)2]} \tag{3.8}$$

$z^2(t)$ has a standard beta distribution with a pdf given as

$$pdf(z^2(\gamma)) = \frac{z^{m-1}(1-z)^m}{\beta(m,\, 1-m)}, \quad 0 \leq z \geq 1 \tag{3.9}$$

where $\beta(x, y)$ is the beta function.

The Markov exponentially correlated process [73], $z(t)$ is given by

$$R_z(\tau) = exp(-\lambda\tau/2) \tag{3.10}$$

where λ is a positive constant.

$$R_y(\tau) = R_x(\tau).exp(\lambda\tau/2) \tag{3.11}$$

If $R_x(\tau)$ is approximated by a correlation function with a rational spectrum, it can be rewritten as

$$R_x(\tau) = \sum_{k=1}^{\infty} c_k^2 exp(-\tau_k|\tau|) \tag{3.12}$$

where c_k is the complex number. By setting $\tau = 0.05min(\tau_k)$, $R_y(\tau)$ defines a proper correlation function of a Gaussian process.

3.4 Proposed Analytical Model for Bit Error Rate Estimation

The WiMAX OFDM system consists of N orthogonal sub-carriers with a frequency spacing ∇f . The cyclic guard is used to combat inter-symbol interference (ISI). Each of the sub-carriers is modulated independently with complex modulation symbol. During an OFDMA symbol transmission, the transmitted signal strength to the antenna [94] is given by

$$S(t) = Re\left\{ e^{j2\pi f_c t} \sum_{k=-(N_{used}-1)/2}^{(N_{used}-1)/2} c_k . e^{2\pi k \nabla f (t-T_g)} \right\} \tag{3.13}$$

where f_c is the center frequency, t is time elapsed since the beginning of the OFDMA symbol, which also specifies a point in a QAM constellation, N_{used} is the number of used subcarrier and T_g is the guard time.

In a high mobility scenario, fading is caused by dynamic multipath effects and doppler shift, and the average received symbol energy to noise ratio ($\overline{\gamma_s}$) of this channel is given by [18, 95]

$$\overline{\gamma_s} = \frac{1}{1 - \frac{1}{N^2}\left[N + 2\sum_{i=1}^{N-1}(N-i)J_0(2\pi f_d T_s i)\right] + \frac{NT_s}{\frac{E_s}{N_0}}} \tag{3.14}$$

where N is the number of the used sub-carrier, j_0 is the Bessel function, T_s is the duration of each M-ary QAM symbol transmitted on a sub-carrier, NT_s is the useful OFDM symbol time, E_s is the average symbol energy, N_0 is the energy of the noise and f_d is the doppler shift of the channel, which is defined as

$$f_d = f_c(\frac{v}{c}) \tag{3.15}$$

where f_c is carrier frequency, v is the speed of the mobile station and c is the speed

Table 3.2: Derived parameters for IEEE 802.16m.

Parameters	Equations
Sampling frequency (F_s)	$F_s = floor(n.BW/8000).8000$
Sub-carrier spacing (∇f)	F_s/N_{fft}
Useful symbol time(T_b)	$1/\nabla F$
Cyclic Prefix (CP) time (T_g)	$G.T_b$
OFDMA symbol time $ofdmT_s$	$T_b + T_g$
Sampling time (T_s)	Sampling time T_b/N_{fft}

of the light.

The average bit energy to noise ratio ($\bar{\gamma_b}$) of a multipath fading is given by

$$\overline{\gamma}_b = \frac{\overline{\gamma_s}}{log_2 M} \tag{3.16}$$

where M is the number of symbol for M-ary QAM modulation scheme (for QPSK $M = 4$ and for 16 QAM $M = 16$). From equation (3.14) (3.16), the bit energy to noise ratio can be written as

$$\overline{\gamma_b}(v) = \frac{\frac{1}{log_2 M}}{1 - \frac{1}{N^2}\left[N + 2\sum_{i=1}^{N-1}(N-i)J_0(2\pi f_c(\frac{v}{c})T_s i)\right] + \frac{NT_s}{log_2 M}\cdot\frac{1}{\frac{E_b}{N_0}}} \tag{3.17}$$

where E_b is the average energy per bit.

For a WiMAX OFDMA air interface, the main source of bit errors is inter-carrier interference instead of interference between OFDMA users. This is because interference between OFDMA users is averaged over many users, and therefore it remains almost constant over time, and is absorbed in the Gaussian thermal noise. AWGN is used successfully to approximate the OFDMA inter-carrier interference [96] [18]. Taking AWGN into consideration, the bit error probability for a generalized ML receiver is given by

$$P_b(v) = Q\left(\sqrt{2\gamma_b(v)}\right) \tag{3.18}$$

where bit error probability P_b and symbol error probability P_M of the OFDM are related to each other in the form of

Table 3.3: List of Parameters used in the proposed analytical model

SL. No	Parameter	Parameter Name
1	$\overline{\gamma_s}$	Energy to noise ratio
2	c	Square root beta modulating component
3	P_b	Bit error probability
4	v	Speed of the MS
5	P_M	Symbol error probability
6	E_b	Average energy per bit
7	$\bar{\gamma}_b$	Bit energy to noise ratio
8	M	Number of symbol for M-ary QAM modulation
9	N	Number of used sub-carrier
10	j_0	Bessel function
11	NT_s	Useful OFDM symbol time
12	E_s	Average symbol energy
13	N_0	Energy of the noise
14	f_c	Carrier frequency
15	f_d	Doppler shift of the channel

$$P_b \approx \frac{P_M}{log_2 M} \tag{3.19}$$

For $M = 2$ or $M = 4$, the average bit error probability is as

$$P_b(v) = \int_0^\infty P_b(x) p_{y_b}(x) dx \tag{3.20}$$

$$P_b(v) = \frac{1}{2}\left[1 - \sqrt{\frac{\bar{\gamma}_b(v)}{1 + \bar{\gamma}_b(v)}}\right] \tag{3.21}$$

Bit error probability for a higher order of M can also be obtained from

$$P_b(v) = \frac{\int_0^\infty p_M(x) P_{\gamma_M(x)dx}}{log_2 M} \tag{3.22}$$

The bit error rate, however, becomes excessively high for the higher order of M (> 4), and therefore is not recommended by the WiMAX forum for use in practical applications in vehicular communications. It is also evident that bit error probability remains almost the same for PSK and QAM for M up to 4, a reason why, in this work we developed an analytical model for QPSK modulation scheme only.

In Nakagami fading, all the sub-carrier frequencies are multiplied by complex channel gains, whose square root beta modulating component (c) arises from the

same parameter distribution, and this modulating component is constant over the OFDM symbol [73]. The i.i.d Gaussian process is conditioned on c, and the average bit energy to noise ratio for Nakagami $m < 1$ fading becomes

$$\tilde{\bar{\gamma}}_b = c\bar{\gamma}_b \tag{3.23}$$

and the bit error probability of a Nakagami-m fading channel is given by:

$$P_b(E) = \int_0^1 P(E|c).P_c(c) = \int_0^1 P(E|z).Pc^2(z)dz \tag{3.24}$$

where $P(E|c)$ is a Rayleigh pdf conditioned on c and $z = c^2$ is distributed according to equation (3.9).

Solving the equation (3.24) using equation 3.21 and equation 3.9, we propose the equation (3.25) to estimate the BEP for QPSK modulation in the WiMAX system using Nakagami-m distribution, the fading becomes:

$$P_b(v) = \int_0^1 \frac{1}{2}\left[1 - \sqrt{\frac{c\gamma_b(v)}{1 + c\gamma_b(v)}}\right] \frac{z^{(m-1)}(1-z)^{-m}}{\beta(m, 1-m)}dz \tag{3.25}$$

In the above mentioned equation, the Nakagami parameter m indicates the fading severity which can be computed using the equation (3.6) from observed data. The m value can be calibrated at various vehicular speeds using data collected from a hardware set-up. This calibrated value of m can be used in equation (3.25) to reflect various fading in different environments such as: Rician ($m > 1$ for LOS fixed communication), Rayleigh fading ($m = 1$ for low speed communication), and Nakagami fading ($m < 1$). Once the m value is calibrated, the proposed analytical model can be used with a resource management scheme (e.g., to compute how much bandwidth is required for a node that moves at a mean speed of 80 km/h) to be used in WiMAX communication at vehicular speeds.

3.5 Simulation Results

The WiMAX standard is developed for operating in the frequency range from 2 -11 GHz and WiMAX forum recommends 2.5 to 3.5 GHz for mobile WiMAX. The doppler spread will vary for various carrier frequencies. For simulation, we selected 2.6 GHz as a representative carrier frequency. and we simulated with 5 MHz and

10 MHz BW. In simulation the 512 and 1024 FFT points were respectively used in QPSK/4-QAM modulation with AMC and PUSC permutation mode. Table-1 summarizes the primitives used for simulating the mobile WiMAX PHY using the Nakagami-m fading model. In this simulation, Derived parameters were taken from table-II. We simulated equation 3.25 using the MATLAB signal processing toolbox for BER analysis at various vehicular speeds from 0 to 200 km/h with different combinations of SNR and Nakagami parameter m.

3.5.1 Simulation Result in AMC Mode

In AMC permutation mode, a total of 433 subcarriers were used for data and pilot transmission where the left guard subcarriers were 40 and the right guard subcarriers were 39 in 512 FFT points. For 1024 FFT point, 865 subcarriers were used for data and pilot transmission, where the left guard subcarriers were 92 and the right guard subcariers were 91. One subcarrier was used for DC or null values for both 512 and 1024 FFT. Figure 3.1 shows the BER at various vehicular speeds from 0 to 50 km/h for different SNR values and $m = 0.5$. It was observed that at low vehicular speeds, SNR has a big impact on overall BER, but as the speed increases, SNR has an insignificant impact on the BER (Figure 3.1 and 3.2) , a reason why special attention is required for resource management at vehicular speeds for facilitating applications requiring high data rates.

It is evident that the BER increases with increasing vehicular speeds and the system experiences severe fading at high vehicular speeds (Figure 3.3). In the Nakagami-m model, the fading severity of the channel is depicted by the parameter m . Figure 3.4 shows BER at 200 km/h speeds for $m = 0.5$.

Figure 3.5 shows BER of the channel for various values of m at a speed ranging from 0 to 200 km/h. Figure 3.6: shows BER of the system, which decreases with increasing Nakagami parameter m. When the value of m is 0.1, BER is relatively high due to the severe fading and when the value of m is 0.9, BER is relatively low. Figure 3.7 shows the BER at 50 km/h and 100 km/h speeds at different values of m with SNR 5 and 10. It is shown in this figure that in a high fading severity channel, impact of low and high SNR is the same.

It is shown in Figure 3.8 that Rayleigh fading fails to model severe fading at high vehicular speeds and the BER increases only marginally even at very high vehicular

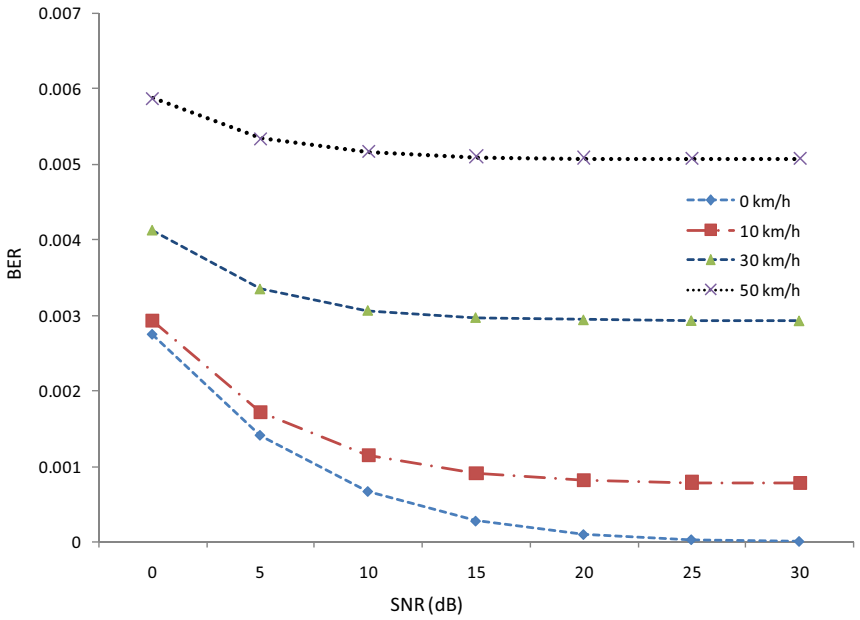

Figure 3.1: BER at vehicular speeds for Nakagami−m (m=0.5) fading channel on 512 FFT point for AMC permutation mode.

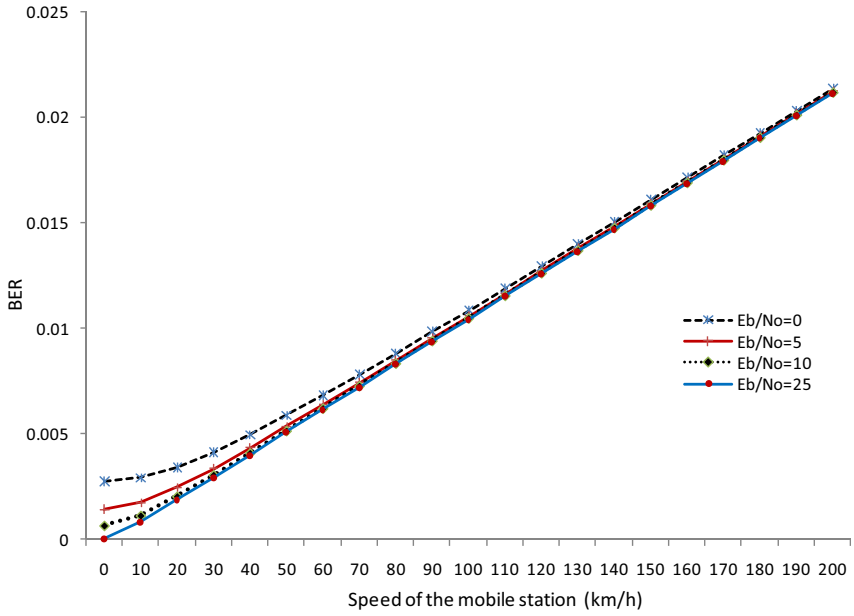

Figure 3.2: Impact of SNR at high speeds.

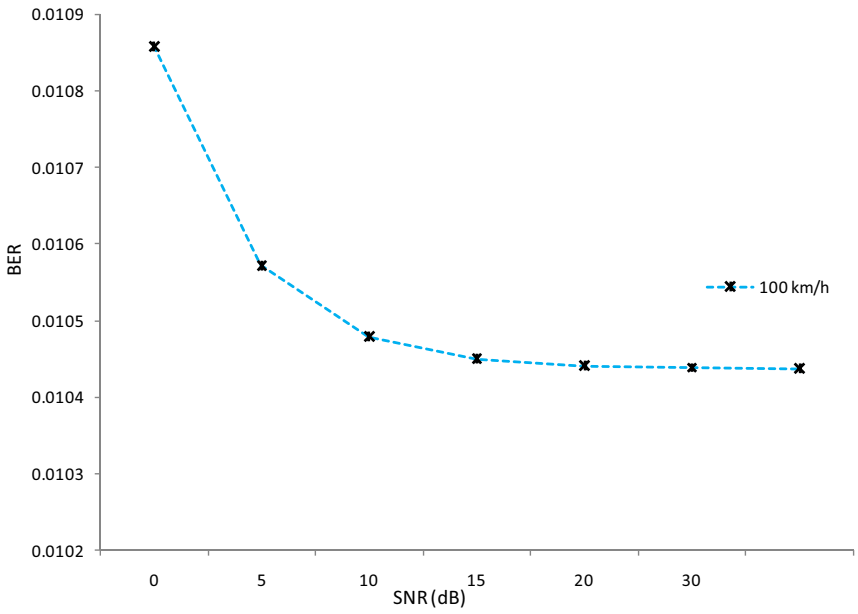

Figure 3.3: BER at 100 km/h for various SNR values on 512 FFT system for AMC permutation mode.

speeds. The biggest advantage of the proposed analytical model (equation 3.25) is that the same model works perfectly fine when the mobile node changes its speed, resulting in various scales of fading severity. For example, when the mobile node is static and has good line of sight communication, the fading model can be modeled using Rician fading and this can be achieved by setting m value greater than 1. When the node moves at low to medium speeds, Rayleigh fading can be modeled by setting the m parameter value as 1. A more severe fading can be reflected by setting the $m < 1$ in Equ. (3.25). As such, the proposed model is a perfect fit for BER estimation in WiMAX communication at vehicular communications.

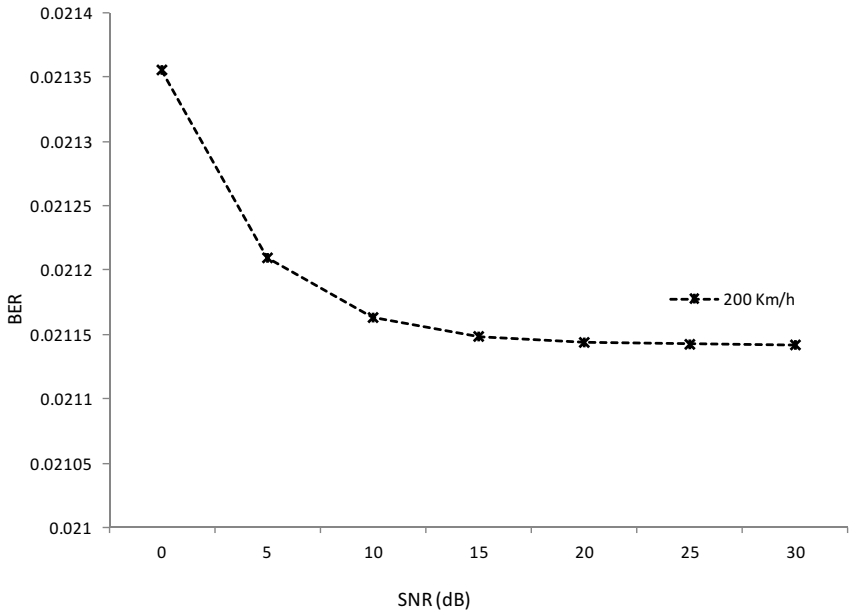

Figure 3.4: BER at 200 km/h speed with different SNR on 512 FFT system for AMC permutation mode..

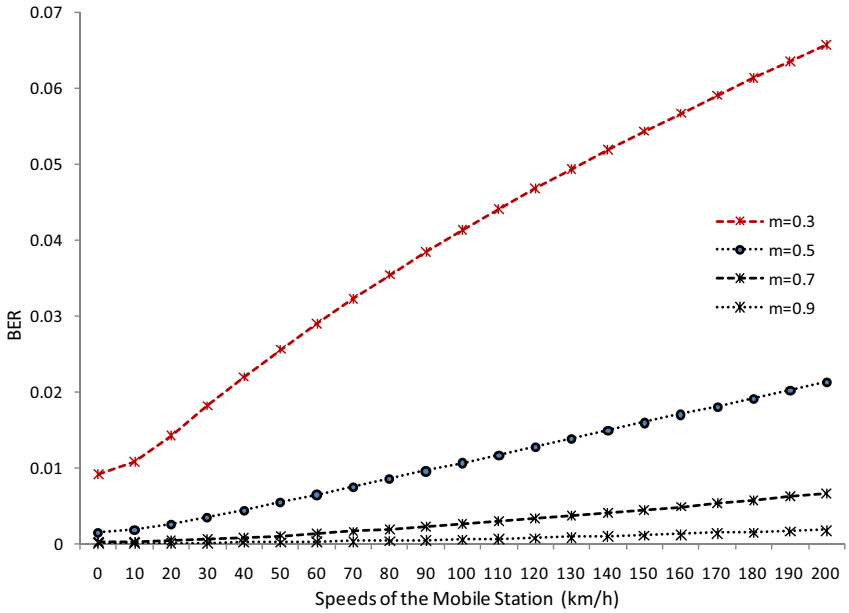

Figure 3.5: BER at various speeds for various values of m on 512 FFT point for AMC permutation mode.

Figure 3.9 shows the BER on different vehicular speeds from 0 to 200 km on 1024 FFT and different values of Nakagami parameter m. Figure 3.10 shows the comparative BER of 512 and 1024 FFT. Results show that at low speeds, SNR has different impacts for both 512 and 1024 FFT but BER shows the same result for both cases. Figure 3.11 shows that at severe fading environment in low speed movement, high SNR improves the BER but at high speed at severe fading, high

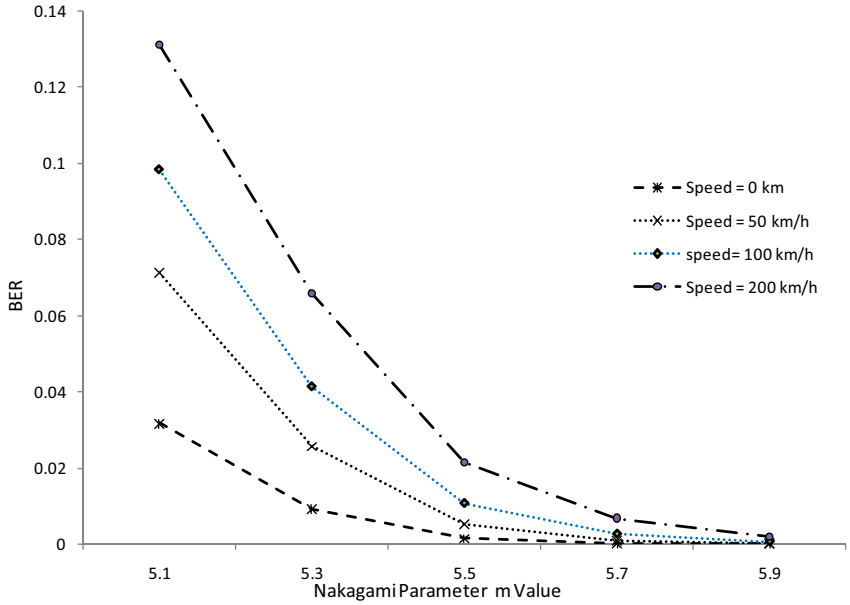

Figure 3.6: BER for different values of Nakagami parameter m on 512 FFT point for AMC permutation mode.

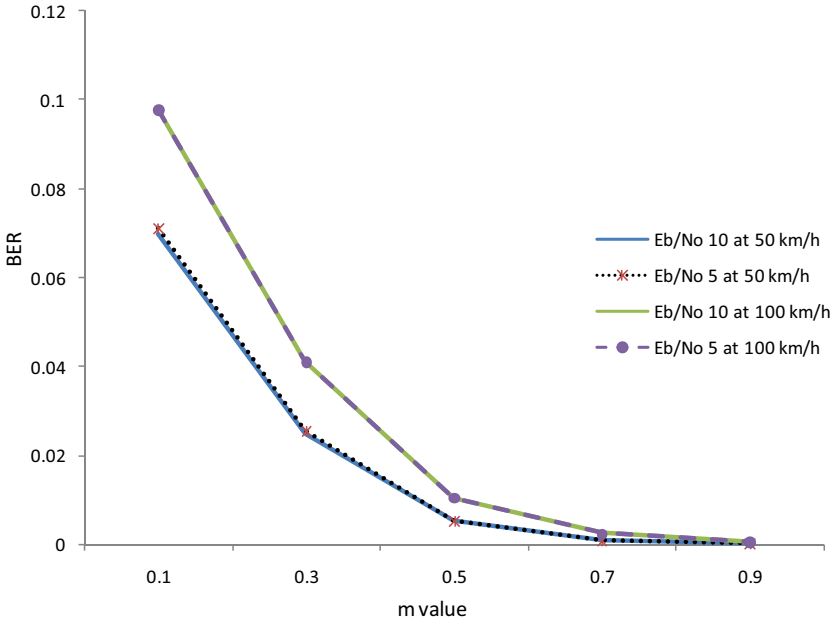

Figure 3.7: BER for different values of m at 50 km/h and 100 km/h with different SNR for 512 FFT.

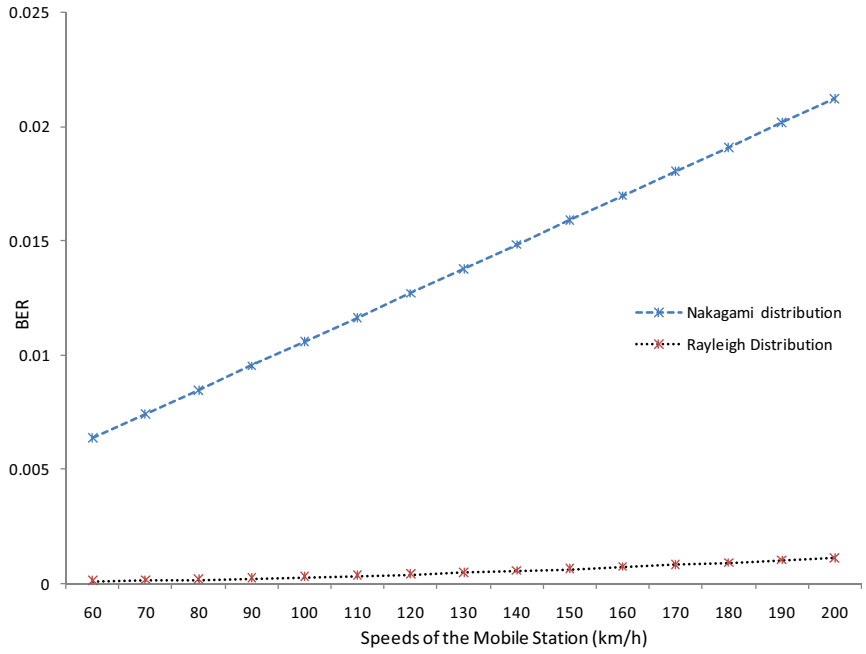

Figure 3.8: Comparative BER at vehicular speeds between Nakagami-m and Rayleigh model on 512 FFT point for AMC permutation mode.

and low SNR values have insignificant impact.

3.5.2 Simulation in PUSC mode DL

We also studied BER performance at high vehicular speeds using PUSC permutation mode. The PUSC is a mandatory permutation mode for mobile WiMAX system [21]. According to IEEE 802.16m standard [20], in UL PUSC mode a total of 409 subcarriers are used for pilot and data transmission; 52 subcarriers for left guard and 51 subcarriers are for right guard on 512 FFT. For 1024 FFT systems, a total of 841 subcarriers are used for data and pilot transmission, with 92 subcarrier for left guard and 91 for right guard. We ran the simulation on PUSC mode for both 512 and 1024 FFT point using QPSK/4-QAM modulation.

Figure 3.12 shows the BER at different vehicular speeds in UL PUSC mode considering the channel is severely fading where the Nakagami constant considered $m = 0.1$. The figure shows that at low speeds it is possible to improve the throughput with increasing SNR, which is the same nature with AMC permutation. But at high speeds it has no impact. It is necessary to find a different technique to improve the throughput at high speeds.

Figure 3.13 shows the BER for UL PUSC mode at different vehicular speeds. The figure shows that BER decreases with increasing speeds. Figure 3.14 shows

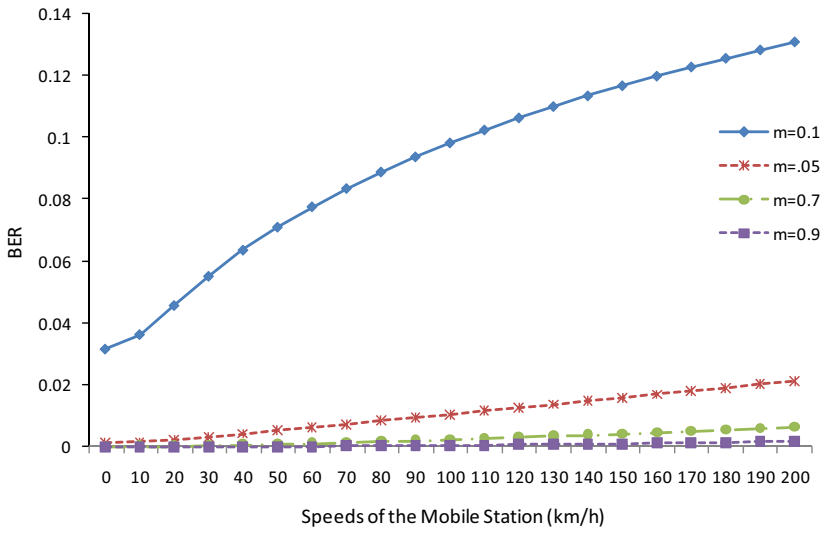

Figure 3.9: BER in a 1024 FFT system with 5 dB SNR for different value of m.

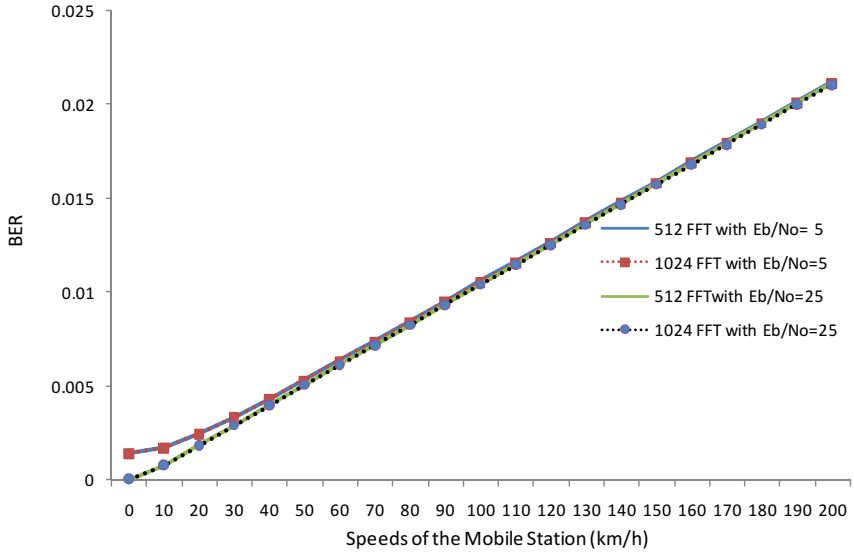

Figure 3.10: Comparative BER of 512 and 1024 FFT mode at different vehicular speeds.

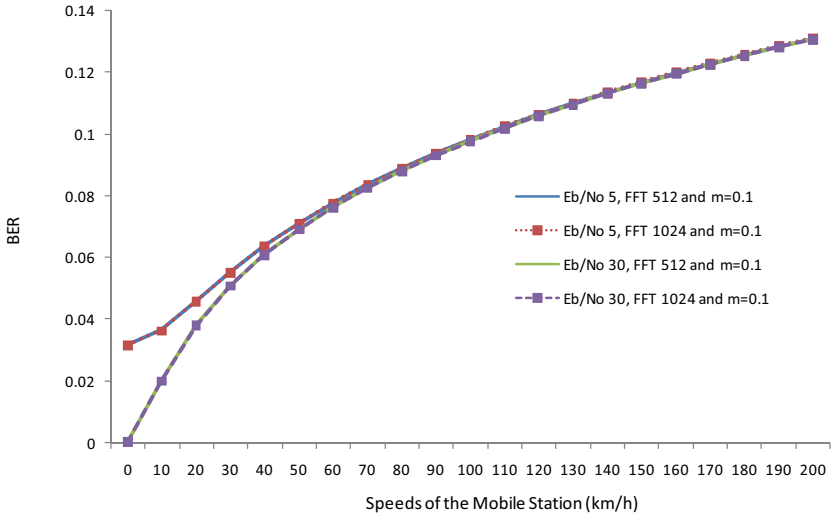

Figure 3.11: BER at Low SNR and high SNR at Nakagami parameter $m = 0.1$.

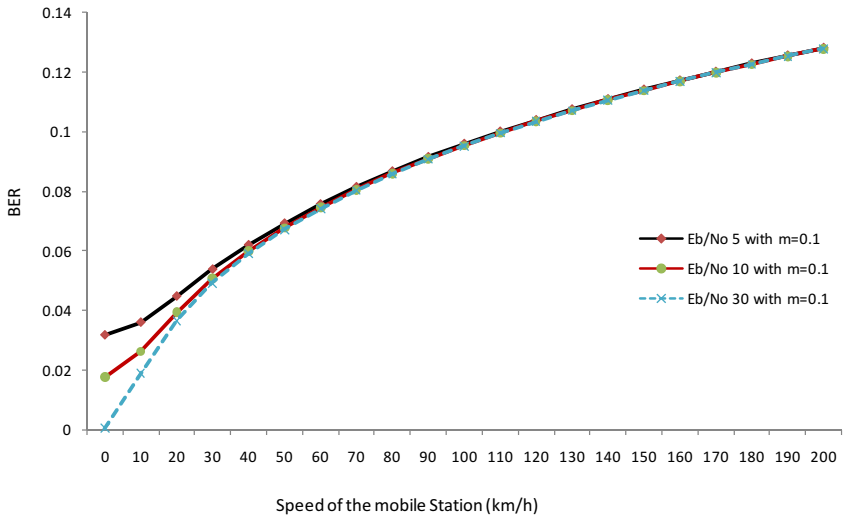

Figure 3.12: BER AT PUSC mode at different vehicular speeds with different SNR and $m = 0.1$.

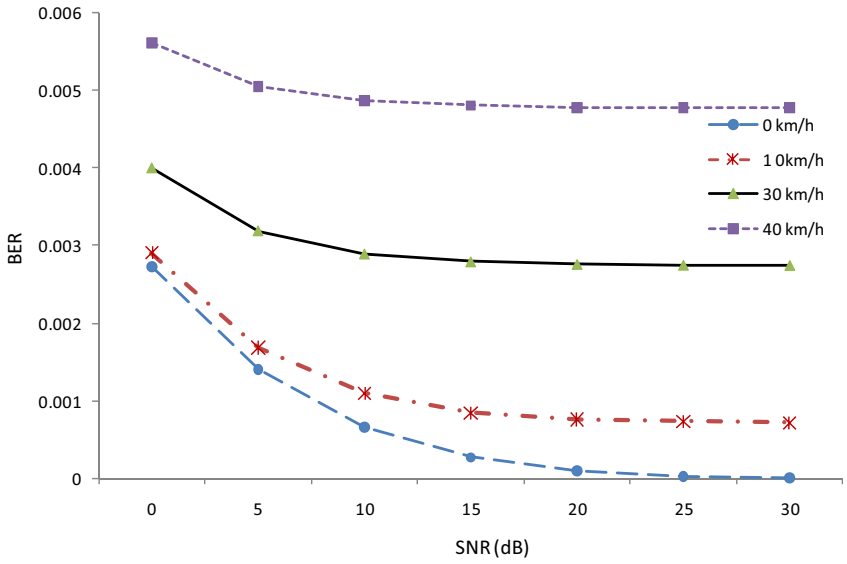

Figure 3.13: BER at various vehicular speeds at UL PUSC mode at $m = 0.5$.

BER at 120 km/h at UL PUSC mode where $m = 0.5$. Figure. 3.15 shows the BER increasing with decreasing m. Figure 3.16 shows comparative BER at 100 km/h speeds between PUSC and AMC permutation mode, at fading parameter $m = 0.5$. The figure shows that the PUSC mode provides a better result than the AMC mode. So we can say at severe fading channel, the PUSC mode performs better then the AMC mode. Figure 3.17 shows that at less fading condition where $m = 0.5$, the BER for both PUSC and AMC are the same, but in severe fading where $m = 0.1$ the BER at PUSC mode is less than the AMC mode. Figure 3.18 shows the comparative BER of PUSC and AMC at 1024 FFT point. The result also shows that at high vehicular speeds the PUSC mode works better than AMC mode.

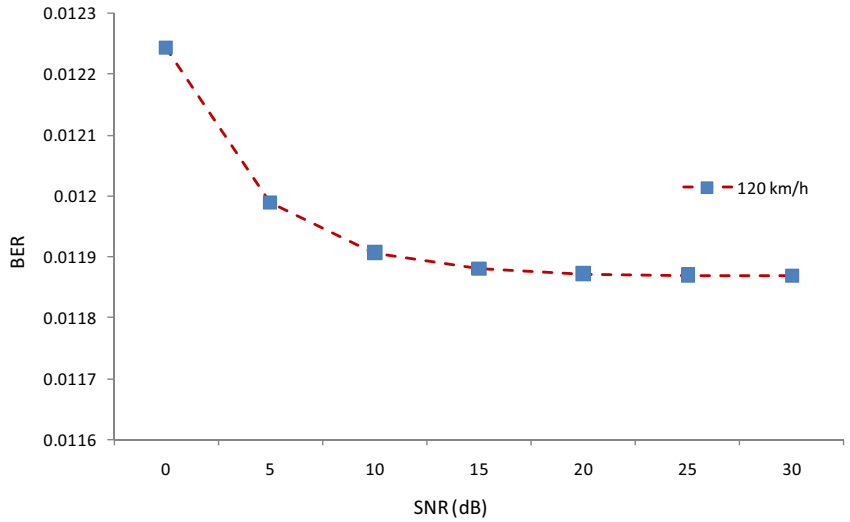

Figure 3.14: BER at the speed of 120 km/h with different SNR and m=0.5.

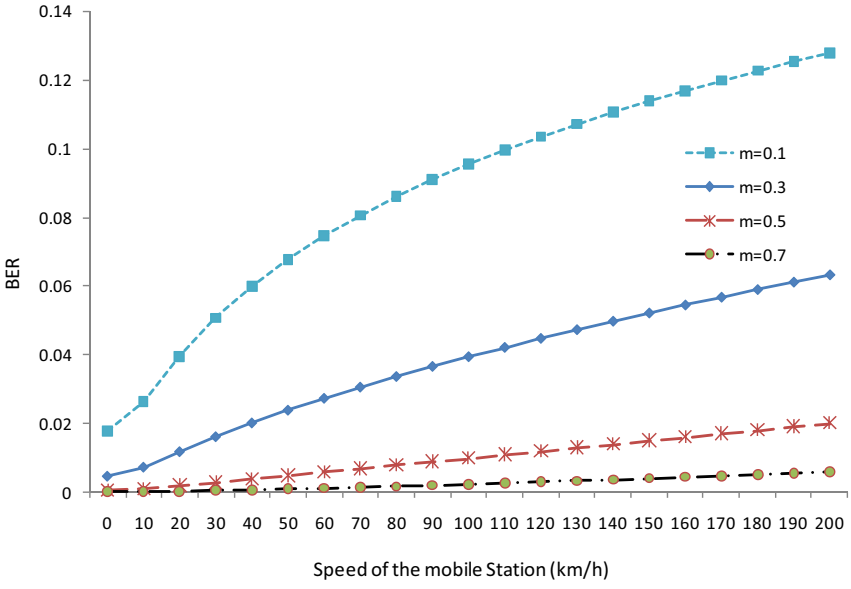

Figure 3.15: BER at various speeds with different values of m in UL PUSC mode .

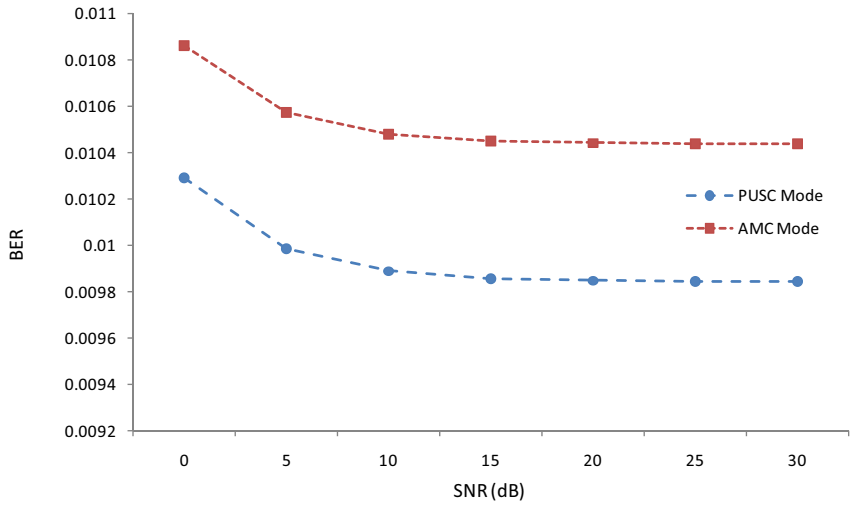

Figure 3.16: BER at 100 km/h speed of mobile station at PUSC and AMC.

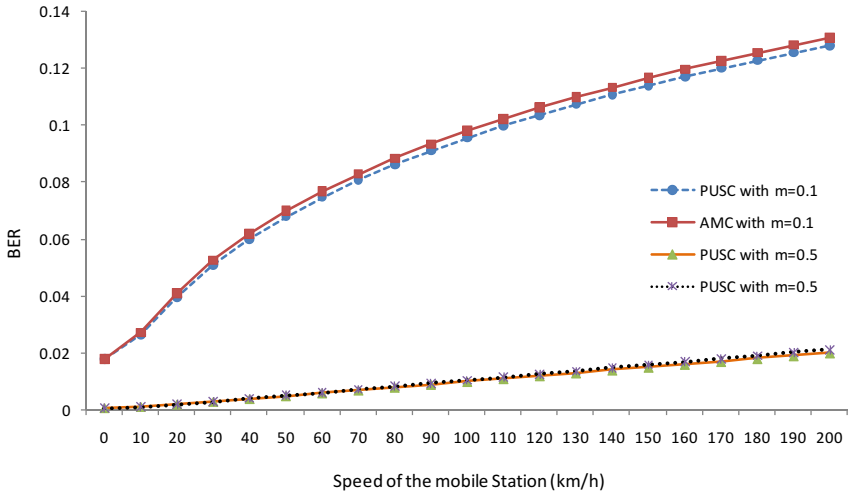

Figure 3.17: BER at severe fading for both PUSC and AMC.

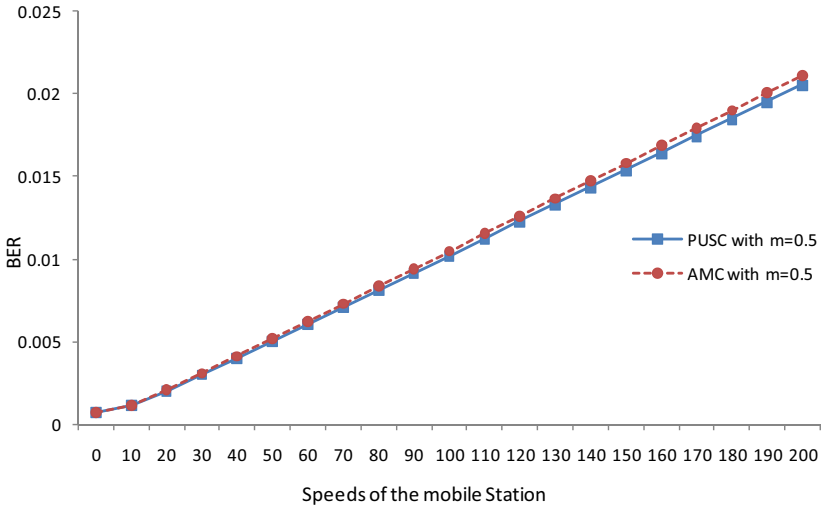

Figure 3.18: BER of 1024 FFT for PUSC and AMC mode.

The BER is a prerequisite measurement to compute a puncturing rate for FEC, and FEC is a part of channel coding to prevent and correct the transmission error of wireless systems. According to the WiMAX system profile, CTC is the mandatory FEC code for mobile WiMAX. The estimated BER at various speeds in this chapter can be used in coding schemes that will proactively adjust its FEC code size, so that packet error rate at the receiver end will be minimized, and this will improve the received throughput. The BER after the FEC process can be taken into account by the CAC scheme while accepting/rejecting new connections. This process will improve the QoS and throughput of on-going connections.

3.6 Summary

In this chapter, an analytical model has been presented that estimates BER in WiMAX communication at vehicular speeds using the Nakagami-m fading model. Due to its high estimation accuracy in wireless communications, the Nakagami-m model has attracted increasing attention from researchers in recent years and challenged the popularity of other models such as the Rayleigh model, The proposed model can also be used with LTE DL channel which uses similar OFDMA technique. Study shows that the BER has a relation with the Nakagami parameter m and BER increases with decreasing m. It is necessary to estimate the accurate m for vehicular speeds. Using the accurate m for specific speed the proposed model will calculate the accurate BER for that speed. In the next chapter, we present a study which

shows the relationship between Nakagami parameter m and vehicular speeds.

Chapter 4

Estimation of Nakagami Parameter m in WiMAX Communication at Vehicular Speeds

Accurate estimation of the Nakagami parameter m is required for an accurate BER calculation in the Nakagami fading channel. It is shown in chapter 3 that the BER increases with increasing fading severity. The Nakagami parameter m defines the fading severity of the channel and the fading increases with decreasing values of m. Accurate estimation of m at specific speeds will provide an accurate BER for that speed. In this chapter, we present an analysis on how the m values changes at various vehicular speeds.

4.1 Introduction

In chapter 3, we showed how to calculate the BER for different values of m. The motivition was to develop a more practical BER estimation technique for nodes moving at vehicular speeds. We used the Nakagami-m distribution model as it is efficient and can be made adaptive in response to the speeds of the moving nodes. The parameter m in the Nakagami-m model is given as

$$m = \frac{\Omega^2}{E[(\gamma_s^2 - \Omega^2)2]} \tag{4.1}$$

where Ω is the local power and γ is the i.i.d random variables. The local power is

derived from the equation

$$\Omega = E[\gamma^2] \tag{4.2}$$

To estimate the local power, it is necessary to determine the Received Signal Strength (RSS) [97] and the instantaneous RSS is treated as a random variable [98] [85] for stochastic distribution used in wireless communication.

To estimate m, we have collected RSS from a commercial WiMAX communication system providing service for Australian stakeholders. The system, environment and data collection procedure and data analysis are described in the following section.

4.2 Systems, Environment and Estimation Procedure

A. System

We have collected data from a BTS of a Vivid wireless system located in Candle wood, Joondalup, WA, Australia (Figure 4.1). The BTS is set up with 4 Argus LLPX310R sectorized antennas which are installed at the top of the mast on a hill. The phase center of the antennas are 35.1 m with upright vertical orientation. The bearing degrees are 45, 150, 270, 50 for sector 1, 2, 3, and 4 respectively. Electrical down tilts (deg) are 0 to 10 (2) for sector 1, 0 to 10 (5) for sector 2, 0 to 10 (2) for sector 3 and 0 to 10 (4) for sector 4. The mechanical downs tilts are 0^0 for all antennas with +45 slant pole for down tilt and -45 slant pole for up tilt of 38.5 dBm and the standard band power per port is 44 dBm. Each of the antennas is 1.125 m long. The center frequency of the systems is 2.3 GHz with 10 MHz BW. The system uses the TDD radio access method with AMC techniques with QPSK, 16-QAM, 64-QAM for DL. The coding techniques are CC and CTC. The QoS management of the systems are ertPS, nrtPS, rtPS and BE.

To estimate the m at first we have collected the RSS using a USB modem. The dimension of the USB modem is 77x28x10 mm and weight is 22g with a plug and play USB 2.0 interface. The transmitter power of the USB is 23 dBm with power consumption <1.75 W. The antenna configuration is 2Rx 1Tx and MIMO configures

Figure 4.1: BTS where the WiMAX transmitters are located

are Matrix A and B. The power control system of the USB are open and closed loop (Adaptive modulation). When it makes connection, the system shows the RSS, data speed and SINR of the signal

The USB modem was installed in a laptop with Windows XP professional 32 bit version with service pack 3 and 2GHz RAM. The desktop recording software CamStudio was installed in the laptop for continuous recording RSS.

B. Environment

The BTS is installed in a heavily populated hilly suburban residential area (Figure 4.1) with huge numbers of trees at both side of the road. Most of the houses are one or two storey buildings with tiles and colour bond or Zinkalume roofes (Figure-4.2). The BS location is at $31^o43'41.18''$ south, $115^o45'52.55''$ east and 75 metre above sea level next to a shopping center (point T in Figure 4.2).

The data was taken in road 1 (Figure 4.4) in the built up area from the point A at $31^o43'54.83''$south, $115^o45'45.22''$ east and 62 metre above sea level to point B of $31^o43'34.92''$south $115^o45'59.00''$ east and 64 metre above sea level . In road-1, from point A to A-1, there is no NOLS communication between car and the Tx, and the terrain is similar between these two points. From point A-1 to A-2, a LOS communication is available and from point A-2 to B, again there is no LOS communication.

In road 2, data was taken from the point C at $31^o43'44.49''$south, $115^o45'48.32''$east and 73 metre high above sea level to point D of $31^o43'46.01''$ south, $115^o45'32.10''$ east and 68 metre above sea level (Figure 4.3). In this road, there is a LOS communication between the car and the Tx from points C and C-1, but from point C-1 to

Figure 4.2: Environment of the location where the BS

point C-2, there is LOS communication and from point C-2 to point D there is no LOS communication again.

In road 3, data was taken from point E at $31^o43'55.12'$ south , $115^o45'28.69''$ east and 67 metre high of the sea level to point F of $31^o43'39.18''$ south, $115^o45'24.35''$east and 43 metre above sea level (Figure 4.3) and there is no LOS communication between the car and the Tx at any point, but the obstruction between points E-1 to F is heavier than the points E to E-1. The roads along 1, 2 and 3 are located in a built up area and there are a number of high trees on both sides of the road. Due to the hilly area, all the roads are undulating and are twisting.

Finally the data was taken in road 4 from point G of $31^o45'04.68''$ south, $115^o45'39.39''$ east and 40 metre above sea level to point H of $31^o43'58.23''$ south, $115^o45'14.62''$ east and 52 metre above sea level (Figure 4.5). In road-4, there is no LOS communication between points G to G-1. But from points G-1 to G-2 there is LOS communication and again from point G-2 to H, there is no NOL communication. It is a freeway with a speed limit of 100 km/h. The freeway consists of three car lanes with two emergency stopping lane each direction. The distance between the two left emergency lanes is around 100 metres.

Figure 4.3: Environment of the Freeway

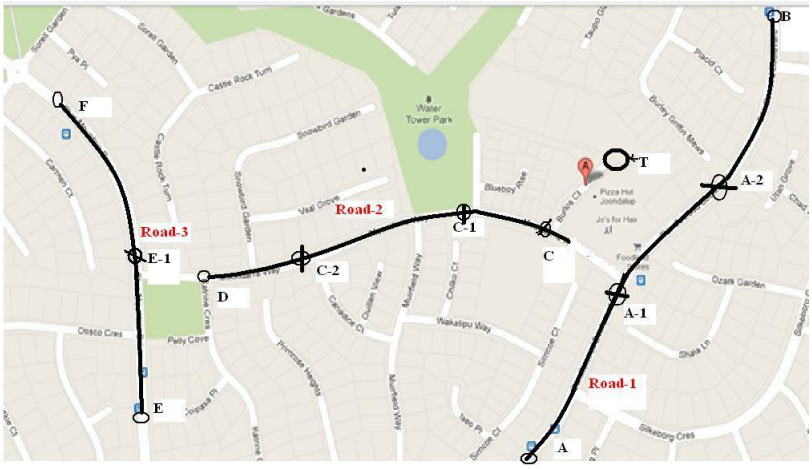

Figure 4.4: Road 1, 2 and 3 where the data has taken from 10 to 50 km/h speeds

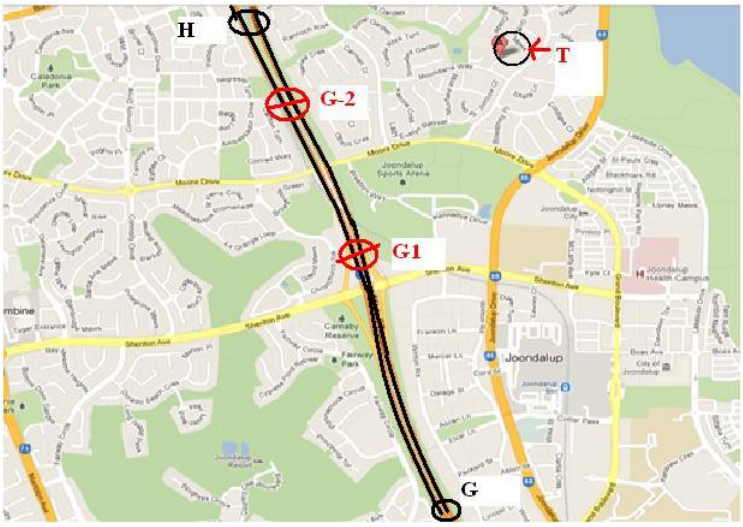

Figure 4.5: Road 4 where the data has taken at 70 to 100km/h speeds

C. Procedure

To record the RSS at vehicular speeds, a laptop was placed in the passenger seat of a car next to the driver. After making the connection using the USB modem the CamStudio software was turned on to record the RSS (Figure 4.6). Firstly the data was taken while stationary at points of every 100 metres approximately.

In the stationary condition, the data was taken in the direction A to B from road 1, direction C to D on road 2 and direction E to F on road 3. Then mobile data was taken at vehicular speeds of 10, 20, 30, 40 and 50 km/h on each direction five times respectively. i.e. total of 5 times each speed each direction, 10 times for both directions for each speed in one road. A total of 50 times each road and 150 times in three roads in the buildup area.

On the freeway, the stationary data was taken in the left emergency lane in each direction every 100 metres as for the built up area road. Then the mobile data has taken at speeds of 60, 70, 80, 90 and 100km/h during the peak hour and off peak hours at night when there was a small number of car on the road. Data was taken 5 times for each speed in both directions. During the peak hour a total of 50 drive tests were taken on the freeway in each direction. To compare the nature of RSS fluctuations 5 drive tests was taken in each direction of 70 km/h in off peak hours. Figure 4.7 shows the RSS nature at peak hours during the day time and off peak hours at mid night when there were a fewer cars on the road. The result shows that there is no significant effect of variation during the peak hours and off peak hours. The study shows that 20 RSS were recorded every minute. So for slower speeds the total recorded data is higher then the higher speeds.

4.3 Result Analysis

The instantaneous RSS is known as the random variable which is treated as data for this study. Figure 4.8 shows the RSS nature at stationary mode in road 1 at 8 different points. It is shown that the RSS is different at different points. The cause of this difference is the nature of the obstruction between the Tx and Rx and the RSS is low when the obstruction is heavier and is mainly due to foliage. This data was taken into consideration in estimating the Nakagami m values of that point. The value of m at these points are 0.6, 0.5, 1.7, 1.5, 2, 0.6, 0.9 and 0.9 for point 1,

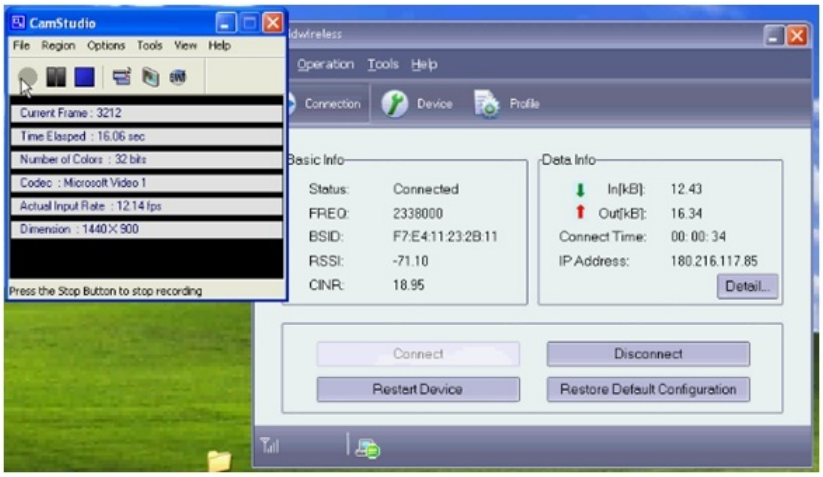

Figure 4.6: Data recording screen shot

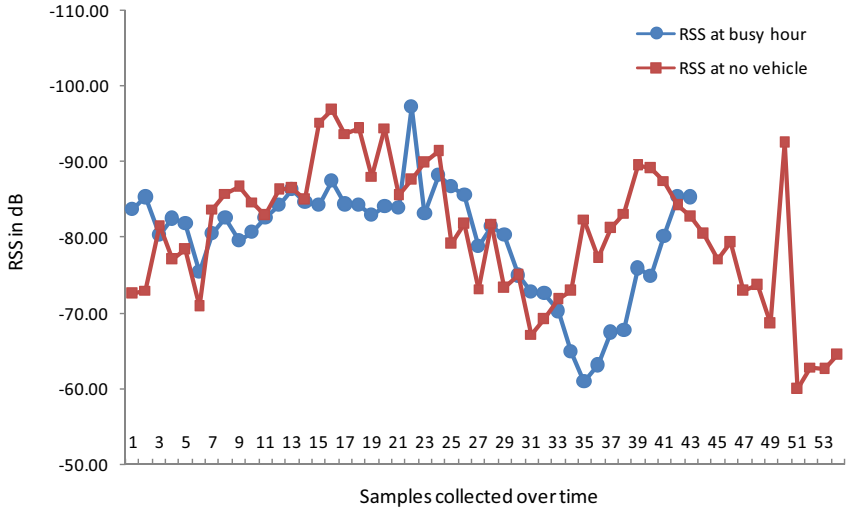

Figure 4.7: Received RSS at 70 km/h during peak hour at day time and off peak hour at midnight.

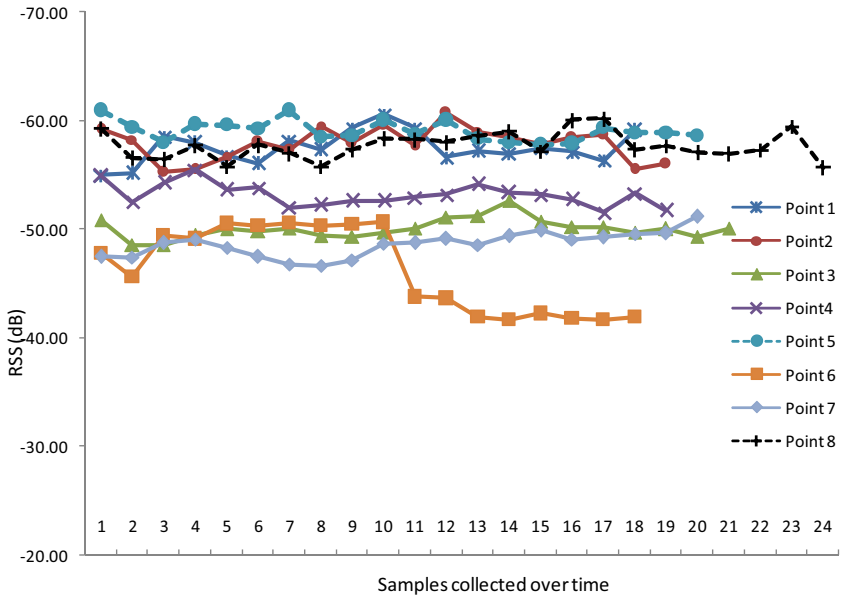

Figure 4.8: RSS fluctuation at static mode in road 1.

Table 4.1: RSS (dB) at stationary mode in road 1 in different points

Min RSS	Max RSS	Diff (dB)	Avg RSS	m	Note
-60.59	-55.00	5.59	-57.53	0.6	NLOS
-60.73	-55.26	5.47	-57.89	0.5	NLOS
-52.62	-48.53	4.09	-50.06	1.7	LOS
-55.49	-51.59	3.90	-53.20	1.5	LOS
-60.97	-57.79	3.18	-59.08	2.09	LOS

point 2, point 3, point 4, point 5, point 6, point 7 and point 8, respectively on the road.

In road 3, data was taken at six different points in stationary mode and the m value becomes 0.7, 2.4, 0.4, 0.5, 0.8 and 0.4 for the point 1, point 2, point3, point4, point5 and point 6, respectively. Table 4.1 shows the RSS for LOS and NLOS communication between Tx and Rx. The table shows that when there is a NLOS communication between the car and Tx, the $m < 1$ and when the communication is LOS, the $m > 1$. Table 4.2 shows the values of m at different points in different roads. It is shown that the fading nature at some points is Rician ($m > 1$), at some points is Rayleigh ($m = 1$) and at some points the fading nature is Nakagami ($m < 1$). It is observed that at some points the values m decrease to 0.2.

Tables 4.3, 4.4 and 4.5 show the maximum, minimum and average RSS on the three roads, respectively, at different vehicular speeds for both directions.

The study shows that the receivers receive RSS every three seconds either at

Table 4.2: Values of Nakagami m parameter at different points in static mode

Road no	P-1	P-2	P-3	P-4	P-5	P-6	P-7	P-8	P-9	P-10	P-11	Direction
Road 1	0.6	0.5	1.7	1.5	2.09	0.6	0.9	0.9	-	-	-	A-B
Road 2	0.8	0.4	0.8	0.6	0.6	0.3	-	-	-	-	-	C-D
Road 3	0.8	2.4	0.4	0.5	0.8	0.4						E-F
Road 4	1	0.3	0.74	2.9	1	0.2	0.4	0.9	1.8	0.5	0.5	G-H
Road 4	2.5	1.9	4	0.7	0.8	0.9	1	0.2	0.5	0.8	0.2	H-G

Table 4.3: RSS (dB) on road 1 in built up area

	Down (From point A to B)			Up (From point B to A)		
Speed	Min RSS	Max RSS	Avg RSS	Min RSS	Max RSS	Avg RSS
10km/h	-66.76	-55.77	-61.04	-63.28	-54.26	-58.88
20km/h	-66.26	-56.84	-61.95	-65.06	-55.58	-60.16
30km/h	-68.75	-55.88	-62.02	-64.80	-54.94	-60.49
40km/h	-67.38	-56.44	-61.97	-67.26	-55.17	-60.75
50km/h	-66.28	-55.38	-61.58	-68.78	-52.93	-61.05

Table 4.4: RSS (dB) in road 2 at built up area

	Down (From point C to D)			Up (From point D to C)		
Speed	Min RSS	Max RSS	Avg RSS	Min RSS	Max RSS	Avg RSS
10km/h	-66.83	-55.76	-62.05	-65.37	-58.83	-62.41
20km/h	-66.56	-54.65	-60.83	-67.25	-57.14	-62.56
30km/h	-67.38	-55.52	-62.23	-67.70	-56.64	-63.71
40km/h	-68.56	-55.46	-63.44	-67.07	-55.27	-60.905
50km/h	-78.28	-54.02	-64.36	-68.89	-53.46	-60.60

Table 4.5: RSS (dB) in road 3 at built up area

	Down (From point E to F)			Up (From point F to E)		
Speed	Min RSS	Max RSS	Avg RSS	Min RSS	Max RSS	Avg RSS
10km/h	-73.16	-64.88	-69.09	-75.54	-63.84	-70.10
20km/h	-74.29	-64.53	-69.44	-79.09	-68.84	-74.76
30km/h	-73.84	-63.19	-68.90	-81.63	-66.38	-74.79
40km/h	-79.67	-64.69	-72.54	-78.40	-64.76	-71.68
50km/h	-84.21	-63.9	-73.15	-85.12	-66.88	-75.53

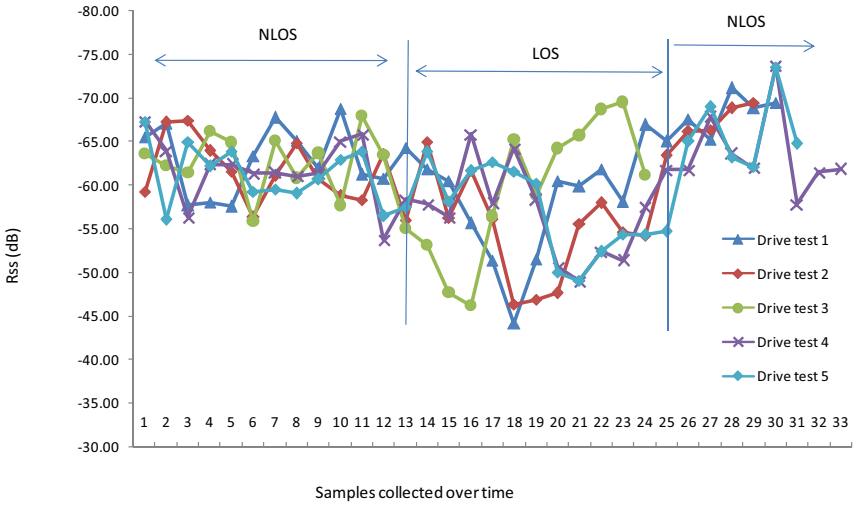

Figure 4.9: Nature of RSS on road 1 for different drives at 30km/h speeds

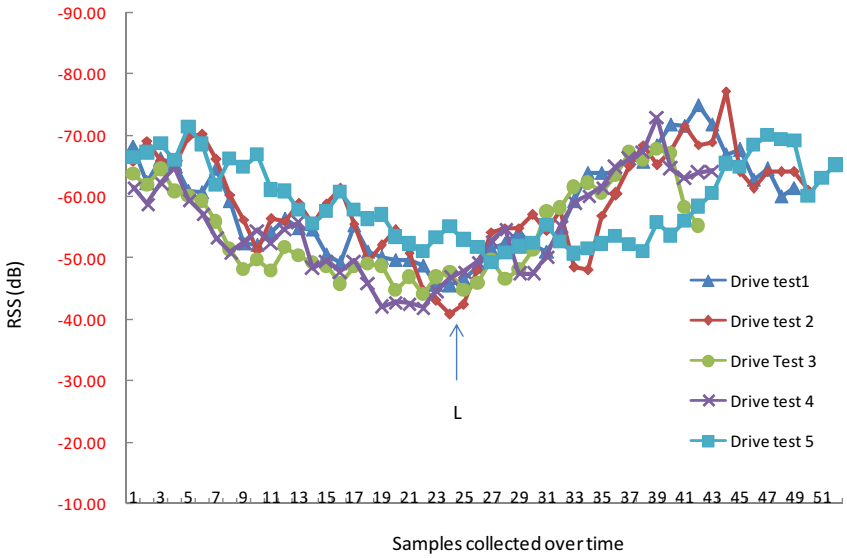

Figure 4.10: Nature of RSS on road 2 for different drives at 10km/h speeds

stationary or mobile mode. Due to the movement of the mobile station after three seconds, the mobile station changes its position and receives the RSS at its new position. The RSS of the new position may be high or low depending on the obstruction between the Rx and Tx. Figure 4.9 shows the nature of the RSS on road 1 at 30 km/h speeds. It shows that at the NLOS area the RSS is lower than the LOS area.

Figure 4.10 shows the RSS on road 2 at 10 km/h increments. It is shown that the RSS changes with time and position. In figure 2, the highest strength of the RSS is received at point L and at this point there is a LOS communication between the

Table 4.6: RSS statistics for different vehicular speeds

Speeds (km/h)	Passing distance (m)/Sec	Passing distance(m) when receive one data
10	2.78	8.33
20	5.56	16.67
30	8.33	25.00
40	11.11	33.33
50	13.89	41.67
60	16.67	50.00
70	19.44	58.33
80	22.22	66.67
90	25.00	75.00
100	27.78	83.33

car and the Tx. At the beginning of this road, obstructions are one story houses and trees. At point L, the obstruction is trees only but there is a LOS communication between the car and the Tx. Again after a certain point, the obstructions are both house and trees. It is shown in this figure that the RSS has increased up to point L and then decreased. It is evidence that the RSS changes with the obstruction. It is observed that at the NLOS area the RSS is lower than the LOS area. Figures 4.9 and 4.10 show that the RSS at a certain point is different from another point. To estimate the Nakagami shape parameter m we considered the received data from the NLOS area.

At different speeds, the RSS are different. It is shown that at 10 km/h speed the system recorded one data (RSS) per 8.3 metre passing distance, but at 50k/h speed the Rx receives one data (RSS) per 42 metre distance. Table 4.6 shows the passing distances of MS for each data receiving time. At the same distance, the number of recorded RSS is higher at low speeds than at high speeds. To estimate the value m, we considered the same number of data for different speeds.

Figure 4.11 shows that the nature of the RSS at vehicular speeds from 70 to 100 km/h. Figure 4.12 shows the RSS nature at 70 km/h speeds for different drives. Figure 4.13 shows the RSS nature at 100 km/h speed on the freeway. It is shown that the nature of the RSS is nearly the same for all the drives at the same speeds.

For any road where the obstructions natures are the same, the study shows that the value of m decreases with increasing speeds. Figure 4.14 shows the m values at different speeds from 10 - 50 km/h on built up suburban roads and figure 4.15

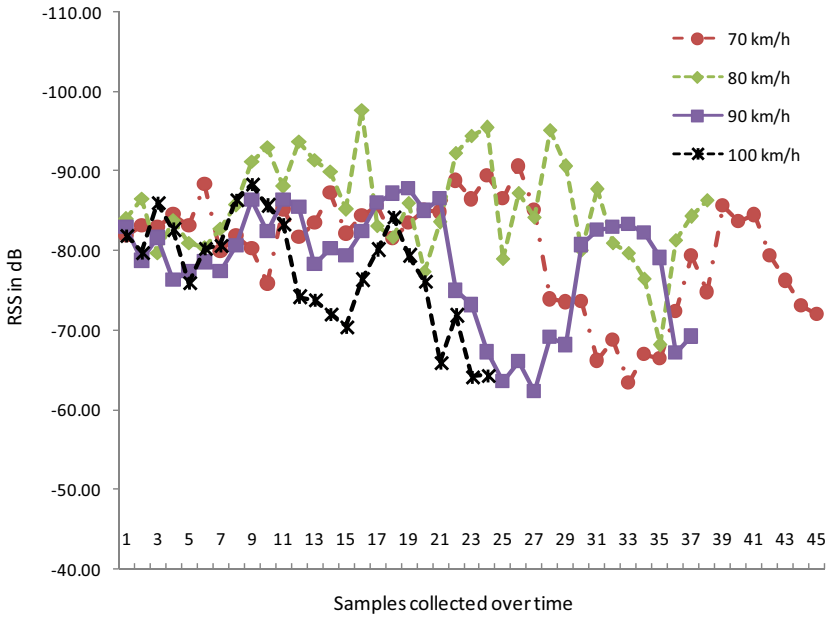

Figure 4.11: Nature of RSS on freeway at different speeds

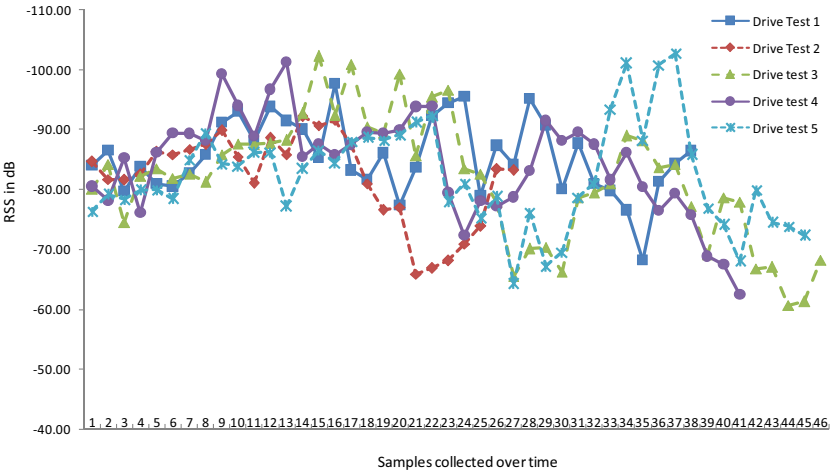

Figure 4.12: Nature of RSS on freeway for different drives at 80km/h speeds

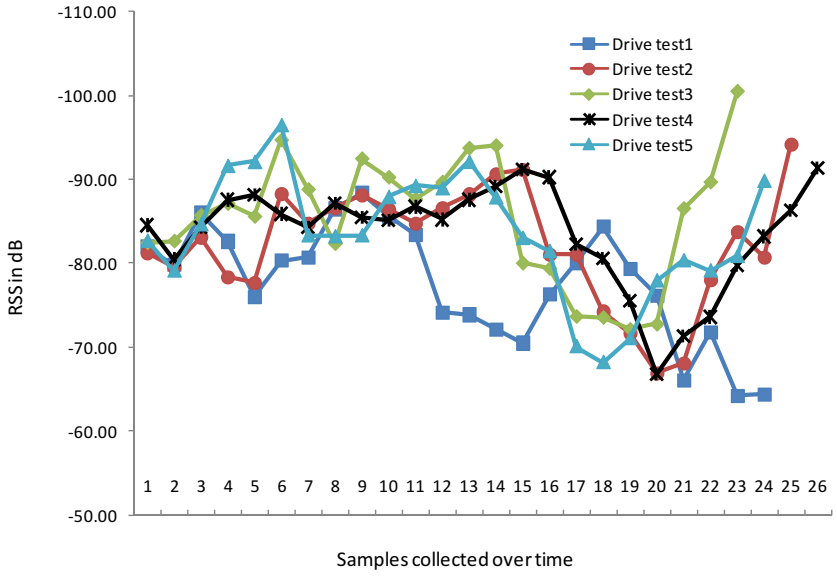

Figure 4.13: Nature of RSS on freeway for different drive at 100 km/h speeds.

shows the m values at different speeds on different roads from 70 - 100 km/h speeds on the freeway. It is shown in the result that the m is different for each direction on any road.

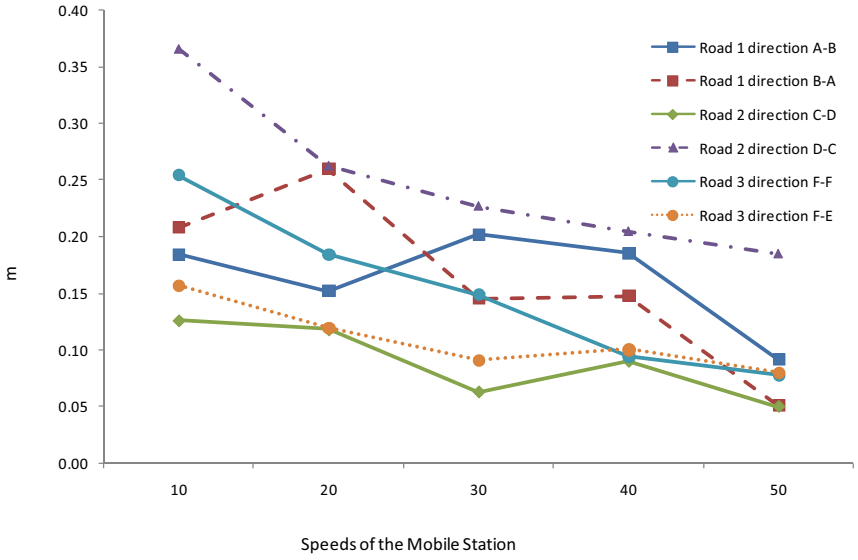

Figure 4.14: Values of m at different vehicular speeds in roads at built up area for both direction

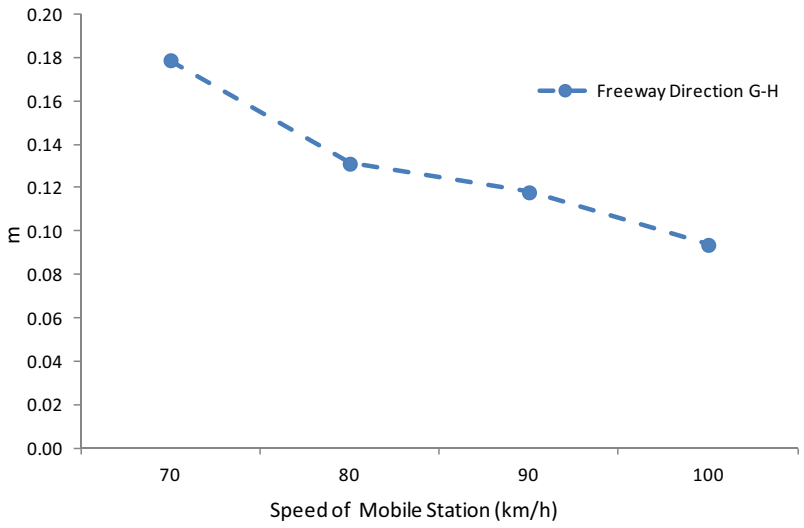

Figure 4.15: m value at freeway for different vehicular speeds from 70 to 100 km/h.

4.4 Sumary

The Nakagami-m distribution model has attracted increasing attention from researchers in recent years. In the Nakagami m distribution, the shape parameter m defines the fading severity of the channel. In this chapter, we estimated the Nakagami m parameter at different vehicular speeds in WiMAX systems. This research shows that during NLOS communication in stationary mode the Nakagami m varies from 0.5 to 2.9 at different points. It is concluded that in a specific road, fading characteristics at some points are Rician, at some points Rayleigh and at some points Nakagami depending on the obstructions between the Tx and Rx. During the vehicular speeds the receiver receive the signal from different points and the instantaneous RSS may be high or low depending on the position of the receiver. For any standard environment, the values of m decreases with increasing speed. As we have seen in chapter 3, the BER changes with m. So an accurate value of m is required for an accurate BER. If we use the estimated values of m for specific speeds in equation 3.25 we can find the accurate BER for that speed.

Chapter 5

Conclusion and Future Works

5.1 Conclusion

The mobile WiMAX system is a good candidate for broadband and vehicle to infrastructure communication architecture, and this research focused on the WiMAX communications at vehicular speeds. The WiMAX system provides high throughput in stationary conditions, but at high vehicular speeds the throughput decreases sharply, to a level which is only sufficient to maintain the connection, but with no assurance of data. The doppler shift and dynamically changed multipath are the main causes behind the low throughput at vehicular speeds. In these circumstances, a proactive measure can improve the throughput at vehicular speeds that can support the transmission of high volume data, especially with multimedia content. BER is a measure of end to end performance of a system and the primary requirement for any proactive measure.

In this thesis, we presented a BER estimation model for estimating the BER at different vehicular speeds. To develop the BER estimation model, we used the Nakagami-m fading model. In the Nakagami-m fading model, the parameter m defines the fading severity of the channel. An accurate BER estimation at a certain speed demands an accurate value of m at that speed. To estimate the accurate m for vehicular speeds, we have collected instantaneous RSS at 10-100 km/h speeds from a WiMAX communication system, and analysed the received RSS for estimating the m value.

We can summarize our main contributions through this research as follows:

1. Firstly we have studied the different fading models that are used for BER

estimation at vehicular speeds. We chose the Nakagami-m fading model and developed a mathematical model for the BER estimation of WiMAX system using the Nakagami-m distribution model.

2. We have estimated the BER using the proposed model at different vehicular speeds. To estimate the BER, we considered the SNR from 0 to 30 dB and the value of the Nakagami parameter m from 0.1 to 0.9. It is shown that the BER increases with the increase of speed and BER decreases with the increase of the Nakagami parameter m. We also compared the BER of the proposed model with the BER from the Rayleigh distribution model.

3. In this thesis, we also estimated the value of m at different vehicular speeds for WiMAX communication systems from 10 to 100km/h. To estimate the value of m, we have collected data on different roads at vehicular speeds around a base station of a commercial WiMAX service provider, located in a hilly built up sub urban area. The study showed that at NLOS communication, the m decreases with increasing speed of the mobile station.

5.2 Future Works

Following the above results, some of the possible extensions of this research are:

1. Improving the throughput of WiMAX communication at vehicular speeds is essential for transmitting multimedia content. FEC is a method for improving the throughput, and for any FEC method, the BER estimation is the basic requirement. The next scope of this research is to develop a FEC process to improve the throughput. The researcher can use this estimated BER for the FEC process.

2. The call admission control (CAC) is a key element for a guaranteed QoS in wireless networks. The design of call admission control algorithms for mobile communication is a challenging issue due to its highly variability at vehicular speeds. The CAC scheme considers currents scenarios while making a decision whether to admit or reject a call. The existing CAC fails when the scenario changes dynamically at vehicular speeds. Following the achieved throughput at high vehicular speeds, the scope of the future research is to develop a new CAC scheme for vehicular application of WiMAX system.

3. The Level Crossing Rate (LCR) is a number of crossings of signals through

a given threshold level, and the Average Fade Duration (AFD) measures how long a signal's envelope stays below a given target threshold which is derived from the level crossing rate. To estimate accurate fading of the channel, the LCR and AFD estimation is essential. Following the proposed mathematical model; LCR and AFD estimation of WiMAX system at vehicular speeds is one of the possible extension of this research.

4. Handoff refers to the process of transferring an ongoing call or data session from one channel connected to the core network to another, and is one of the major issue for mobility management at vehicular networks. Handoff at high speed causes packet loss and service interruptions. Following the estimated LCR and AFD, future research is to develop new schemes for handoff at vehicular speeds.

5. The value of the Nakagami parameter m defines the fading severity of the channel. The estimated values of m can be used for further research to find out the threshold BER at different vehicular speeds.

Bibliography

[1] M. Salazar-Palma, T. Sarkar, and D. Sengupta, "The father of radio: A brief chronology of the origin and developments of wireless communication and supporting electronics," in *Telecommunications Conference (HISTELCON), 2010 Second IEEE Region 8 Conference on the History of*, nov. 2010, pp. 1 –8.

[2] "All about the technology, www.itu.int/osg/spu/ni/3g/technology/index.html, last accessed 26 june 2012."

[3] P. K. Kaveh Pahlavan, *Principle of Wireless Network*, ser. Prentice Hall communications Engineering and Emerging Technologies Series. New Jersey 07458: Prentice Hall PTR, 2002.

[4] "Report itu-r m.2134, "requirements related to technical performance for imt-advanced radio interface(s)" 2008," ITU, Tech. Rep.

[5] D. J. s. D. Amit Kumar, Dr. Yunfei Liu, "Evolution of mobile wireless communication network: 1g to 4g," *International Jounrnal of electronics and Communication Technology*, vol. 1, pp. 484–486, December 2010.

[6] D. Locke, "Research report on wimax and lte," Pyramid Research, 10 Central park, Tech. Rep., 2010.

[7] L. Garber, "Mobile wimax: The next wireless battle ground," *Computer*, vol. 41, no. 6, pp. 16–18, 2008.

[8] IEEE, "Draft ieee 802.16m requirments, ieee802.16m broadband wireless access working group, www.ieee802.org/16/tgm/docs/80216m-070-024r.pdf,, last accessed 23 sep 2011."

[9] P. Lombardo, G. Fedele, and M. Rao, "Mrc performance for binary signals in nakagami fading with general branch correlation," *Communications, IEEE Transactions on*, vol. 47, no. 1, pp. 44 –52, jan 1999.

[10] K.-W. Yip and T.-S. Ng, "A simulation model for nakagami-m fading channels, m lt;1," *Communications, IEEE Transactions on*, vol. 48, no. 2, pp. 214 –221, feb 2000.

[11] J. G. A. R. M. Arunabha Ghosh, Jun Zang, *Fundamentals of LTE*, 1st ed., ser. The Prentice Hall. Boston: Pearson Education, 2010.

[12] T. Koon Hoo, T. Zhifeng, and Z. Jinyun, "The mobile broadband wimax standard [standards in a nutshell]," *Signal Processing Magazine, IEEE*, vol. 24, no. 5, pp. 144–148, 2007.

[13] "A socio-economic analysis of wimax," in *Application of Information and Communication Technologies, 2009. AICT 2009. International Conference on*, oct. 2009, pp. 1 –6.

[14] S. Murawwat and K. Ahmed, "Performance analysis of 3g and wimax as cellular mobile technologies," in *Electrical Engineering, 2008. ICEE 2008. Second International Conference on*, 2008, pp. 1–5.

[15] W. C. Inc., "Can wimax address your application?" WiMAX Forum, Tech. Rep., 24 October 2005.

[16] L. Chaari and L. Kamoun, "An overview of mobility management over ieee802.16e," in *Telecommunications, 2009. ICT '09. International Conference on*, may 2009, pp. 334 –339.

[17] F. Wang, A. Ghosh, C. Sankaran, P. Fleming, F. Hsieh, and S. Benes, "Mobile wimax systems: performance and evolution," *Communications Magazine, IEEE*, vol. 46, no. 10, pp. 41 –49, october 2008.

[18] I. Ahmad and D. Habibi, "A novel mobile wimax solution for higher throughput," in *Networks, 2008. ICON 2008. 16th IEEE International Conference on*, dec. 2008, pp. 1 –5.

[19] "Ieee 802.16m approved as imt-advanced technology, www.wimaxforum.org, wimax forum, press release,20 october 2010."

[20] "Ieee standard for local and metropolitan area networks part 16: Air interface for broadband wireless access systems amendment 3: Advanced air interface," *IEEE Std 802.16m-2011(Amendment to IEEE Std 802.16-2009)*, pp. 1 –1112, 5 2011.

[21] W. ForumTM, "Wimax forumtm mobile system profile specification ,common part,wmf,t23001r015v01," 2009-08-01 2009.

[22] R. K. Jurgen, "Smart cars and highways go global," *Spectrum, IEEE*, vol. 28, no. 5, pp. 26–36, 1991.

[23] E. S. Steven, "Applications of wireless communications to cooperative its in the california path program," in *ITS Telecommunications Proceedings, 2006 6th International Conference on*, 2006, pp. P8–P9.

[24] Z. Peng, G. Li, H. Wang, and Q. Wu, "A wireless transmission mechanism of the wireless cbtc system and performance analysis," in *Audio, Language and Image Processing, 2008. ICALIP 2008. International Conference on*, july 2008, pp. 443 –448.

[25] W. Fei-Yue, Z. Daniel, and Y. Liuqing, "Smart cars on smart roads: An ieee intelligent transportation systems society update," *Pervasive Computing, IEEE*, vol. 5, no. 4, pp. 68–69, 2006.

[26] B. Kamali, "Some applications of wireless communications in intelligent vehicle highway systems," *Aerospace and Electronic Systems Magazine, IEEE*, vol. 11, no. 11, pp. 8–12, 1996.

[27] J. Kay, "Advanced traffic management systems - an element of intelligent vehicle-highway systems," in *Transportation Electronics, 1990. Vehicle Electronics in the 90's: Proceedings of the International Congress on*, 1990, pp. 73 –84.

[28] D. Roper and G. Endo, "Advanced traffic management in california," *Vehicular Technology, IEEE Transactions on*, vol. 40, no. 1, pp. 152 –158, feb 1991.

[29] J. Lam, J. Kerr, P. Korpal, and C. Rayman, "Development of compass an advanced traffic management system," in *Vehicle Navigation and Information Systems Conference, 1993., Proceedings of the IEEE-IEE*, oct 1993, pp. 200 –203.

[30] M. C. B. I. D.McCoy, K.Morrison, "Development and deployment of an advanced traffic management system (atms) in auckland, new zealand," Tech. Rep., 10 March 1999.

[31] P. Kumar, V. Singh, and D. Reddy, "Advanced traveler information system for hyderabad city," *Intelligent Transportation Systems, IEEE Transactions on*, vol. 6, no. 1, pp. 26 – 37, march 2005.

[32] D. Jeffery and R. Meekums, "Advanced traveller information systems in the uk: experience from the pleiades and romanse projects," in *Vehicle Navigation and Information Systems Conference, 1994. Proceedings., 1994*, aug-2 sep 1994, pp. 309 –313.

[33] S. Shladover, "The california path program of ivhs research and its approach to vehicle-highway automation," in *Intelligent Vehicles '92 Symposium., Proceedings of the*, July 1992, pp. 347 –352.

[34] D. Symes, "Automatic vehicle monitoring: A tool for vehicle fleet operations," *Vehicular Technology, IEEE Transactions on*, vol. 29, no. 2, pp. 235 – 237, may 1980.

[35] B. Robinson and R. Troxell, "The balkan digitization initiative," in *Military Communications Conference, 2001. MILCOM 2001. Communications for Network-Centric Operations: Creating the Information Force. IEEE*, vol. 2, 2001, pp. 775 – 779.

[36] M. Aguado, E. Jacob, J. Matias, C. Conde, and M. Berbineau, "Deploying cctv as an ethernet service over the wimax mobile network in the public transport scenario," in *Communications Workshops, 2009. ICC Workshops 2009. IEEE International Conference on*, 2009, pp. 1–5.

[37] H. Aodeikat, "Euro-scout's adaptability to paradigm shift in transportation policy," in *Vehicle Navigation and Information Systems Conference, 1993., Proceedings of the IEEE-IEE*, oct 1993, pp. 702 –705.

[38] K. Takada, Y. Tanaka, A. Igarashi, and D. Fujita, "Road/automobile communication system (racs) and its economic effect," in *Vehicle Navigation and Information Systems Conference, 1989. Conference Record*, sep 1989, pp. A15 –A21.

[39] Y. Sunachi and T. Tajima, "Infrared beacon for urban express ways," in *Intelligent Vehicles Symposium, 2000. IV 2000. Proceedings of the IEEE*, 2000, pp. 424 –429.

[40] M. Sugimoto, K. Aoyama, and A. Kongoh, "Improvement of traffic control system by means of infrared beacon two-way communication," in *Intelligent Transportation Systems, 2000. Proceedings. 2000 IEEE*, 2000, pp. 258 –263.

[41] R. Pascoe and T. Eichorn, "What is communication-based train control?" *Vehicular Technology Magazine, IEEE*, vol. 4, no. 4, pp. 16 –21, december 2009.

[42] M. Aguado, E. Jacob, P. Saiz, J. Unzilla, M. Higuero, and J. Matias, "Railway signaling systems and new trends in wireless data communication," in *Vehicular Technology Conference, 2005. VTC-2005-Fall. 2005 IEEE 62nd*, vol. 2, sept., 2005, pp. 1333 – 1336.

[43] K. Kwon, J. Choi, J. Choi, Y. Hwang, K. Lee, and J. Ko, "A 5.8 ghz integrated cmos dedicated short range communication transceiver for the korea/japan electronic toll collection system," *Microwave Theory and Techniques, IEEE Transactions on*, vol. 58, no. 11, pp. 2751 –2763, nov. 2010.

[44] C. B. Carolyn Anderson, "Redline connects passengers ot utah transit authority's high speed commuter train, www.redlinecommunications.com, press release," September 3 2008).

[45] C.-M. Chou, C.-Y. Li, W.-M. Chien, and K. chan Lan, "A feasibility study on vehicle-to-infrastructure communication: Wifi vs. wimax," in *Mobile Data Management: Systems, Services and Middleware, 2009. MDM '09. Tenth International Conference on*, may 2009, pp. 397 –398.

[46] A. Costa, P. Pedreiras, J. Fonseca, J. Matos, H. Proenca, A. Gomes, and J. Gomes, "Evaluating wimax for vehicular communication applications," in *Emerging Technologies and Factory Automation, 2008. ETFA 2008. IEEE International Conference on*, sept. 2008, pp. 1185 –1188.

[47] M. Aguado, J. Matias, E. Jacob, and M. Berbineau, "The wimax asn network in the v2i scenario," in *Vehicular Technology Conference, 2008. VTC 2008-Fall. IEEE 68th*, sept. 2008, pp. 1 –5.

[48] V. Riihimaki, T. Vaaramaki, J. Vartiainen, and T. Korhonen, "Techno-economical inspection of high-speed internet connection for trains," *Intelligent Transport Systems, IET*, vol. 2, no. 1, pp. 27 –37, march 2008.

[49] N. Doyle, N. Jaber, and K. Tepe, "Improvement in vehicular networking efficiency using a new combined wimax and dsrc system design," in *Communications, Computers and Signal Processing (PacRim), 2011 IEEE Pacific Rim Conference on*, aug. 2011, pp. 42 –47.

[50] K. Shafiee, A. Attar, and V. Leung, "Wlan-wimax double-technology routing for vehicular networks," in *Vehicular Technology Conference (VTC Fall), 2011 IEEE*, sept. 2011, pp. 1 –6.

[51] M. Tran, G. Zaggoulos, A. Nix, and A. Doufexi, "Mobile wimax: Performance analysis and comparison with experimental results," in *Vehicular Technology Conference, 2008. VTC 2008-Fall. IEEE 68th*, 2008, pp. 1–5.

[52] K. Hye-Soo, N. Hyeong-Min, J. Jae-Yun, K. Soo-Hyung, and K. Sung-Jea, "Measurement based channel-adaptive video streaming for mobile devices over mobile wimax," *Consumer Electronics, IEEE Transactions on*, vol. 54, no. 1, pp. 171–178, 2008.

[53] O. Alim, N. Elboghdadly, M. Ashour, and A. Elaskary, "Simulation of channel estimation and equalization for wimax phy layer in simulink," in *Computer Engineering Systems, 2007. ICCES '07. International Conference on*, nov. 2007, pp. 274 –279.

[54] M. F. Mohamad, M. A. Saeed, and A. U. Priantoro, "Downlink channel estimation and tracking in mobile wimax systems," in *Computer and Communication*

Engineering, 2008. ICCCE 2008. International Conference on, 2008, pp. 1340–1343.

[55] O. Arafat and K. Dimyati, "Performance parameter of mobile wimax : A study on the physical layer of mobile wimax under different communication channels," in *Computer Engineering and Applications (ICCEA), 2010 Second International Conference on*, vol. 2, march 2010, pp. 533 –537.

[56] G. Zaggoulos, A. Nix, and A. Doufexi, "Wimax system performance in highly mobile scenarios with directional antennas," in *Personal, Indoor and Mobile Radio Communications, 2007. PIMRC 2007. IEEE 18th International Symposium on*, sept. 2007, pp. 1 –5.

[57] P. Neves, R. Matos, B. Sousa, G. Landi, S. Sargento, K. Pentikousis, M. Curado, and E. Piri, "Mobility management for ngn wimax: Specification and implementation," in *World of Wireless, Mobile and Multimedia Networks Workshops, 2009. WoWMoM 2009. IEEE International Symposium on a*, june 2009, pp. 1 –10.

[58] H. Min, J. Kim, H. Kim, D. Kim, D. S. Kwon, and D. Hong, "New pilot designs and ici mitigation for ofdm downlink systems based on ieee 802.16m standards over high speed vehicular channels," in *Wireless Communications and Networking Conference, 2009. WCNC 2009. IEEE*, april 2009, pp. 1 –5.

[59] A. Rottinghaus, R. Hariharan, X. Guo, A. Rangarajan, R. Avivi, A. Busch, and B. Conner, "Supporting high speed on wimax: From theory to practice," in *Vehicular Technology Conference (VTC Spring), 2011 IEEE 73rd*, may 2011, pp. 1 –6.

[60] R. Colda, T. Palade, E. Pucchita, I. Vermecan, and A. Moldovan, "Mobile wimax: System performance on a vehicular multipath channel," in *Antennas and Propagation (EuCAP), 2010 Proceedings of the Fourth European Conference on*, april 2010, pp. 1 –5.

[61] N. Begam, F. Rahman, and K. Ahmed, "Analysis of propagation model performance in wimax (ieee 802.16e)-based wireless mobile vehicular networks," in

Electrical and Computer Engineering (ICECE), 2010 International Conference on, dec. 2010, pp. 714 –717.

[62] B. Wang, I. Sen, and D. Matolak, "Performance evaluation of 802.16e in vehicle to vehicle channels," in *Vehicular Technology Conference, 2007. VTC-2007 Fall. 2007 IEEE 66th*, 30 2007-oct. 3 2007, pp. 1406 –1410.

[63] I. Ahmad and D. Habibi, "High utility video surveillance system on public transport using wimax technology," in *Wireless Communications and Networking Conference (WCNC), 2010 IEEE*, april 2010, pp. 1 –5.

[64] R. Bultitude, Y. de Jong, J. Pugh, S. Salous, and K. Khokhar, "Measurement and modelling of emergency vehicle-to-indoor 4.9 ghz radio channels and prediction of ieee 802.16 performance for public safety applications," in *Vehicular Technology Conference, 2007. VTC2007-Spring. IEEE 65th*, april 2007, pp. 397 –401.

[65] J.-H. Lee, H.-W. Kim, Y.-H. Choi, J. Park, and K. Lee, "Predictive l3 handover in ieee 802.16 vehicular networks," in *Ubiquitous Information Technologies and Applications (CUTE), 2010 Proceedings of the 5th International Conference on*, dec. 2010, pp. 1 –6.

[66] I. Ahmad, D. Habibi, and Z. Rahman, "An improved fec scheme for mobile wireless communication at vehicular speeds," in *Telecommunication Networks and Applications Conference, 2008. ATNAC 2008. Australasian*, 2008, pp. 312–316.

[67] I. Ahmad and D. Habibi, "Call admission control scheme for the ieee 802.16e at vehicular speeds," in *High Performance Computing and Communications (HPCC), 2010 12th IEEE International Conference on*, 2010, pp. 413–418.

[68] B. Ouarzazi, M. Berbineau, I. Dayoub, and A. Menhaj-Rivenq, "Channel estimation of ofdm system for high data rate communications on mobile environments," in *Intelligent Transport Systems Telecommunications,(ITST),2009 9th International Conference on*, 2009, pp. 425–429.

[69] K. Zhengjiu, Y. Kung, and F. Lorenzelli, "Nakagami-m fading modeling in the frequency domain for ofdm system analysis," *Communications Letters, IEEE*, vol. 7, no. 10, pp. 484–486, 2003.

[70] J. Cheng and N. Beaulieu, "Precise bit error rate calculation for asynchronous ds-cdma in nakagami fading," in *Global Telecommunications Conference, 2000. GLOBECOM '00. IEEE*, vol. 2, 2000, pp. 980 –984.

[71] M. Assaad and D. Zeghlache, "Analytical model of hsdpa throughput under nakagami fading channel," *Vehicular Technology, IEEE Transactions on*, vol. 58, no. 2, pp. 610 –624, feb. 2009.

[72] D. Zheng, J. Cheng, and N. C. Beaulieu, "Accurate error-rate performance analysis of ofdm on frequency-selective nakagami-m fading channels," *Communications, IEEE Transactions on*, vol. 54, no. 2, pp. 319–328, 2006.

[73] S. P. Vanja Subotic, "Ber analysis of equalized ofdm systems in nakagami, m $<$ 1 fading," *Wireless Personal Communications*, vol. 40,, no. 3, pp. 281–290, 2006.

[74] X. Chen, Q. Liu, and M. Hu, "Performance analysis of mimo-ofdm systems on nakagami-m fading channels," in *Future Computer and Communication (ICFCC), 2010 2nd International Conference on*, vol. 3, 2010, pp. V3–396–V3–400.

[75] G. Rui and L. Ji-lin, "Ber performance analysis of rcpc encoded mimo-ofdm in nakagami-m channels," in *Information Acquisition, 2006 IEEE International Conference on*, 2006, pp. 1416–1420.

[76] P. V. S. S. Srigowri, Prabhakara Rao, "Performance of dqpsk-ofdm systems over slowly nakagami-m fading channels," in *World Congress on Engineering and Computer Science*, San Francisco, USA, 2007.

[77] P. K. Vivek K. Dwivedi and G. Singh, "Performance analysis of ofdm communication systems over a correlated nakagami-m fading channel," in *Electronics Research symposium*, March 2007, pp. 1495 –1498.

[78] V. Dwivedi and G. Singh, "Improved ber analysis of ofdm communication system on correlated nakagami-m fading channel," in *Recent Advances in Microwave Theory and Applications, 2008. MICROWAVE 2008. International Conference on*, nov. 2008, pp. 536 –539.

[79] A. Mills, D. Lister, M. De Vos, and Y. Ji, "The impact of ms velocity on the performance of frequency selective scheduling in ieee 802.16e mobile wimax," in *Consumer Communications and Networking Conference (CCNC), 2010 7th IEEE*, jan. 2010, pp. 1 –5.

[80] H. Balta, M. Kovaci, and A. de Baynast, "Performance of turbo-codes on nakagami flat fading (radio) transmission channels," in *Signals, Systems and Computers, 2005. Conference Record of the Thirty-Ninth Asilomar Conference on*, 2005, pp. 606–610.

[81] A. Ramesh, A. Chockalingam, and L. B. Milstein, "Bounds on the performance of turbo codes on nakagami fading channels with diversity combining," in *Global Telecommunications Conference, 2001. GLOBECOM '01. IEEE*, vol. 2, 2001, pp. 1199–1204.

[82] R. Annavajjala, A. Chockalingam, and L. B. Milstein, "Performance analysis of coded communication systems on nakagami fading channels with selection combining diversity," *Communications, IEEE Transactions on*, vol. 52, no. 7, pp. 1214–1220, 2004.

[83] N. Sood, A. K. Sharma, and M. Uddin, "Ber performance of ofdm-bpsk and-qpsk over nakagami-m fading channels," in *Advance Computing Conference (IACC), 2010 IEEE 2nd International*, 2010, pp. 88–90.

[84] S. Cotton, "Characterization and modeling of the indoor radio channel at 868 mhz for a mobile bodyworn wireless personal area network," *Antennas and Wireless Propagation Letters, IEEE*, vol. 6, pp. 51 –55, 2007.

[85] S. Cotton and W. Scanlon, "An experimental investigation into the influence of user state and environment on fading characteristics in wireless body area networks at 2.45 ghz," *Wireless Communications, IEEE Transactions on*, vol. 8, no. 1, pp. 6 –12, jan. 2009.

[86] J. Yin, G. Holland, T. ElBatt, F. Bai, and H. Krishnan, "Dsrc channel fading analysis from empirical measurement," in *Communications and Networking in China, 2006. ChinaCom '06. First International Conference on*, oct. 2006, pp. 1 –5.

[87] C. Yeh, C. Chow, Y. Liu, S. Wen, S. Chen, C. Sheu, M. Tseng, J. Lin, D. Hsu, and S. Chi, "Theory and technology for standard wimax over fiber in high speed train systems," *Lightwave Technology, Journal of*, vol. PP, no. 99, pp. 1–1, 2010.

[88] NIC, "Impulse response model of a multipath channel, developer zone, national instrument corporation http://zone.ni.com/devzone/cda/ph/p/id/331, last accessed 5 august 2010," pp. 1–12.

[89] I. Ahmad and D. Habibi, "Improving quality of service in wimax communication at vehicular speeds: A new call admision control solution (in press doi:10.1002/wcm.111)„" *Wireless communication and mobile computing,2011.*

[90] P. V. David Tser, *Wireless Communication*, first reprinted edition ed. Edinburgh Building, Cambridge, CB2 2RU, UK: Cambridge University Press, 2005.

[91] B. Skler, "Rayleigh fading channels in mobile digital communication systems part 1: Characterization," *IEEE Communications Magazine*, pp. 136–146, September 1997.

[92] V. Subotic and S. Primak, "A new vector channel simulator for sub rayleigh fading," in *Wireless Technology, 2004. 7th European Conference on*, 2004, pp. 49 – 52.

[93] K.-W. Yip and T.-S. Ng, "A simulation model for nakagami-m fading channels, m lt;1," *Communications, IEEE Transactions on*, vol. 48, no. 2, pp. 214 –221, feb 2000.

[94] "Ieee standard for local and metropolitan area networks part 16: Air interface for broadband wireless access systems amendment 3: Advanced air interface," *IEEE Std 802.16m-2011(Amendment to IEEE Std 802.16-2009)*, pp. 1 –1112, 5 2011.

[95] S. Mukherjee, K. Leung, and G. Rittenhouse, "Protocol and control mechanisms to save terminal energy in ieee 802.16 networks," in *Communications, Computers and signal Processing, 2005. PACRIM. 2005 IEEE Pacific Rim Conference on*, aug. 2005, pp. 5 – 8.

[96] G. Stuber, *Principles of Mobile Communication*, second edition ed. Boston, MA: Kluwer Academic Publisher, 2002.

[97] C. Tepedelenlioglu and P. Gao, "Estimators of the nakagami-m parameter and performance analysis," *Wireless Communications, IEEE Transactions on*, vol. 4, no. 2, pp. 519 – 527, march 2005.

[98] A. Abdi and M. Kaveh, "Performance comparison of three different estimators for the nakagami m parameter using monte carlo simulation," *Communications Letters, IEEE*, vol. 4, no. 4, pp. 119 –121, apr 2000.

Appendix A

Algorithms Referred in this Thesis

Appendix A presents photographs and algorithms to support our design and experiments in the thesis. Algorithm-1 is the related function of the BER analytical model. Algorithm-2, combines the WiMAX system parameters and OFDM and algoithm-3 is the algorithm for the proposed BER analytical model of chapter 3. Algorithm-4 is the algorithm for estimation of Nakagami parameter m in chapter 4 of this thesis.

A.1 Photograph

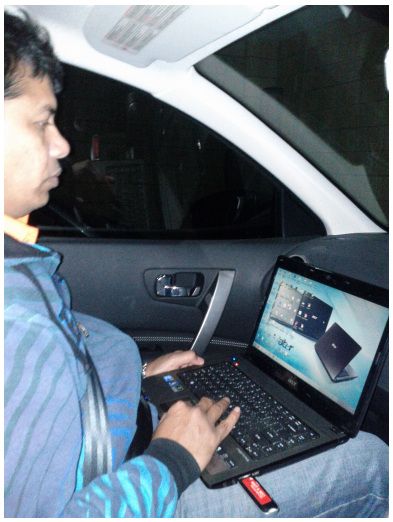

Figure A.1: Laptop position inside the car

A.2 Algorithm

Algorithm A.1 Mobile WiMAX system and OFDM configuration algorithm

```
clear;
%primitive parameter
bw=5*10^6; % bandwidth for 512 FFT on OFDMA( mobile WiMAX)
nfft=512; % number of fft
nused=433;% number of used subcarriers
n=28/25; % Sampling factor
fc= 2.6 *10^9; %carrier frequency
c=3*10^8; % meter per sec, speed of light
%drived parameter
fs= floor(n*(5*10^6)/8000)*8000; %sampling frequency
df=fs/nfft; %subcarrier spacing
Tb= 1/df; % useful symbol time
g=1/8; %cyclic prefix guard time constant
Tg=g*Tb; %CP time ( guard band duration) ofdm
Ts=Tb+Tg; %total ofdm symbol time
Ts=Tb/nfft; % Sampling time
%Estimation of doppler shift
vmin=0;
vmax=200;
sp =vmin:10:vmax;
for p = 1:length(sp)
v(p) = sp(p)*1000/3600; % speed of mobile station
end
fd=v*fc/c; %Doppler shift
%Estimation of energy per bit to noise ration
M=4; % 4 for qpsk and 16 for Qam modulation
EbNo= 5; %energy per bit to noise ratio
nebnr=10^(EbNo/10); % numerical values of EbNo
%Nakagami parameter
m=5;
% estimation Bit energy to noise ratio
a1=1/(nused.^2);
a=0;
for k=1:nused-1
a = a+(nused-k)*besselj(0,2*pi*fd*Ts*k);
end
a2 = (nused+2*a)/nused^2;
a3 =(Tb/log2(M))/nebnr;
% Energy per bit to noise ratio
for i=1:length(a2)
a4(i) = 1-a2(i)+a3;
end
for q=1:length(a4)
yb(q)=1/log2(M)/a4(q);
end
% bit error at Rayleigh Fading
for r=1:length(yb)
rpb(r)=1/2*(1-sqrt(yb(r)/(1+yb(r))));
end
```

Algorithm A.2 Functions for proposed BER estimation model for WiMAX communication

```
function A=ber(yb,m) % (yb and m came from algorithm A.22)
M=100000;
x=linspace(0,1,M);
x1=zeros(M-1,1);
for i=1:M-1
x1(i)=(x(i+1)+x(i))/2;
end
ybn=size(yb,2);
A=zeros(ybn,1);
for j=1:ybn
y1=zeros(M-1,1);
for i=1:M-1
y1(i)=P(x1(i),m,yb(j));
end
dx=1/(M-1);
s=0;
for i=1:M-1 s=s+y1(i);
end
A(j)=s*dx;
end
figure plot(A,yb)
```

Algorithm A.3 Algorithm for BER estimation at high vehicular speeds in WiMAX communications using Nakagami-m distribution model

```
function y=P(x,m,yb)
y=0.5*(1-sqrt(yb*x/(1+yb*x)))*(x^(m-1)*(1-x)^(-m))/beta(m,1-m);
```

Algorithm A.4 Algorithm for Nakagami parameter m estimation

```
y= data; %received data
for i=1:length(y)
rv(i)=10.^(y(i)/10); % numerical values of RSSI
end
for k=1:length(rv)
R=rv.^2;
end
omega=mean(R.^2);
for j=1:length(R)
p(j)=R(j).^2-omega;
end
%mv=mean(rssi);
z=p.^2;
w=mean(z);
m=omega.^2/w;
```

Appendix B

Abbreviations Referred in this Thesis

1G First Generation.

2G The Second Generation.

3G Third Generation .

4G Fourth Generation.

AAS Advanced Antenna Subsystems.

AIC Akakie Information Criterion

AMC Adaptive Modulation and Coding

AMC Adaptive Modulation and Coding

AME Approximate Moment Estimator.

AMPS Advanced Mobile Phone System.

APTS Advanced Public Transportation Systems.

ARDIS Advanced Radio Data Information Services.

ATIS Advanced Traveler Information Systems.

ATMS Advanced Traffic Management Systems.

AVCS Advanced Vehicle Control Systems.

AWGN Additive White Gaussian Noise.

BEP Bit Error Probability.

BER Bit Error Rate.

BF Beam Forming.

BS Base Station.

BSC Base Station Controller.

BSC Base Station Controller.

BTC Block Turbo Code.

BTS Base Transceiver Station.

BTS Base Station Transceiver System.

BW Band Width.

BWA Broadband Wireless Access.

CCTV Closed Circuit Television.

cdf Cumulative Distribution Function.

CDMA Code Division Multiple Access.

CDPD Cellular Digital Packet Data.

CF Characteristics Function.

CFSK Coded Frequency Shift Keying.

CINR Carrier Interference to Noise Ratio.

CIR Channel Impulse Response.

CN Core Network.

COFDM Coded OFDM.

CP Cyclic Prefix.

CPE Customer Premises Equipment.

CPS The Common Part Sublayer.

CPU Central Processing Units.

CQI Channel Quality.

CS Convergence Sublayer.

CSC Connectivity Service Controller.

CTBC Communication Based Train Control.

CTC Convolution Turbo code.

CTC Convolutional Turbo Codes.

CVO Commercial Vehicle Operation.

DC Direct Current.

DL Down Link.

DSRC Dedicated Short Range Communication.

DSSS Direct Sequence Spread Spectrum.

EDGE Enhanced Data rates for GSM Evolution.

EGC Equal Gain Combining.

EPC Evolved Packet Core.

ERTMS European Rail Network management system.

ETSI European Telecommunications Standards Institute.

EU User Equipment.

E-UTRAN Evolved UMTS Terrestrial Radio Access Network.

EVDO EVolution Data Only.

FDD Frequency Division Duplex.

FDM Frequency Division Multiplexing.

FDMA Frequency Division Multiple Access.

FEC Forward Error Correction.

FER Frame Error Rate.

FFT First Furrier Transformation.

FHSS Frequency Hopping Spread Spectrum.

FUSC Full Use of Sub-carrier.

GPRS General Packet Radio Service.

GSM Global System for Mobile Communications.

HARQ Hybrid Automatic Repeat Request.

H-FDD Half-Duplex FDD.

HSDPA High Speed Downlink Packet Access.

HSPA High Speed Packet Access.

HSUPA High Speed Uplink Packet Access.

i.i.d independent and identically distributed.

ICI Inter Carrier Interference.

IEEE Institute of Electrical and Electronics Engineers.

IFFT Inverse First Fourier Transformation.

IMT-2000 Advanced International Mobile Telecommunication-2000.

IMT-Advanced International Mobile Telecommunication-Advanced.

IP Internet Protocol.

ISI Inter Symbol Interference.

ISM Industrial, Scientific and Medical.

ITS Intelligent Transportation systems.

ITSS Intelligent Transportation Systems Society.

ITU International Telecommunication Union.

IVHS Intelligent Vehicle Highway System.

JDC Japanese Digital Cellular.

LDAR Light Detection And Ranging.

LDPC Low Density Parity-Check.

LLC Logical Link Control.

LMS Least mean squares.

LMSC LAN/MAN Standards Committee.

LOS Line of Site.

LS Least Square.

LTE Long Term Evolution.

LTE-A Long Term Evolution-Advanced.

MAC Media Access Control.

MGF Moment Generating Function.

MiMO Multiple Input Multiple Output.

MIP Mobile IP.

ML Maximum Likelihood.

MM Mobility Manager.

MMSE Minimum Mean Squared Error.

MRC Maximal Ratio Combing.

MS Mobile Station.

MSE Mean Square Erroir.

MSS Mobile Satellite Service.

Mu-MIMO Multiuser MIMO.

NLOS Non Line of Site.

NMT Nordic mobile Telephony.

NSS Network Switching Subsystem.

OFDM Orthogonal Frequency Division Multiplexing.

OFDMA Orthogonal Frequency Division multiple Access.

OSI Open Systems Interconnection.

P2M Point to Multipoint.

P2P Point to Point.

PCS Personal Communication Systems.

PDA Personal Digital Assistant.

pdf Probability Density Function.

PEP Pairwise Error Probability.

PER Packet Error Rate.

PHY Physical Layer.

PMP Point to Multi-point.

PMR Professional Mobile Radio.

PRU Physical Resource Unit.

PSC Public Safety Communication.

PSD Power Spectrum Density.

PSK Phase-Shift Keying.

PSTN Public Switched Telephone Network.

PTA Public Transport Authority.

PUSC Partial Use of Sub-Carrier.

QAM Quadrature Amplitude Modulation.

QoS Quality of Service.

RADAR Radio Detection And Ranging.

RCPC Rate-Compatible Punctured Convolution.

rms Root Mean Square.

RNC Radio Network controller.

RSC Recursive Systematic Convolution.

RS-CC Reed-Solomon Convolutional Code.

RSS Received Signal Strength.

RSS Received Signal Strength.

Rx Receiver.

SAE System Architecture Evolution .

SC Selection Combining.

SER Symbol Error Rate.

SFN Signal Frequency Network.

SISO Single Input Single Output.

SNR Single to Noise Ratio.

SOFDMA Scalable OFDMA.

SS Subscriber Station.

STBC Space Time Block Coding.

STC Space Time Coding.

STDMA Space Time Division Multiple Access.

SUI Stanford University Interim.

SU-MIMO Single User MIMO.

TCP/IP Transmission Control Protocol/Internet Protocol.

TDD Time Division Duplex

TDL Tapped Delay Line.

TDMA Time Division Multiple Access.

TETRA Terrestrial European Trunked Radio.

TGPP Third Generation Partnership Project.

THSR Taiwan High Speed Rail.

TIGER Topologically Integrated Geographic Encoding and Referencing.

TUSC Tile Uses of Subchannel.

Tx Transmitter.

UL Up Link.

UMTS Universal Mobile Telephone System.

UTA Utah transit Authority.

UTMS Universal Traffic Management Systems.

V2I Vehicle to infrastructure.

V2V Vehicle to Vehicle.

VICS Vehicle Information and Communication System.

VoIP Voice Over Internet Protocol.

WBN Wireless Body area Network.

WCDMA Wideband CDMA.

WiFi Wireless Fidelity.

WiMAX Worldwide Interoperability of Microwave Access.

WLAN Wireless Local Area Network.

WMAN Wireless Metropolitan Area Network.

WPAN Wireless Personal area Network.

WWAN Wireless Wide Area Network.

WWDTR WiMAX Double-Technology Routing .

WWWW World Wide Wireless Web.

YRP Research Park